НАЦІОНАЛЬНА АКАДЕМІЯ НАУК УКРАЇНИ
ІНСТИТУТ ЗАГАЛЬНОЇ ТА НЕОРГАНІЧНОЇ ХІМІЇ імені В. І. ВЕРНАДСЬКОГО
КИЇВСЬКИЙ НАЦІОНАЛЬНИЙ УНІВЕРСИТЕТ імені ТАРАСА ШЕВЧЕНКА

УКРАЇНСЬКИЙ ХІМІЧНИЙ ЖУРНАЛ

№ 2
Том 92 / Vol. 92
2026
https://ucj.org.ua

UKRAINIAN CHEMISTRY JOURNAL

Зміст

Contents

УДК [543.442.2+543.421/.424.54-74]:54-386(546.742+547.484.34+547.824) doi: 10.33609/2708-129X.92.2.2026.3-12

СТРУКТУРА КОМПЛЕКСУ БІС(ЦИКЛОГЕКСИЛАЦЕТОАЦЕТАТО)НІКЕЛЮ(II) З N,N-ДІЕТИЛНІКОТИНАМІДОМ

***Ольгерд О. Штоквиш*[1],** https://orcid.org/0000-0002-0164-9456
***Вікторія В. Дьяконенко*[1, 2],** https://orcid.org/0000-0003-4613-172X
***Людмила І. Коваль*[1*],** https://orcid.org/0000-0001-5266-988X

[1] *Інститут загальної та неорганічної хімії ім. В.І. Вернадського НАН України, просп. академіка Палладіна, 32–34, Київ 03142, Україна;*
[2] *Інститут хімії функціональних матеріалів НТК "Інститут монокристалів" НАН України, просп. Науки, 60, Харків 61001, Україна*
** e-mail: : kamila6719@gmail.com*

Синтезовано та досліджено методами рентгеноструктурного аналізу та ІЧ-спектроскопії нову координаційну сполуку Ni(II) з циклогексилацетоацетатом та N,N-діетилнікотинамідом. Молекулярна структура відповідає формулі $[Ni(C_{10}H_{15}O_3)_2(C_{10}H_{14}N_2O)_2]$, кристали моноклінної сингонії, просторова група $P2_1/c$, a = 7.0360(15) Å, b = 13.233(4) Å, c = 23.619(5) Å, α = γ =90°, β = 93.301(12)°. Координаційний поліедр атома Ni(II) – викривлений октаедр, який утворено чотирма атомами оксигену двох депротонованих молекул β-кетоестеру та двома атомами нітрогену піридинових кілець двох аксіально розташованих молекул N,N-діетилнікотинаміду. Кристалічна упаковка – шари вздовж площини (001), які стабілізовано слабкими С-Н…π взаємодіями між сусідніми молекулами комплексу.

Ключові слова: нікель, β-дикарбонільні комплекси, циклогексилацетоацетат, N,N-діетилнікотинамід, кристалічна структура.

ВСТУП. Координаційні сполуки металів із β-дикарбонільними лігандами відомі вже багато десятиліть і досить широко досліджені [1]. Стосується це зокрема і комплексів нікелю з різними нітрогенвмісними додатковими лігандами, як монодентатними – піридином та його похідними [2, 3, 4], так і полідентатними – етилендіаміном, фенатроліном тощо [5]. Координація N-основ β-дикарбонільними металохелатами, внаслідок заповнення координаційної сфери металу надає останнім певних фізико-хімічних властивостей і робить більш функціонально придатними для конкретних практичних застосувань [5]. Наприклад, комплекси з алкілдіамінами використовують як леткі прекурсори для отримання тонких плівок оксидів металів методом хімічного осадження з парової фази [6, 7], нерозчинні полімерні металохелати з 4,4'-біпіридином – як каталізатори окиснення в органічних реакціях [8], з бідентатними

P-,N-вмісними лігандами – як хромотропні матеріали [9]. β-Дикарбоніли Ni(II) з піридином, піколіном та амінопіридином широко застосовують у фундаментальних фізичних дослідженнях [10, 11]. Поліядерні піридинвмісні β-дикетонати Ni(II), які мають особливу кубанову структуру, представляють інтерес для створення молекулярних магнетиків [12].

Суттєвий потенціал мають β-дикарбонільні металохелати для фармацевтичних застосувань [13, 14]. У зв'язку з цим потенційно цікавими лігандами є похідні нікотинової кислоти – нікотинамід та N,N-діетилнікотинамід. Нікотинова кислота, що в організмі людини трансформується в нікотинамід (вітамін РР), є біологічно активною сполукою, залученою до ключових метаболічних процесів, її широко застосовують у медичній практиці у антигістамінних та вітамінних препаратах. N,N-діетиламід нікотинової кислоти як ефективний стимулятор центральної нервової системи [15] використовують у невідкладній медицині. Сполуки металів з означеними лігандами також проявляють біологічну активність, часто є більш ефективними порівняно з вільними лігандами [16, 17, 18].

У відомих кристалічних структурах комплексів перехідних металів молекули N,N-діетилнікотинаміду переважно виступають як монодентатні ліганди, координовані до металу через атом нітрогену піридинового кільця. Значно рідше вони функціонують як бідентатні місткові ліганди, сприяючи утворенню димерних або полімерних координаційних сполук [15]. У літературі описано змішанолігандні комплекси Ni(II) з N,N-діетилнікотинамідом у поєднанні з такими органічними лігандами, як бензойна кислота та її похідні [16, 19, 20, 21, 22, 23].

У попередній роботі було досліджено та охарактеризовано структурно комплекси Co(II) та Ni(II) з циклогексилацетоацетатом та піридином [24]. Альтернативою токсичному піридину для металохелатів з екологічно прийнятними β-кетоестерами є нікотинамід та N,N-діетилнікотинамід. β-Дикарбонільні металокомплекси з означеними лігандами в літературі не описано. У цій статті представлено результати синтезу та дослідження структурних і спектральних властивостей нового комплексу нікелю(II) складу $[NiL_2NK_2]$, що містить циклогексилацетоацетат (HL) як хелатуючий ліганд та N,N-діетилнікотинамід (NK) як додатковий нейтральний ліганд.

ЕКСПЕРИМЕНТ І ОБГОВОРЕННЯ РЕЗУЛЬТАТІВ. У роботі [25] наведено методику отримання комплексів низки 3d-металів (Co(II), Ni(II), Zn(II)) з β-кетоестерами вищих спиртів у кристалічній формі. Цю методику було модифіковано для синтезу змішанолігандних комплексів Co(II) та Ni(II) з циклогексилацетоацетатом та піридином [24], а також комплексу $[NiL_2NK_2]$, який досліджують у цій роботі.

До 0,89 мл розчину $NiCl_2{\cdot}6H_2O$ у суміші етанол: вода 9:1 із концентрацією солі 0,05 г/мл (0,19 ммоль металу) додавали 0,068 мл циклогексилацетоацетату (0,38 ммоль) та 0,4 мл водного розчину N,N-діетилнікотинаміду з концентрацією 0,25 г/мл (0,57 ммоль), суміш струшували. Пробірку з реакційною сумішшю та окрему пробірку з 0,14 мл (0,76 ммоль) триетиламіну вміщували в посудину, яку герметизували й залишали в холодильнику. Подібно до інших комплексів нікелю з β-кетоестерами

та похідними піридину в умовах наведеного синтезу, сполука схильна до утворення пересичених розчинів. За кілька місяців утворилися слабко забарвлені блакитні і голчасті кристали. Їх фільтрували на скляному фільтрі № 40, промивали декілька разів етанолом і сушили на повітрі не більше кількох годин. Вихід – 0,04 г (28,6 %).

ІЧ-спектр комплексу реєстрували у таблетках із KBr на спектрометрі Specord M-80 в області 4000–400 $см^{-1}$. У спектрі спостерігають інтенсивні широкі смуги поглинання валентних коливань спряжених у хелатному циклі зв'язків C=O та C=C (1625, 1502 $см^{-1}$), а також інші характеристичні для β-дикарбонільних комплексів смуги поглинання, зокрема вузький сигнал при 775 $см^{-1}$ позаплощинного деформаційного коливання C–H хелатного циклу [26]. У високочастотній області спектру спостерігаються сигнали валентних коливань алканових C–H зв'язків (2855–2990 $см^{-1}$) та слабкі сигнали валентних коливань C-H піридинового кільця (3080–3110 $см^{-1}$). Для вільного N,N-діетилнікотинаміду характеристичні смуги поглинання пов'язані з амідною групою ($\nu_{C=O}$ 1620–1650 $см^{-1}$) та піридиновим кільцем ($\nu_{C=C}$, $\nu_{C=N}$ 1500–1600 $см^{-1}$), у спектрі комплексу вони перекриваються зі смугами коливань хелатних циклів та не можуть бути однозначно ідентифіковані. Ще одна характеристична смуга поглинання N,N-діетилнікотинаміду відповідає валентними коливанням C-N амідної групи, її спостерігають як у спектрі вільного ліганду, так і в спектрі комплексу при 1300 $см^{-1}$. Смуги низької інтенсивності, що з'являються в спектрі комплексу в області 600–400 $см^{-1}$, відповідають коливанням зв'язків Ni–N та Ni–O.

Кристали комплексу $C_{40}H_{58}N_4NiO_8$ (M = 781.61 г/моль): моноклінна сингонія, просторова група $P2_1/c$, a = 7.0360(15) Å, b = 13.233(4) Å, c = 23.619(5) Å, α = γ = 90°, β = 93.301(12)°, V = 2195.(9) $Å^3$, Z = 2, T = 294 K, $\mu(Mo K\alpha) = 0.492 мм^{-1}$, $D_{обч} = 1.182 г/см^3$, виміряно 13 892 відбиттів, 3 746 незалежних (R_{int} = 0.1496, R_{sigma} = 0.1335). Кінцеві значення R_1 = 0.0953 (для відбиттів з інтенсивністю $I > 2\sigma(I)$) та wR2 = 0.2219 (для всіх відбиттів).

Параметри елементарної комірки та інтенсивності відбиттів для $C_{48}H_{84}Ni_2O_{20}$ виміряно на дифрактометрі Bruker APEX-II (MoKα випромінювання, λ= 0.71073 Å, CCD-детектор, графітовий монохроматор). Використовуючи програму Olex2 [27], структуру розшифровано за допомогою програми SHELXT [28] і уточнено по F^2 повноматричним МНК в анізотропному наближенні для неводневих атомів у комплексі програм SHELXL [29]. Положення атомів гідрогену отримано з карти електронної густини та уточнено з використанням моделі «вершника» $U_{iso} = nU_{eq}$ (n = 1.5 для метильних груп і n = 1.2 для інших атомів гідрогену). Координати атомів, а також повні таблиці довжин зв'язків і валентних кутів депоновано до Кембриджського банку кристалографічних даних (https://www.ccdc.cam.ac.uk/structures), вони доступні із зазначенням номеру CCDC 2539164.

За даними рентгеноструктурного аналізу структура $C_{40}H_{58}N_4NiO_8$ ($[NiL_2NK_2]$, де L^- – єнолат-аніон циклогексилацетоацетату, а NK – N,N-діетилнікотинамід) являє собою моноядерний комплекс, який знаходиться в спеціальному положенні відносно центру інверсії.

Координаційний поліедр атому Ni(II) – це викривлений октаедр, який утворено

чотирма атомами оксигену двох депротонованих молекул циклогексилацетоацетату та двома атомами нітрогену двох молекул N,N-діетилнікотинаміду (рис. 1). Останні координуються атомом нітрогену піридинового кільця в аксіальному положенні відносно площини хелатних лігандів. Довжини зв'язків Ni-O та Ni-N у координаційному поліедрі змінюються в діапазоні 2.080(4) ÷ 2.109(4) Å та 2.164(5) Å відповідно, а валентні кути O-Ni-O та O-Ni-N – у діапазоні 84.48(17) ÷ 92.52(17) ° (табл. 1).

У кристалі молекули комплексу пов'язані слабкими C-H…π взаємодіями (C20-H20…C14'(π) (x, 1-y, z) H…C 2.94 Å, C-H…C 147.23 °) і утворюють шари в площині (001), що чергуються між собою (рис. 2).

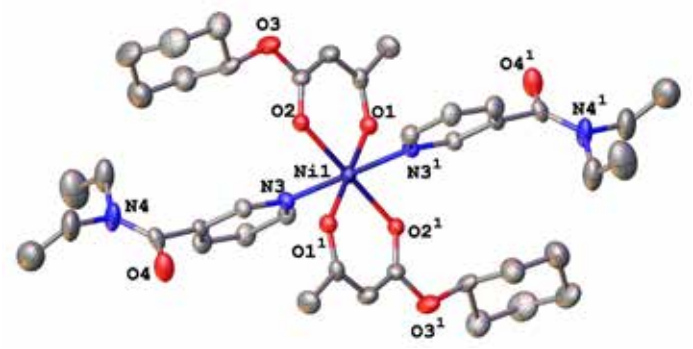

Рис.1. Молекулярна будова комплексу NiL_2NK_2. (операція симетрії [1] 2-x,-y,1-z). Атоми гідрогену прибрано для спрощення

Fig. 1. Molecular structure of the complex NiL_2NK_2. (symmetry code [1]2-x,-y,1-z). The H-atoms are omitted for clarity.

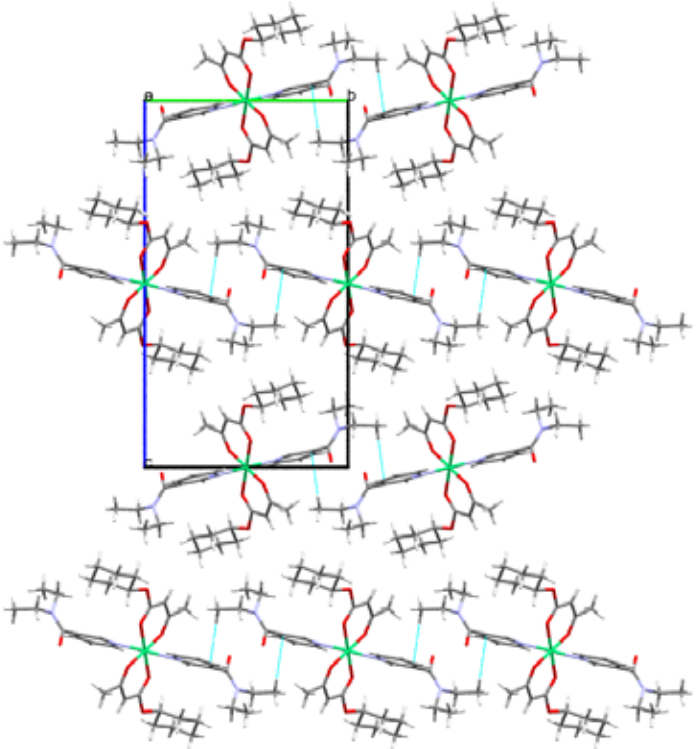

Рис. 2. Кристалічна будова комплексу NiL_2NK_2

Fig. 2. The crystal packing of NiL_2NK_2 complex.

Табл. 1

Деякі довжини зв'язків (Å) та валентні кути (град.) у комплексі NiL_2NK_2 (операція симетрії [1] 2-x,-y,1-z)

Table 1.

Some bond lengths (Å) and bond angles (deg.) in the NiL_2NK_2 complex (symmetry operation [1] 2-x,-y,1-z).

Ni1—O1	2.080 (4)	Ni1—N3	2.164 (5)
Ni1—O2	2.109 (4)		
O1—Ni1—O2	91.34 (16)	O1^{i}—Ni1—N3	87.62 (18)
O1^{i}—Ni1—O2	88.66 (16)	O2—Ni1—N3^{i}	92.52 (17)
O1—Ni1—N3	92.38 (18)	O2—Ni1—N3	87.48 (17)

ВИСНОВКИ. Синтезовано та структурно охарактеризовано нову сполуку – змішанолігандний комплекс Ni(II) з циклогексилацетоацетатом та N,N-діетилнікотинамідом. Комплекс моноядерний, координаційний поліедр атому Ni(II) – викривлений октаедр, який утворено чотирма атомами оксигену двох депротонованих молекул β-кетоестеру та двома атомами нітрогену піридинових кілець аксіально розташованих молекул N,N-діетилнікотинаміду. В кристалах молекули комплексу розташовуються шарами, між сусідніми молекулами в шарах спостерігаються слабкі C-H…π взаємодії, що стабілізують кристалічну упаковку. Будова координаційного поліедру описаної сполуки подібна до будови аддуктів β-дикарбонільних комплексів d-металів із піридином.

ДЕТАЛІЗАЦІЯ ВКЛАДУ АВТОРІВ У ПІДГОТОВЦІ РУКОПИСУ / DETAILED DESCRIPTION OF THE AUTHORS' CONTRIBUTION

Ольгерд О. Штоквиш / Olherd O. Shtokvysh – проведення експериментальних досліджень, первинне оброблення результатів / conducting experimental research, initial processing of results.

Вікторія В. Дьяконенко / Viktoriya V. Dyakonenko – проведення рентгеноструктурних досліджень, розшифрування структури та опис результатів / conducting X-ray structural studies, deciphering the structure and describing the results.

Людмила І. Коваль / Lyudmila I. Koval – пошук і аналіз наукової літератури, оброблення результатів, написання рукопису / literature search and analysis, processing results, writing the manuscript.

Усі автори ознайомилися з результатами дослідження та схвалили остаточну версію статті / All authors reviewed the study results and approved the final version of the article.

Роботу виконано в межах держбюджетної теми «Синтез і фізико-хімічні дослідження нових лігандів та координаційних сполук d-, f-металів із каталітичною і біологічною активністю для медичних і технічних застосувань», державний реєстраційний номер: 0126U002304.

UDK [543.442.2+543.421/.424.54-74]:54-386 (546.742+547.484.34+547.824)
doi: 10.33609/2708-129X.92.2.2026.3-12

STRUCTURE OF THE BIS(CYCLOHEXYLACETOACETATO)NICKEL(II) COMPLEX WITH N,N-DIETHYLNICOTINAMIDE.

Olherd O. Shtokvysh[1], Viktoriya V. Dyakonenko[1, 2], Lyudmila I. Koval[1*]

[1] *Vernadsky Institute of General and Inorganic Chemistry of National Academy of Sciences of Ukraine, 32–34 Acad. Palladin Avenue, 03142 Kyiv, Ukraine;*
[2] *Institute of Functional Materials Chemistry, SSI «Institute for Single, Crystals» of National Academy of Sciences of Ukraine, 60 Nauki Ave, 61001 Kharkiv, Ukraine*
** e-mail: : kamila6719@gmail.com*

A new coordination compound of Ni(II) with cyclohexylacetoacetate and N,N-diethylnicotinamide was synthesized and characterized by IR spectroscopy and X-ray analysis. The IR spectrum exhibits intense broad absorption bands corresponding to the stretching vibrations of the C=O and C=C bonds conjugated within the chelate ring (1625, 1502 cm^{-1}), as well as other absorption bands characteristic of β-dicarbonyl complexes, in particular a sharp band at 775 cm^{-1} attributed to the out-of-plane bending vibration of the C–H bond in the chelate ring. In the high-frequency region of the spectrum, there are signals of stretching vibrations of the C-H bonds of alkyl groups (2855–2990 cm^{-1}) and weak signals of stretching vibrations of the C-H of the pyridine ring (3080–3110 cm^{-1}). The absorption bands of the amide group ($\nu_{C=O}$ 1620–1650 cm^{-1}) and the pyridine ring ($\nu_{C=C}$, $\nu_{C=N}$ 1500–1600 cm^{-1}) of N,N-diethylnicotinamide overlap with the vibration bands of the chelate rings and cannot be unambiguously assigned. The medium-intensity band at 1300 cm^{-1}, present in both the free ligand and the complex, is assigned to C–N stretching vibrations of the amide group. The low-intensity bands in the 600–400 cm^{-1} region are assigned to Ni–N and Ni–O vibrations. According to X-ray data, the crystal system of NiL_2NK_2 complex is monoclinic, space group $P2_1/c$, a = 7.0360(15) Å, b = 13.233(4) Å, c = 23.619(5) Å, α = γ = 90°, β = 93.301(12)°. The structure corresponds to the formula $[Ni(C_{10}H_{15}O_3)_2(C_{10}H_{14}N_2O)_2]$ and represents a mononuclear complex located in a special position relative to the inversion center. The central Ni atom has a O_4N_2 distorted octahedral environment. The axial positions of the coordination polyhedron are occupied by the nitrogen atoms of the pyridine ring of N,N-diethylnicotinamide. The molecules of chelating ligands, coordinated through oxygen atoms, occupy an equatorial position with a *trans* configuration relative to each other. In the crystal, the complex molecules are bound by weak C-H…π interactions and form layers in the (001) plane, alternating with each other. The structure of the coordination polyhedron of the described compound is similar to the structure of adducts of β-dicarbonyl complexes of d-metals with pyridine.

Keywords: nickel, β-dicarbonyl complexes, cyclohexyl acetoacetate, N,N-diethylnicotinamide, crystal structure.

ЛІТЕРАТУРА

1. Vigato P.A., Peruzzo V., Tamburini S. The evolution of β-diketone or β-diketophenol ligands and related complexes, Coord Chem Rev. 2009. **253.** P. 1099–1201. doi:10.1016/j.ccr.2008.07.013.
2. Syamal A. Hexa-coordinated Complexes of Nickel(II) bis(methylacetoacetate) with aromatic heterocyclic amines. *J. Prakt. Chem.* 1969. **311.** P. 884–888. https://doi.org/10.1002/prac.19693110603.
3. Elder R. C. Conformations and crystal packing. The crystal and molecular structure of trans-bis(2,4-pentanedionato)dipyridinenickel(II), Ni(AA)2(py)2. *Inorg. Chem.* 1968. **7** (11). P. 2316–2322. DOI: 10.1021/ic50069a028.
4. Boutebdja M., Beghidja A., Beghidja C. Bis(acetylacetonato-κ2O,O′)bis(pyridine-κN) nickel(II) dehydrate. *Acta Cryst. E,* 2013. **69.** P. 131. https://doi.org/10.1107/S1600536813002699.
5. Harding P., Harding D. J., Phonsri W., Saithong S., Phetmung H. Synthesis and electrochemical studies of octahedral nickel b-diketonate complexes. *Inorg. Chim. Acta*. 2009. **362.** P. 78–82. doi:10.1016/j.ica.2008.03.014.
6. Invernizzi C., Tabacchi G., Seraglia R, Benedet M., Roverso M., Maccato C., Bogialli S., Barreca D., Fois E. On the Fragmentation of Ni(II) β-Diketonate-Diamine Complexes as Molecular Precursors for NiO Films: A Theoretical and Experimental Investigation. *Molecules.* 2024. **29.** 642. https://doi.org/10.3390/molecules29030642.
7. Cosham S.D., Richards S.P., Manning T., Hill M.S., Johnson A.L., Molloy K.C. Precursors for p-type Nickel Oxide: Atmospheric Pressure MOCVD of Nickel Oxide thin films with high work functions. *Eur. J. Inorg. Chem.* 2017. **13.** P. 1868–1876. https://doi.org/10.1002/ejic.201601419.
8. Angelescua E., Pavela O. D., Ionescua R., Birjegab R., Badeac M., Z˘avoianua R. Transition metal coordination polymers MeX_2(4,4 bipyridine) (Me = Co, Ni, Cu; X = Cl^-, CH_3OCO^-, acetylacetonate) selective catalysts for cyclohexene epoxidation with molecular oxygen and isobutyraldehyde. *J. of Mol. Catalysis A: Chemical.* 2012. **352.** P. 21–30.
9. Arakawa M., Suzuki N., Kishi S., Hasegawa M., Satoh K., Horn E., Fukuda Y. Synthesis, Crystal Structure, and Chromotropic Properties of Mixed-Ligand Nickel(II) Complexes with 1,3-Diketonate and P–N Bidentate Ligands. *Bull. Chem. Soc. Jpn.* 2008. **81.** P. 127–135. doi:10.1246/bcsj.81.127.
10. Maitani T., Chikuma M., Tanaka H. Isotropic proton nuclear magnetic resonance shifts of adducts of bis(β-ketoesterato)nickel(II) complexes. *J. Inorg. Nucl. Chem.* 1979. **41.** P. 1115–1120.
11. Ohtsu H., Tanaka K. Equilibrium of Low- and High-Spin States of Ni(II) Complexes Controlled by the Donor Ability of the Bidentate Ligands. *Inorg. Chem.* 2004. **43** (9). P. 3024–3030. https://doi.org/10.1021/ic035486.
12. Petit S., Neugebauer P., Pilet G., Chastanet G., Barra A.-L., Antunes A.B., Wernsdorfer W., Luneau D. Condensation of a Nickel Tetranuclear Cubane into a Heptanuclear Single-Molecule Magnet. *Inorg. Chem.* 2012. **51.** P. 6645–6654. https://pubs.acs.org/doi/10.1021/ic3001637.
13. Sechi M., Bacchi A., Carcelli M., Compari C., Duce E., Fisicaro E., Rogolino D., Gates P., Derudas M., Al-Mawsawi L.Q., Neamati N. From Ligand to Complexes: Inhibition of Human Immunodeficiency Virus Type 1 Integrase by β-Diketo Acid Metal Complexes. *J. Med. Chem.* 2006. **49** (14). P. 4248–4260 https://doi.org/10.1021/jm060193m.
14. Pröhl M, Schubert US, Weigand W, Gottschaldt M. Metal complexes of curcumin and curcumin derivatives for molecular imaging and anticancer therapy. *Coord Chem Rev.*

2016; **307.** P. 32–41.
https://doi.org/10.1016/j.ccr.2015.09.001.

15. Ondrejkovičová I., Galková S., Mroziński J., Kłak J., Lis T., Olejnik Z. New polymeric thiocyanatoiron(II) complex with *N*,*N*′-diethylnicotinamide – Synthesis, structure, magnetic and spectral properties. *Inorg. Chim. Acta*. 2008. **361** (8). P. 2483–2490.
16. Koëse D. A., Necefoglu H., Icbudak H. Synthesis and characterization of N,N-diethylnicotinamide-acetylsalicylato complexes of Co(II), Ni(II), Cu(II), and Zn(II). *J. Coord. Chem.* 2008. **61** (21). P. 3508–3515.
http://dx.doi.org/10.1080/00958970802074555.
17. Çataldağ E., Köse D.A., Özlük G., Şahin O. Novel mixed-ligand metal complexes containing anisic acid/nicotinamide ligands. Their synthesis, structural characterization and biological applications. *Polyhedron*. 2025. **269.** 117410.
https://doi.org/10.1016/j.poly.2025.117410.
18. Yildirim T., Dursun Ali Köse D.A., Avci E., Özer D., Şahin O. Novel mixed ligand complexes of acesulfame / nicotinamide with some transition metals. Synthesis, crystal structural characterization, and biological properties. *J. Mol. Struc.* 2019. **1176.** P. 576–582.
https://doi.org/10.1016/j.molstruc.2018.08.099.
19. Hökelek T., Dal H., Tercan B., Özbek F. E., Necefoğlu H. Diaquabis(2-chlorobenzoato-κO)bis(N,N-diethylnicotinamide-κN^1)nickel(II). *Acta Cryst. E.* 2009. **65.** P. m545–m546.
https://doi.org/10.1107/S1600536809014226.
20. Sertçelik M., Tercan B., Şahin E., Necefoğlu H., Hökelek T. Diaquabis(*N*,*N*-diethylnicotinamide-κN^1)bis(4-formylbenzoato-κ*O*)nickel(II). *Acta Cryst. E.* 2009. **65.** P. m326–m327.
https://doi.org/10.1107/S1600536809006345.
21. Hökelek T., Süzen Y., Tercan B., Aybirdi Ö., Necefoğlu H. Diaquabis(*N*,*N*-diethylnicotinamide-κN^1)bis[4-(dimethylamino)benzoato-κ*O*]nickel(II). *Acta Cryst. E.* 2009. **65.** P. m1015–m1016.
https://doi.org/10.1107/S1600536809030098.
22. Köse D. A., Gökçe G., Gökçe S., Uzun I. bis(N,N-diethylnicotinamide) p-chlorobenzoate complexes of Ni(II), Zn(II) and Cd(II). Synthesis and characterization. *J. Therm. Analysis and Calorimetry*. 2009. **95** (1). P. 247–251. DOI: 10.1007/s10973-008-9150-8.
23. Çataldağ E., Köse D.A., Özlük G., Şahin O. Novel heteroleptic metal cation complexes of anisic acid/N,N-diethylnicotinamide ligands and biological applications. *J. Mol. Struc.* 2026. **1357.** 145219.
https://doi.org/10.1016/j.molstruc.2025.145219.
24. Штоквиш О., Коваль Л., Дьяконенко В., Хоменко Б., Пехньо В. Синтез та кристалічна структура комплексів кобальту(II) та нікелю(II) з циклогексилацетоацетатом і піридином. *Chem. Met. Alloys.*2021. **14.** P. 38–42.
25. Штоквиш О. О., Коваль Л. І., Пехньо В. І. Синтез та дослідження комплексів кобальту (II) з естерами ацетооцтової кислоти первинних, вторинних і третинних спиртів. *Укр. хім. журн.* 2015. **81** (12). С. 92–98.
26. Накамото К. ИК-спектры и спектры КР неорганических и координационных соединений. М.: Мир, 1991. 536 с.
27. Dolomanov O.V., Bourhis L.J., Gildea R.J., Howard J.A.K., Puschmann H. Olex2: A complete structure solution, refinement and analysis program. *J. Appl. Cryst*. 2009. **42.** P. 339–341.
https://doi.org/10.1107/S0021889808042726.
28. Sheldrick G.M., SHELXT-Integrated space-group and crystal-structure determination. *Acta Cryst.* 2015. **A71.** P. 3–8.
https://doi.org/10.1107/ S2053273314026370.
29. Sheldrick G.M. Crystal structure refinement with SHELXL. *Acta Cryst.* 2015. **C71.** P. 3–8.
https://doi.org/10.1107/S2053229614024218.

REFERENCES

1. Vigato P.A., Peruzzo V., Tamburini S. The evolution of β-diketone or β-diketophenol ligands and related complexes, Coord Chem Rev. 2009. **253**: 1099–1201. doi:10.1016/j.ccr.2008.07.013.
2. Syamal A. Hexa-coordinated Complexes of Nickel(II) bis(methylacetoacetate) with aromatic heterocyclic amines. *J. Prakt. Chem.* 1969. **311:** 884–888. https://doi.org/10.1002/prac.19693110603.
3. Elder R. C. Conformations and crystal packing. The crystal and molecular structure of trans-bis(2,4-pentanedionato)dipyridinenickel(II), Ni(AA)2(py)2. *Inorg. Chem.* 1968. **7** (11): 2316–2322. DOI: 10.1021/ic50069a028.
4. Boutebdja M., Beghidja A., Beghidja C. Bis-(acetylacetonato-κ2O,O′)bis(pyridine-κN) nickel(II) dehydrate. *Acta Cryst. E,* 2013. **69:** m131. https://doi.org/10.1107/S1600536813002699.
5. Harding P., Harding D. J., Phonsri W., Saithong S., Phetmung H. Synthesis and electrochemical studies of octahedral nickel b-diketonate complexes. *Inorg. Chim. Acta*. 2009. **362**: 78–82. doi:10.1016/j.ica.2008.03.014.
6. Invernizzi C., Tabacchi G., Seraglia R, Benedet M., Roverso M., Maccato C., Bogialli S., Barreca D., Fois E. On the Fragmentation of Ni(II) β-Diketonate-Diamine Complexes as Molecular Precursors for NiO Films: A Theoretical and Experimental Investigation. *Molecules*. 2024. **29:** 642. https://doi.org/10.3390/molecules29030642.
7. Cosham S.D., Richards S.P., Manning T., Hill M.S., Johnson A.L., Molloy K.C. Precursors for p-type Nickel Oxide: Atmospheric Pressure MOCVD of Nickel Oxide thin films with high work functions. *Eur. J. Inorg. Chem.* 2017. **13**: 1868–1876. https://doi.org/10.1002/ejic.201601419.
8. Angelescua E., Pavela O. D., Ionescua R., Birjegab R., Badeac M., Z˘avoianua R. Transition metal coordination polymers MeX_2(4,4 bipyridine) (Me = Co, Ni, Cu; X = Cl^-, CH_3OCO^-, acetylacetonate) selective catalysts for cyclohexene epoxidation with molecular oxygen and isobutyraldehyde. *J. of Mol. Catalysis A: Chemical.* 2012. **352**: 21–30.
9. Arakawa M., Suzuki N., Kishi S., Hasegawa M., Satoh K., Horn E., Fukuda Y. Synthesis, Crystal Structure, and Chromotropic Properties of Mixed-Ligand Nickel(II) Complexes with 1,3-Diketonate and P–N Bidentate Ligands. *Bull. Chem. Soc. Jpn.* 2008. **81:** 127–135. doi:10.1246/bcsj.81.127.
10. Maitani T., Chikuma M., Tanaka H. Isotropic proton nuclear magnetic resonance shifts of adducts of bis(β-ketoesterato)nickel(II) complexes. *J. Inorg. Nucl. Chem.* 1979. **41:** 1115–1120.
11. Ohtsu H., Tanaka K. Equilibrium of Low- and High-Spin States of Ni(II) Complexes Controlled by the Donor Ability of the Bidentate Ligands. *Inorg. Chem.* 2004. **43** (9): 3024–3030. https://doi.org/10.1021/ic035486.
12. Petit S., Neugebauer P., Pilet G., Chastanet G., Barra A.-L., Antunes A.B., Wernsdorfer W., Luneau D. Condensation of a Nickel Tetranuclear Cubane into a Heptanuclear Single-Molecule Magnet. *Inorg. Chem.* 2012. **51**: 6645–6654. https://pubs.acs.org/doi/10.1021/ic3001637.
13. Sechi M., Bacchi A., Carcelli M., Compari C., Duce E., Fisicaro E., Rogolino D., Gates P., Derudas M., Al-Mawsawi L.Q., Neamati N. From Ligand to Complexes: Inhibition of Human Immunodeficiency Virus Type 1 Integrase by β-Diketo Acid Metal Complexes. *J. Med. Chem.* 2006. **49 (14)**: 4248–4260. https://doi.org/10.1021/jm060193m.
14. Pröhl M, Schubert US, Weigand W, Gottschaldt M. Metal complexes of curcumin and curcumin derivatives for molecular imaging and anticancer therapy. *Coord Chem Rev.* 2016; **307.** P. 32–41. https://doi.org/10.1016/j.ccr.2015.09.001

15. Ondrejkovičová I., Galková S., Mroziński J., Kłak J., Lis T., Olejnik Z. New polymeric thiocyanatoiron(II) complex with *N*,*N*′-diethylnicotinamide – Synthesis, structure, magnetic and spectral properties. *Inorg. Chim. Acta*. 2008. **361 (8)**: 2483–2490.
16. Koëse D. A., Necefoglu H., Icbudak H. Synthesis and characterization of N,N-diethylnicotinamide-acetylsalicylato complexes of Co(II), Ni(II), Cu(II), and Zn(II). *J. Coord. Chem.* 2008. **61 (21):** 3508–3515. http://dx.doi.org/10.1080/00958970802074555.
17. Çataldağ E., Köse D.A., Özlük G., Şahin O. Novel mixed-ligand metal complexes containing anisic acid/nicotinamide ligands. Their synthesis, structural characterization and biological applications. *Polyhedron*. 2025. **269:** 117410. https://doi.org/10.1016/j.poly.2025.117410.
18. Yildirim T., Dursun Ali Köse D.A., Avci E., Özer D., Şahin O. Novel mixed ligand complexes of acesulfame / nicotinamide with some transition metals. Synthesis, crystal structural characterization, and biological properties. *J. Mol.r Struc.* 2019. **1176:** 576–582. https://doi.org/10.1016/j.molstruc.2018.08.099.
19. Hökelek T., Dal H., Tercan B., Özbek F. E., Necefoğlu H. Diaquabis(2-chlorobenzoato-κO) bis(N,N-diethylnicotinamide-κN^1)nickel(II). *Acta Cryst. E.* 2009. **65:** m545–m546. https://doi.org/10.1107/S1600536809014226.
20. Sertçelik M., Tercan B., Şahin E., Necefoğlu H., Hökelek T. Diaquabis(*N*,*N*-diethylnicotinamide-κ*N*^{1})bis(4-formylbenzoato-κ*O*)nickel(II). *Acta Cryst. E.* 2009. **65:** m326–m327. https://doi.org/10.1107/S1600536809006345.
21. Hökelek T., Süzen Y., Tercan B., Aybirdi Ö., Necefoğlu H. Diaquabis(*N*,*N*-diethylnicotinamide-κ*N*^{1})bis[4-(dimethylamino)benzoato-κ*O*]nickel(II). *Acta Cryst. E.* 2009. **65:** m1015–m1016. https://doi.org/10.1107/S1600536809030098.
22. Köse D. A., Gökçe G., Gökçe S., Uzun I. bis-(N,N-diethylnicotinamide) p-chlorobenzoate complexes of Ni(II), Zn(II) and Cd(II). Synthesis and characterization. *J. Therm. Analysis and Calorimetry*. 2009. **95 (1):** 247–251. DOI: 10.1007/s10973-008-9150-8.
23. Çataldağ E., Köse D.A., Özlük G., Şahin O. Novel heteroleptic metal cation complexes of anisic acid/N,N-diethylnicotinamide ligands and biological applications. *J. Mol. Struc.* 2026. **1357:** 145219. https://doi.org/10.1016/j.molstruc.2025.145219.
24. Shtokvysh O., Koval L., Dyakonenko V., Homenko B., Pekhnyo V. Syntes ta krystalichna struktura kompleksiv kobaltu (II) ta nikel'u (II) z cycloheksylacetoacetatom i pirydynom. *Chem. Met. Alloys.* 2021. **14:** 38–42. (*in Ukrainian*).
25. Shtokvysh O.O., Koval L.I., Pekhnyo V.I. Syntes ta doslidzhennia kompleksiv kobaltu (II) z esteramy atsetootsotovoi kysloty pervynnykh, vtorynnykh i tretynnykh spyrtiv. Ukr. khim. zhurn. 2015. **81** (12): 92–98. (*in Ukrainian*).
26. Nakamoto K. Infrared and Raman Spectra of Inorganic and Coordination Compounds. M.: Mir, 1991. 536 p. (*in Russian*).
27. Dolomanov O.V., Bourhis L.J., Gildea R.J., Howard J.A.K., Puschmann H. Olex2: A complete structure solution, refinement and analysis program. *J. Appl. Cryst*. 2009. **42**: 339–341. https://doi.org/10.1107/S0021889808042726.
28. Sheldrick G.M., SHELXT-Integrated space-group and crystal-structure determination. *Acta Cryst.* 2015. **A71**: 3–8. https://doi.org/10.1107/ S2053273314026370.
29. Sheldrick G.M. Crystal structure refinement with SHELXL. *Acta Cryst.* 2015. **C71**: 3–8. https://doi.org/10.1107/S2053229614024218.

Стаття надійшла: 24.02.2026
Стаття прийнята до друку: 05.03.2026
Стаття опублікована:25.03.2026

УДК 615.07: 543.544 doi: 10.33609/2708-129X.92.2.2026.13-25

ВАЛІДАЦІЯ ВЕРХ-МЕТОДИКИ ВИЗНАЧЕННЯ РИВАРОКСАБАНУ ДЛЯ ПОРІВНЯЛЬНИХ ДОСЛІДЖЕНЬ СТУПЕНЯ ВИЛУЧЕННЯ ПРИ ВИВЧЕННІ ДОСТАВКИ ЛІКАРСЬКОГО ЗАСОБУ ЧЕРЕЗ НАЗОГАСТРАЛЬНИЙ ЗОНД *IN VITRO*

***А. В. Єгорова*[1],** https://orcid.org/0000-0002-6979-553X
***О. В. Сисенко*[2],** https://orcid.org/0009-0009-7150-9879
***Ю. В. Скрипинець*[1],** https://orcid.org/0000-0001-5826-1914
***І. І. Чеботарська*[1],** https://orcid.org/0000-0003-2116-9166
***Д. І. Александрова*[1],** https://orcid.org/0000-0002-8443-0221
***С. М. Кашуцький*[2] ,** https://orcid.org/0000-0001-8075-757X

[1]Фізико-хімічний інститут ім. О. В. Богатського НАН України, Люстдорфська дорога, 86, Одеса 65080, Україна;
[2]ТДВ «ІНТЕРХІМ», Люстдорфська дорога, 86, Одеса 65080, Україна,
e-mail: yegorovalla@gmail.com

Валідовано ВЕРХ-методику кількісного визначення ривароксабану, придатну для дослідження повноти вилучення лікарського засобу «РИВАРОКСАБАН», таблетки по 20 мг після доставки через назогастральний зонд за показниками: специфічність, точність, правильність, лінійність у вивченому діапазоні концентрацій. Підтверджено стабільність випробовуваних розчинів та порівняння розчинів у разі їхнього зберігання за кімнатної температури протягом 8 год.

Проведено моніторинг повноти вилучення ривароксабану після суспендування у середовищі (деіонізованій воді) розтертих таблеток досліджуваного та референтного лікарських засобів та їхньої доставки через назогастральний зонд. Встановлено, що понад 90 % ривароксабану вилучається після ентерального введення, а препарати є еквівалентними за варіабельністю ступеня вилучення.

Ключові слова: ривароксабан, високоефективна рідинна хроматографія, назогастральний зонд, валідація.

ВСТУП. Ентеральне введення ліків через зонд є кращим методом для пацієнтів, які не можуть безпечно їх ковтати. Для назогастрального введення перевагу надають рідким формам. Перед застосуванням твердих форм слід оцінити можливість їхнього подрібнення та суспендування. Ефективність доставки лікарських засобів через назогастральний (НГ) зонд визначається правильним вибором лікарської форми, характеристиками трубки, усуванням ризику закупорювання зондів. Також необхідно

підтверджувати, що генеричний лікарський засіб є терапевтично еквівалентним до референтного, визначаючи повноту його вилучення [1]. Для цього необхідно розробляти аналітичні методики кількісного визначення препаратів.

В останні роки зросла кількість публікацій з вивчення ефективності доставки деяких лікарських препаратів через НГ-зонд, що є необхідним для фармацевтичного досьє та промислового випуску. В цих роботах розглядають подібність між схемами прийому інтактних і подрібнених таблеток та встановлюють вивільнення лікарських препаратів різними аналітичними методами [2–5].

Для цих досліджень важливою є валідація аналітичних методик – невід'ємна частина належної виробничої практики (GMP), яка гарантує, що вибрана методика буде давати відтворювані та достовірні результати відповідно до поставлених цілей. Набір досліджуваних валідаційних характеристик залежить від призначення аналітичної методики. Типові валідаційні характеристики – це правильність, точність, збіжність, внутрішньолабораторна точність, специфічність, межа виявлення, межа кількісного визначення, лінійність, діапазон застосування [6].

У порівняльних випробуваннях *in vitro* потрібно провести дослідження, виконуючи по 12 або 6 тестів для досліджуваного та референтного лікарських засобів, суспендованих в обраному середовищі в початковій точці (0 хвилин) та протягом максимально допустимого обраного часу змочування відповідно.

Ривароксабан 5-хлоро-N-[[(5S)-2-оксо-3-[4-(3-оксоморфолін-4-іл)феніл]-1,3-оксазолідин-5-іл]метил]тіофен-2-карбоксамід – представник класу прямих антикоагулянтів.

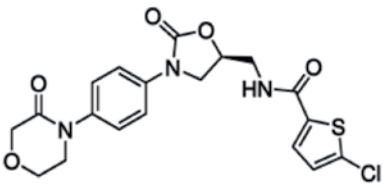

(1S,2S,3R,5S)-3-[7-[[(1R,2S)-2-(3,4-дифторфеніл)циклопропіл]аміно]-5-(пропілсульфаніл)-3H-[1,2,3]триазоло[4,5-d]піримідин-3-іл]-5-(2-гідроксиетокси)циклопентан-1,2-діол

Основна дія – гальмування перетворення протромбіну в тромбін, внаслідок чого проходить блокування як внутрішнього, так і зовнішнього каскаду зсідання крові. Застосовують для лікування гострих тромбозів глибоких вен нижніх кінцівок або тромбоемболії легеневої артерії.

Необхідно було провести валідацію ВЕРХ-методики кількісного визначення ривароксабану, для дослідження ступеня вилучення, готового лікарського засобу «РИВАРОКСАБАН», таблетки, вкриті плівковою оболонкою, по 20 мг, за показниками: специфічність, точність, правильність, лінійність у вивченому діапазоні концентрацій відповідно до вимог Державної Фармакопеї України [6]. Провести моніторинг повноти вилучення генеричного та референтного препаратів після доставки через назогастральний зонд для вивчення біоеквівалентності.

ЕКСПЕРИМЕНТ І ОБГОВОРЕННЯ РЕЗУЛЬТАТІВ. У роботі використовували реактиви кваліфікації не нижче ч. д. а. Для приготування розчинів застосовували деіонізовану воду (воду для хроматографії). У роботі використовували робочий стандартний зразок (РСЗ) ривароксабану (ТДВ «ІНТЕРХІМ»).

У роботі використовували ваги лабораторні електронні AUX220 (SHIMADZU, Японія) і магнітну мішалку ARE (VELP Scientifica, Італія).

Воду для хроматографії отримували з використанням системи очищення води arium® pro UV фірми Sartorius.

pH розчинів вимірювали на pH-метрі серії Seven Easy фірми Mettler Toledo.

Об'єктом дослідження був препарат «РИВАРОКСАБАН», таблетки, вкриті плівковою оболонкою, по 20 мг (виробник – ТДВ «ІНТЕРХІМ», Україна) та референтний препарат «КСАРЕЛТО»,® таблетки, вкриті плівковою оболонкою, по 20 мг (Байєр АГ).

Умови проведення дослідження зазначено у FDA Draft Guidance on Rivaroxaban [7], інструкції для медичного застосування референтного препарату «КСАРЕЛТО»®: кількість таблеток – 1 шт; дозування – 20 мг; середовище для суспендування – деіонізована вода (вода для хроматографії); об'єм – 50,0 мл; друга часова точка – час змочування 240 хв; пероральний шприц – трикомпонентний одноразовий стерильний з поліпропілену. Назогастральний зонд: матеріал полівінілхлорид, розмір трубки – 8; внутрішній діаметр – 2,7 мм; довжина 1200 мм.

Хроматограми реєстрували на рідинному хроматографі 1260 Infinity з УФ-детектором (Agilent Technologies, США).

1. *Випробовуваний розчин 1 для часу змочування 0 хв*

Готують суспензію так: подрібнюють 1 таблетку (20 мг) за допомогою ступки та товкача протягом 60 секунд, додають 30 мл води для хроматографії, та перемішують упродовж

60 секунд за допомогою товкача, набирають суспензію в шприц. Додають у ступку 20 мл води для хроматографії, перемішують суспензію за допомогою товкача, набирають суспензію в шприц і перемішують її протягом 15 секунд. Проводять введення суспензії через шприц у трубку НГ-зонду. Збирають суспензію в контейнер для збору (мірний стакан). У стакані вимірюють pH суспензії після проходження через НГ-зонд, переносять суспензію у мірну колбу на 200,0 мл. Промивають електрод у 5 мл води для хроматографії над ступкою, далі додають 15 мл води для хроматографії, обмивають мірний стакан, товкач і ступку. Обмивши посуд, промивні води зі ступки набирають у шприц, проштовхують через шприц у трубку НГ-зонду для додаткового промивання, збирають промивні води у мірну колбу на 200,0 мл. Загальна кількість використаної води – 70 мл.

2. *Випробовуваний розчин 1 для часу змочування 240 хв*

Приготовану суспензію набирають у шприц, залишають на 240 хвилин у горизонтальному положенні у стані спокою. Промивні води (10 мл) наливають у ступку з товкачем та залишають на 240 хвилин. По закінченню часу ретельно перемішують суспензію в шприці протягом 15 секунд, проштовхують її через шприц в трубку НГ-зонду, далі в контейнер для збору (мірний стакан). У стакані вимірюють pH суспензії після проходження через НГ- зонд, переносять суспензію у мірну колбу на 200,0 мл.

Промивають електрод 5 мл води для хроматографії над ступкою, далі додають 5 мл води для хроматографії, обмивають мірний стакан, товкач і ступку. Обмивши посуд, промивні води зі ступки набирають у шприц, проштовхують через шприц в трубку НГ-зонду для додаткового промивання,

збирають промивні води у мірну колбу на 200,0 мл. Загальна кількість використаної води – 70 мл.

Методика визначення

Випробовуваний розчин 2. До випробовуваного розчину 1 додають 8,0 мл розчину А1, 120 мл ацетонітрилу, перемішують упродовж 30 хв на магнітній мішалці, доводять об'єм розчину водою для хроматографії до об'єму 200,0 мл та перемішують. Одержаний розчин фільтрують крізь мембранний фільтр (0,20 мкм; RC 25).

20,0 мг РСЗ ривароксабану поміщають у мірну колбу місткістю 100,0 мл, додають

75 мл суміші розчинників, перемішують упродовж 30 хв на магнітній мішалці та доводять об'єм розчину сумішшю розчинників до позначки та перемішують.

5,0 мл одержаного розчину доводять сумішшю розчинників до 10,0 мл та перемішують. Одержаний розчин фільтрують крізь мембранний фільтр (0,20 мкм; RC 25) (розчин порівняння).

Розчин А. 0,67 мл фосфорної кислоти доводять до 1000 мл водою для хроматографії.

Розчин А1. 6,7 мл фосфорної кислоти доводять до 1000 мл водою для хроматографії.

Суміш розчинників: розчин А : ацетонітрил (40 : 60 об/об).

Розчини використовують свіжоприготованими.

Хроматографування проводять на рідинному хроматографі з УФ-детектором у ізократичному режимі за таких умов:

- колонка з нержавіючої сталі розміром 0,10 м × 4,6 мм, заповнена силікагелем для хроматографії октадецилсилільним Р, (3,5 мкм);
- температура колонки: 45 °С;
- рухома фаза А: ацетонітрил : розчин А (8:92 об/об) (70%);
- рухома фаза В: ацетонітрил (30%);
- швидкість рухомої фази: 1,0 мл/хв;
- детектування за довжини хвилі: 250 нм;
- об'єм інжекції: 10 мкл;
- час хроматографування: 5 хв.

Хроматографують випробовуваний розчин та розчин порівняння.

Вміст ривароксабану (X) у випробовуваному розчині 2, в міліграмах, обчислюють за формулою:

$$X = \frac{S \cdot m_0 \cdot 200 \cdot 5 \cdot P}{S_0 \cdot 100 \cdot 10 \cdot 100} \cdot \left(1 - \frac{W}{100}\right) = \frac{S \cdot m_0 \cdot P}{S_0 \cdot 100} \cdot \left(1 - \frac{W}{100}\right),$$

де: S – площа піка ривароксабану на хроматограмі випробовуваного розчину;

S_0 – площа піка ривароксабану на хроматограмі розчину порівняння;

m_0 – маса наважки РСЗ ривароксабану, у міліграмах;

P – вміст основної речовини в РСЗ ривароксабану, у відсотках;

W – вміст вологи в РСЗ ривароксабану, у відсотках.

Ступінь вилучення

Ступінь вилучення (RF) ривароксабану, у відсотках, обчислюють за формулою:

$$RF = \frac{X \cdot 100}{1 \cdot B},$$

де: X – вміст ривароксабану у випробовуваному розчині, в міліграмах;

B – середній вміст ривароксабану у таблетці (за результатами тесту «Кількісне визначення»), у міліграмах;

1 – кількість таблеток на одне визначення, шт.

ISSN 2708-129X. Укр. хім. журн., 2026

Специфіка методу полягає в можливості достовірно визначати вміст ривароксабану в таблетці за присутності допоміжних речовин, її досягають шляхом використання зовнішніх стандартів. При розробленні методики було встановлено, що допоміжні речовини не заважають визначенню основної речовини.

На хроматограмі випробовуваного розчину час утримування піка ривароксабану (рисунок 1) збігається з часом утримування піка ривароксабану на хроматограмі розчину порівняння (рисунок 2), що підтверджує ідентичність ривароксабану у лікарському засобі «РИВАРОКСАБАН», таблетки, вкриті плівковою оболонкою, по 20 мг та в розчині порівняння.

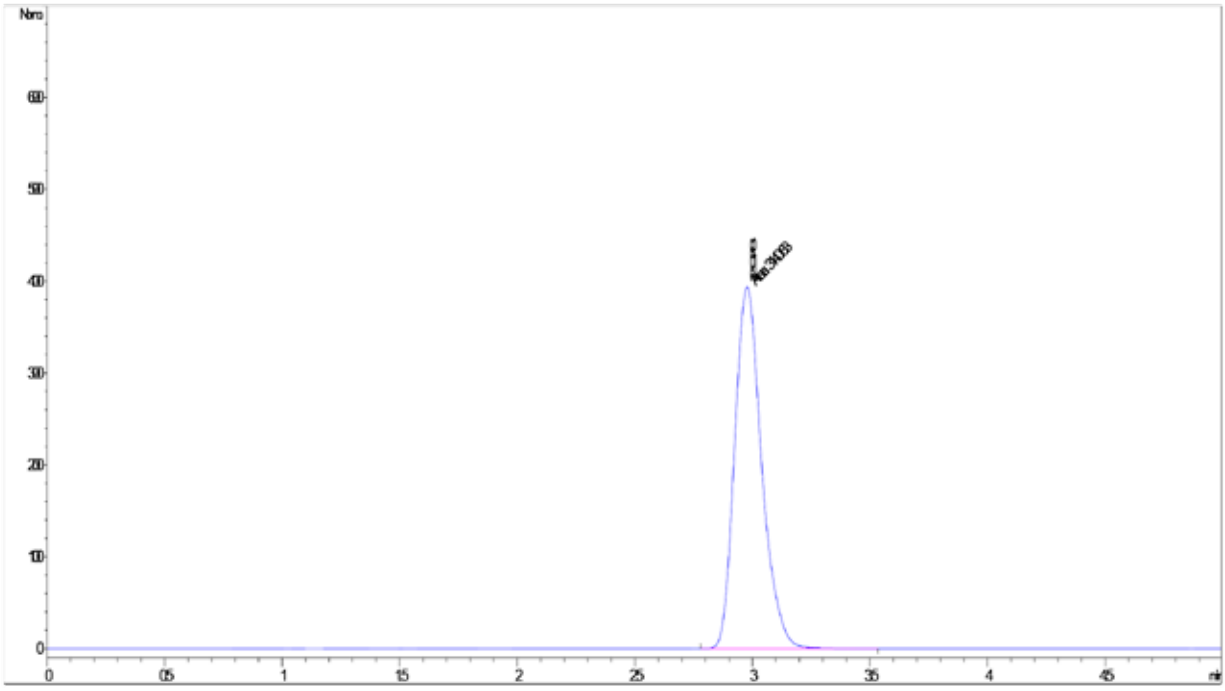

Рис. 1. Хроматограма випробовуваного розчину

Fig. 1. Chromatogram of the test solution.

Лінійна залежність методу характеризує здатність отримання аналітичних сигналів, прямопропорційних вмісту визначуваних речовин у випробовуваному зразку. Лінійність методики оцінювали в діапазоні від 50 % до 130 %. Як 100 % точку обрано концентрацію 0,2 мг/мл.

Побудова градуювального графіка

Вихідний розчин РСЗ ривароксабану. 50 мг *РСЗ ривароксабану* поміщають у мірну колбу місткістю 50,0 мл, додають 30 мл суміші розчинників, перемішують упродовж 30 хв на магнітній мішалці, доводять об'єм розчину тим самим розчинником до позначки та перемішують.

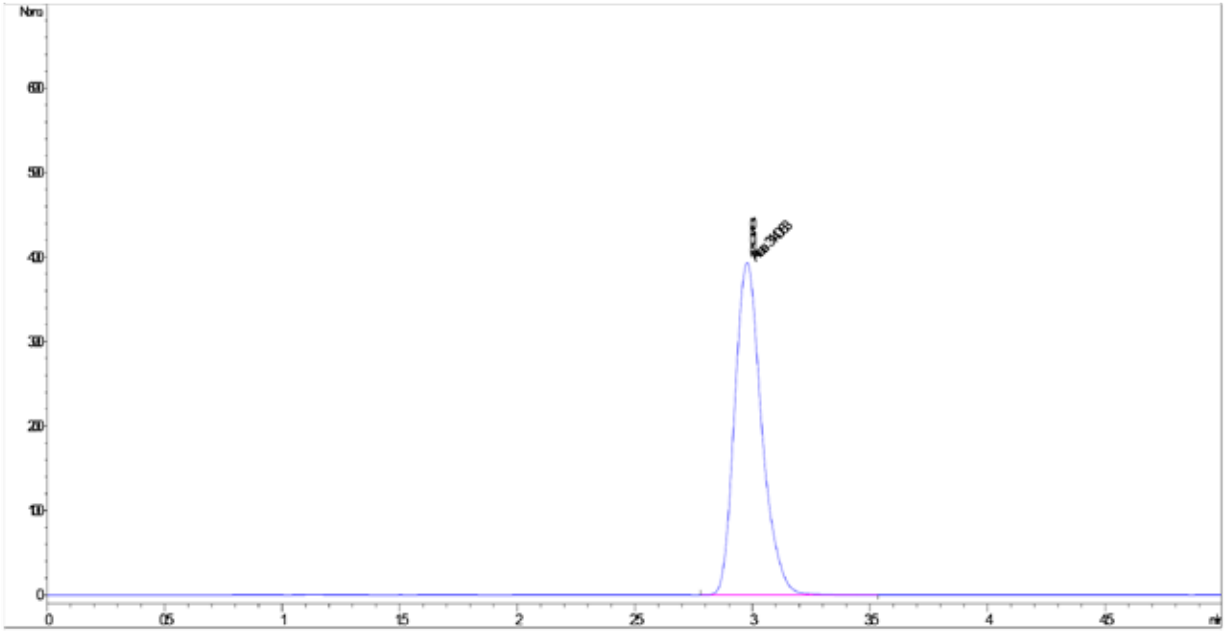

Рис. 2. Хроматограма розчину порівняння

Fig. 2. Chromatogram of the reference solution.

Випробовувані розчини. У мірні колби місткістю 25,0 мл вносять 2,5; 3,5; 3,75; 4,0; 4,5; 5,0; 5,5; 6,0 і 6,5 мл вихідного розчину *РСЗ ривароксабану*, доводять об'єми розчинів сумішшю розчинників до позначки та перемішують. Одержані розчини фільтрують крізь мембранні фільтри (0,20 мкм; RC).

Розчини використовують свіжоприготованими.

Результати представлено графічно у вигляді залежності площі піка ривароксабану від концентрації в нормалізованих координатах.

У нормалізованих координатах вміст ривароксабану *(X)*, у відсотках, обчислювали за формулою:

$$X = \frac{C_n \cdot 100\%}{C_0},$$

де: C_n – концентрація ривароксабану в n-ом аналітичному розчині;

C_0 – концентрація ривароксабану в розчині порівняння.

Площу піка ривароксабану *(S)*, у відсотках, обчислювали за формулою:

$$S = \frac{S_n \cdot 100\%}{S_0},$$

де: S_n – площа піка ривароксабану на хроматограмі n-ого аналітичного розчину;

S_0 – площа піка ривароксабану на хроматограмі розчину порівняння.

На рисунку 3 представлено лінійну залежність для визначення ривароксабану, яку описують рівнянням:

$$S = - 0{,}34958 + 1{,}00646 \cdot x,$$

де: *x* – вміст ривароксабану в розчині, у відсотках;

S – площа піка ривароксабану, у відсотках.

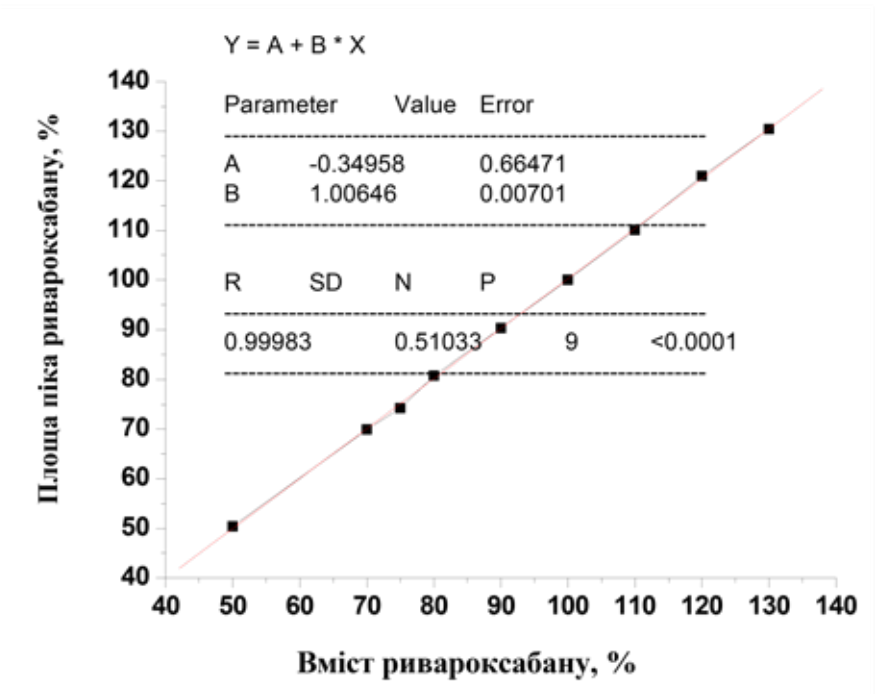

Рис. 3. Лінійна залежність площі піка від концентрації в нормалізованих координатах для визначення ривароксабану

Fig. 3. Linear dependence of peak area on concentration in normalized coordinates for the determination of rivaroxaban.

Табл. 1

Метрологічні характеристики лінійної залежності

Table 1.

Metrological characteristics of linear dependence.

Величина	Значення	Допуски		Висновок
b	1,00646	Близько до 1		відповідає
|a|	0,34958	статистич.	≤1,26	відповідає
		практич.	≤1,02	відповідає
R	0,99983	≥ 0,99946		відповідає

Метрологічні характеристики лінійної залежності для визначення ривароксабану наведено в таблиці 1.

Правильність оцінювали за результатами аналізу таблеток (три наважки по три паралельних визначення) з різних наважок.

Результати кількісного визначення ривароксабану в інтервалі вмісту від 14 мг до 26 мг (70–130 % від 20 мг) у модельних сумішах, що відповідають складу лікарського засобу «РИВАРОКСАБАН», таблетки, вкриті плівковою оболонкою, по 20 мг представлено в таблиці 2.

Вміст ривароксабану, у міліграмах, досягали введенням в модельні суміші різних наважок АФІ ривароксабану.

Табл. 2

Результати визначення ривароксабану в модельних сумішах

Table 2.

Results of rivaroxaban determination in model mixtures.

Введено X_i, мг	Знайдено Y_i, мг	$Z_i = Y_i/X_i \cdot 100$ %
14,03	13,8294	98,57
14,06	14,0234	99,74
14,05	13,9390	99,21
20,00	19,7980	98,99
20,02	20,1161	100,48
20,05	20,2385	100,94
26,06	26,0913	100,12
26,04	25,8890	99,42
26,02	25,7910	99,12
	середнє $\overline{Z}$, %	99,62
	S_Z, %	0,77
	$\delta\% = \lvert\overline{Z} - 100\rvert$	0,38

Величина	Значення	Критерій		Висновок
d %	0,38	статистич.	≤ 0,48	Відповідає
		практич.	≤ 0,51	Відповідає

ISSN 2708-129X. Укр. хім. журн., 2026

Як видно з наведених розрахунків, усі вимоги до статистичної та практичної незначущості систематичної похибки виконано. Таким чином, правильність методики відповідає необхідним вимогам.

Внутрішньолабораторну прецизійність було оцінено за результатами визначення та метрологічними характеристиками методики кількісного визначення ривароксабану, зроблену в різні дні одним аналітиком (таблиця 3).

Табл. 3

Результати визначення та метрологічні характеристики методики кількісного визначення ривароксабану (f = 5; P = 0,95; t (P, f) = 2,57)

Table 3.

Results of determination and metrological characteristics ofthe method for quantitative determination of rivaroxaban (f = 5; P = 0.95; t (P, f) = 2.57).

№ п/п	x_i, мг	$\overline{X}$, мг	S^2	S	$\Delta\overline{X}$, мг	$\varepsilon=\frac{\Delta\overline{X}}{\overline{X}}\cdot 100$, %
1 день	19,17 19,55 19,32 19,36 19,54 19,75 19,39	19,4483	0,0423	0,2057	0,2158	1,11
2 день	19,41 19,42 19,34 19,17 19,37	19,3500	0,0086	0,0927	0,0973	0,50

Для результатів, наведених в таблиці 3: m =2; f =10; t =2,23.

$$S_0=\sqrt{\frac{0,0423+0,0086}{2}}=0,16$$

$$|19,4483-19,3500|\le\sqrt{2}\cdot 2,23\cdot\frac{0,16}{\sqrt{6}}$$

$$0,0983 \le 0,2052$$

Наведені розрахунки свідчать про задовільну внутрішньолабораторну прецизійність.

Результати порівняльного дослідження ступеня вилучення при вивченні доставки досліджуваного та референтного лікарських засобів через назогастральний зонд наведено в таблиці 4.

Табл. 4

Результати порівняльного дослідження ступеня вилучення при вивченні доставки лікарського засобу через НГ-зонд

Table 4.

Results of a comparative study of the degree of extraction in the study of drug delivery through an NG tube.

Препарат	Початковий pH води (середнє)	Ступінь вилучення (*RF*), %		
		статистичний показник (n = 12)	час змочування	
			0 хв	240 хв
Досліджуваний	5,95 (0 хв)	арифметичне середнє	97,86	98,03
		мінімальне	95,13	90,85
	6,08 (240 хв)	максимальне	101,40	118,50
		CV, %	1,85	7,56
Референтний	5,93 (0 хв)	арифметичне середнє	98,16	100,88
		мінімальне	93,25	94,02
	6,04 (240 хв)	максимальне	110,93	119,68
		CV, %	6,07	7,88

Точкова оцінка *RGM*, коефіцієнт варіації *CV* та 90 % довірчий інтервал відношення середньогеометричних значень ступенів вилучення досліджуваного та референтного препаратів ривароксабану наведено у таблиці 5.

Табл. 5

Точкова оцінка *RGM*, коефіцієнт варіації *CV* та 90 % довірчий інтервал відношення середньогеометричних значень ступеня вилучення при вивченні доставки досліджуваного та референтного лікарських засобів через назогастральний зонд (рівень значущості 5 %, *df* = 20)

Table 5.

RGM point estimate, CV coefficient of variation and 90% confidence interval of the ratio of geometric mean values of the degree of extraction in the study of delivery of test and reference drugs via nasogastric tube (significance level 5%, *df* = 20).

Час змочування	Точкова оцінка *RGM*, %	Коефіцієнт варіації *CV*, %	Межі 90%-го довірчого інтервалу, %	
0 хв	100,84	1,70	Нижня межа, *LL* %	96,89
			Верхня межа, *LU* %	104,95
240 хв	98,99	2,06	Нижня межа, *LL* %	92,50
			Верхня межа, *LU* %	105,95

Значення нижньої та верхньої меж 90 % довірчих інтервалів для двох етапів дослідження (час змочування 0 хв та 240 хв) задовольняють вимогам (80,00 %; 125,00 %) на рівні значущості 5 %. Тобто, досліджуваний та референтний препарати ривароксабану є еквівалентними за ступенем вилучення при доставці через НГ-зонд.

ВИСНОВКИ. За результатами валідації встановлено, що наведена методика є специфічною, характеризується коректною правильністю, прецизійністю, лінійною залежністю у вивченому діапазоні концентрацій, що дозволяє використовувати її для проведення порівняльних досліджень ступеня вилучення при вивченні доставки лікарського засобу через назогастральний зонд *in vitro.*

Проведені дослідження підтвердили, що досліджуваний препарат «РИВАРОКСАБАН» та референтний препарат «КСАРЕЛТО»® забезпечують понад 90 % вилучення активної речовини після суспендування у воді та введення через назогастральний зонд. Такий рівень переходу свідчить про низький ризик закупорювання або непрохідності зонда.

Отримані результати демонструють еквівалентність препаратів за варіабельністю ступеня вилучення, що підтверджує їхню взаємозамінність у клінічній практиці при застосуванні НГ-зонда й забезпечує стабільність та відтворюваність доставки «Ривароксабану» пацієнтам, які не можуть приймати препарат перорально.

Роботу виконано в межах держбюджетної теми «Застосування аналітичних методів для оцінки in vitro ефективності доставки деяких лікарських препаратів через назогастральний зонд», державний реєстраційний номер: 0125U000370.

ДЕТАЛІЗАЦІЯ ВКЛАДУ АВТОРІВ У ПІДГОТОВЦІ РУКОПИСУ. Автори роботи зробили рівнозначний внесок у розроблення концепції та дизайну дослідження, збір, систематизацію, аналіз та інтерпретацію отриманих даних. Автори брали участь у підготовці та редагуванні статті. Усі автори ознайомилися з результатами дослідження та схвалили остаточну версію статті.

VALIDATION OF HPLC METHOD FOR THE DETERMINATION OF RIVAROXABAN FOR COMPARATIVE EXTRACTION IN STUDYING THE DELIVERY OF THE DRUG VIA NASOGASTRIC TUBE *IN VITRO.*

A.V. Yegorova[1], O.V. Sysenko[2], Yu.V. Skrypynets[1], I.I. Chebotarska[1], D.I. Aleksandrova[1], S.N. Kashutskyy[2]

[1]A.V. Bogatsky Physico-Chemical Institute of the National Academy of Sciences of Ukraine, 86 Lustdorfska doroga, 65080 Odesa, Ukraine; [2]"INTERCHEM", 86 Lustdorfska doroga, 65080 Odesa, Ukraine
e-mail: yegorovalla@gmail.com

Enteral administration of drugs via a tube is the preferred method for patients who cannot swallow safely. For nasogastric administration, liquid formulations are preferred. Before using solid formulations, the possibility of their grinding and suspension should be evaluated. The effectiveness of drug delivery via a nasogastric (NG) tube is determined by the correct choice of dosage form, tube characteristics, and elimination of the risk of tube blockage. It is also necessary to confirm that the generic drug is therapeutically equivalent to the reference drug by determining the completeness of its extraction. For this, it is necessary to

develop analytical methods for the quantitative determination of drugs.

In this work, the HPLC method for quantitative determination of rivaroxaban, suitable for studying the completeness of the extraction of the drug RIVAROXABAN, 20 mg tablets after delivery via a nasogastric tube, was validated for the following criteria: specificity, accuracy, precision, and linearity in the studied concentration range. The stability of the test solutions and reference solutions when stored at room temperature for 8 hours was confirmed.

In our developed method there is no need to use special chemical reagents, high percentage of organic solvent, high flow rate. Chromatographic system consists of ODS column (100 mm × 4.6 mm × 3.5 μm). Mobile phase A was prepared by mixing acetonitrile : solution A (0.67 ml of phosphoric acid is made up to 1000 ml with water for chromatography) (8:92), flow rate 1.0 ml / min, detection wavelength 250 nm, using an injection volume of 10 μl. The linearity of the method for supernatural houses was assessed in the concentration range of 50–130%. The concentration of 0.2 mg/mL was selected as the 100% point. The method demonstrated satisfactory regression linearity (0.99983) with a good repeatability range (0.5–1.1%).

The completeness of the extraction of rivaroxaban was monitored after suspension in the medium (deionized water) of crushed tablets of the test and reference drugs and their delivery via a nasogastric tube. It was established that more than 90% of rivaroxaban is extracted after enteral administration, and the drugs are equivalent in terms of the variability of the degree of extraction.

Keywords: rivaroxaban, high-performance liquid chromatography, nasogastric tube, validation.

ЛІТЕРАТУРА

1. Oral Drug Products Administered Via Enteral Feeding Tube: In Vitro Testing and Labeling Recommendations Guidance for Industry. DRAFT GUIDANCE. June 2021, Pharmaceutical Quality.
2. Tanaka R., Eto D., Goto K., Ohchi Y., Yasuda N., Suzuki Y., Tatsuta R., Kitano T., Itoh H. Pharmacokinetic and adsorptive analyses of administration of oral voriconazole suspension via enteral feeding tube in intensive care unit patients. *Biol. Pharm. Bull.* 2021. **44** (5). P. 737–741.
doi: 10.1248/bpb.b20-00796
3. Desai A., Helmick M., Heo N., Moy S., Stanhope S., Goldwater R., Martin N. Pharmacokinetics and bioequivalence of isavuconazole administered as isavuconazonium sulfate intravenous solution via nasogastric tube or orally in healthy subjects. *Antimicrob Agents Chemother.* 2021. **65** (9). P. e0044221.
doi: 10.1128/AAC.00442-21
4. Karkossa F., Bading A., Klein S. What to consider for successful administration of oral liquids via enteral feeding tubes? A case study with paediatric ibuprofen suspensions. *Int. J. Pharm.* 2024. **5** (649). P. 123628.
doi: 10.1016/j.ijpharm.2023.123628
5. Santangelo M., Wood J.A., Barnett K.L., Wooding F.G.G., Bartlett J.A. In vitro assessment for dose preparation and simulated administration of azithromycin suspensions via enteral feeding tubes. *Hosp. Pharm.* 2022. **57** (2). P. 260–267.
doi: 10.1177/00185787211024216
6. Державна Фармакопея України: в 3 т. / Державне підприємство «Український науковий фармакопейний центр якості лікарських засобів». 2-е вид. Доповнення 4. Харків: Державне підприємство «Український науковий фармакопейний центр якості лікарських засобів», 2020. С. 123–236.
7. FDA Draft Guidance on Rivaroxaban, 2020.

REFERENCES

1. Oral Drug Products Administered Via Enteral Feeding Tube: In Vitro Testing and Labeling Recommendations Guidance for Industry. DRAFT GUIDANCE. June 2021, Pharmaceutical Quality.
2. Tanaka R., Eto D., Goto K., Ohchi Y., Yasuda N., Suzuki Y., Tatsuta R., Kitano T., Itoh H. Pharmacokinetic and adsorptive analyses of administration of oral voriconazole suspension via enteral feeding tube in intensive care unit patients. *Biol. Pharm. Bull.* 2021. **44** (5): 737–741.
   doi: 10.1248/bpb.b20-00796
3. Desai A., Helmick M., Heo N., Moy S., Stanhope S., Goldwater R., Martin N. Pharmacokinetics and bioequivalence of isavuconazole administered as isavuconazonium sulfate intravenous solution via nasogastric tube or orally in healthy subjects. *Antimicrob Agents Chemother.* 2021. **65** (9): e0044221.
   doi: 10.1128/AAC.00442-21
4. Karkossa F., Bading A., Klein S. What to consider for successful administration of oral liquids via enteral feeding tubes? A case study with paediatric ibuprofen suspensions. *Int. J. Pharm.* 2024. **5** (649): 123628.
   doi: 10.1016/j.ijpharm.2023.123628
5. Santangelo M., Wood J.A., Barnett K.L., Wooding F.G.G., Bartlett J.A. In vitro assessment for dose preparation and simulated administration of azithromycin suspensions via enteral feeding tubes. *Hosp. Pharm.* 2022. **57** (2): 260–267.
   doi: 10.1177/00185787211024216
6. Derzhavna Farmakopeia Ukrainy: v 3 t. / Derzhavne pidpryiemstvo «Ukrainskyi naukovyi farmakopeinyi tsentr yakosti likarskykh zasobiv». 2-e vyd. Dopovnennia 4. Kharkiv: Derzhavne pidpryiemstvo «Ukrainskyi naukovyi farmakopeinyi tsentr yakosti likarskykh zasobiv», 2020. 123–236. (in Ukrainian).
7. FDA Draft Guidance on Rivaroxaban, 2020.

Стаття надійшла: 15.02.2026
Стаття прийнята до друку: 30.02.2026
Стаття опублікована: 25.03.2026

UDC 546.26-162: 541.13:549.21 doi: 10.33609/2708-129X.92.2.2026.26-82

RECENT ADVANCES IN PHOTOCHEMICAL SYNTHESIS OF FLUORINE-CONTAINING HETEROCYCLES (review).

***Alicja Wzorek*[1],** https://orcid.org/0000-0001-9041-7034
***Taizo Ono*[2],** https://orcid.org/0009-0002-3268-2344
***Daniel Baecker*[3],** https://orcid.org/0000-0002-1963-9838
***Wei Zhang*[4],** https://orcid.org/0000-0002-6097-2763
***Vadim A. Soloshonok*[5*],** https://orcid.org/0000-0003-0681-4526

[1] *Institute of Chemistry, Jan Kochanowski University in Kielce, Uniwersytecka 7, 25-406 Kielce, Poland;*
[2] *National Institute of Advanced Industrial Science and Technology (AIST), 2266-98, Anagahora, Shimoshidami, Moriyama-ku, Nagoya, 463-8560, Japan;*
[3] *Department of Pharmaceutical and Medicinal Chemistry, Institute of Pharmacy, Freie Universität Berlin, Königin-Luise-Straße 2+4, 14195 Berlin, Germany;*
[4] *Department of Chemistry, University of Massachusetts Boston, Boston MA 02125, Unites States of America;*
[5] *IKERBASQUE, Basque Foundation for Science, María Díaz de Haro 3, Plaza Bizkaia, 48013 Bilbao, Spain*
e-mail: vadimsoloshonok@gmail.com

Abstract:

Fluorine-containing heterocycles occupy a central position in pharmaceutical, agrochemical, and materials science due to their unique physicochemical properties and broad functional relevance. The pursuit of efficient and sustainable synthetic methodologies has catalyzed the emergence of photochemistry as a compelling alternative to conventional thermal, acid–base, or redox-based approaches. Indeed, many of the transformations highlighted in this review would be unattainable under traditional reaction conditions, underscoring the distinctive reactivity enabled by light-driven processes.

This review surveys key advances over the past decade in the photochemical synthesis of fluorinated heterocyclic compounds. It begins with an overview of fundamental photochemical principles and the most commonly employed photocatalysts. The discussion then proceeds to categorize reactions into unimolecular, bimolecular, and trimolecular classes. Unimolecular (intramolecular) reactions typically involve the cyclization of strategically designed substrates capable of forming heterocyclic frameworks upon photoactivation. Unimolecular (intramolecular) reactions represent the most prevalent class, wherein two distinct components contribute complementary fragments to construct the target heterocycle. Trimolecular (three-component) photochemical reactions, by contrast, are exceedingly rare due to the inherent mechanistic, kinetic, and spatial constraints associated with three-body interactions under photochemical conditions.

For each transformation discussed, we detail the photocatalyst employed, the irradiation source, reaction conditions, and the specific fluorination pattern introduced. Photochemistry redefines light not merely as an energy source but as a precise and sustainable reagent—unlocking synthetic pathways with elegance, selectivity, and minimal environmental impact.

This work aims to serve as a comprehensive resource for researchers and practitioners seeking to harness photochemical strategies for the synthesis of fluorinated heterocycles, with an emphasis on catalytic efficiency, structural diversity, and ecological responsibility.

Keywords: Fluorine Chemistry, Heterocycles, Organofluorine Compounds, Photoredox Catalysis, Structural Diversity, Green Chemistry, Sustainable Methodologies, Environmental Impact.

INTRODUCTION.

Photochemistry is the science of chemical transformation driven by light. At its heart lies the interaction between photons—primarily in the ultraviolet and visible regions—and molecules capable of absorbing this energy and responding through chemical change [1–4]. These light-induced reactions often proceed via excited electronic states, enabling transformations that would be improbable or even inaccessible under standard thermal conditions [5–7].

Historically, photochemistry traces its lineage back to early observations by Herschel and Faraday, who recognized that light was more than illumination—it could influence matter [8–11]. However, the field matured significantly with the advent of spectroscopy, quantum mechanics, and laser-based technologies, which allowed scientists to probe and manipulate excited-state dynamics with precision. Pioneers like Porter and Miyaura helped unveil the molecular choreography underlying these light-driven processes [12–14].

The foundational concept begins when a molecule absorbs a photon, shifting from its ground electronic state to an excited state. This higher-energy configuration can initiate a variety of pathways: bond formation or cleavage, electron transfer, energy migration, isomerization, or radical generation. These reactions are typically non-thermal, unfolding not through vibrational excitation but via electronic transitions [15–17].

A molecule's ability to absorb light depends on the availability of suitable electronic transitions, such as $\pi \rightarrow \pi^*$ or $n \rightarrow \pi^*$, governed by the Beer–Lambert law [18–20]. The excited states accessed—singlet (S_1) or triplet (T_1)—carry distinct chemical potentials and lifetimes, shaping their reactivity. Processes like intersystem crossing and internal conversion dictate whether the molecule reacts chemically or returns to the ground state via photophysical emission. The quantum yield (Φ) quantifies the efficiency of these photochemical events, indicating how many molecular transformations occur per photon absorbed [21–23].

A crucial distinction exists between photochemistry and photophysics: photochemistry results in permanent chemical change, while photophysics involves energy release without altering molecular structure, as seen in fluorescence and phosphorescence [24].

Photochemistry permeates numerous disciplines. In organic synthesis, it enables selective reactions such as [2+2] cycloadditions, oxidations, and rearrangements [25–27]. In materials

science, photochemical processes underpin technologies like photoresists, light-curable polymers, and organic light emitting diode (OLED) displays [28–31]. In biochemistry, light governs critical pathways including photosynthesis, visual perception, and DNA damage and repair [32]. Environmental chemistry harnesses solar light to degrade pollutants and activate photocatalysts, providing green solutions to industrial waste [33–35].

In essence, photochemistry offers more than just reactivity—it provides a lens through which light becomes a tool of molecular design, capable of unlocking pathways shaped not by heat, but by photons sculpting the structure and destiny of chemical species. Photochemistry has become a cornerstone of modern organic synthesis, offering reactivity pathways that are often inaccessible or impractical under conventional thermal conditions. By harnessing the energy of light—typically in the ultraviolet or visible spectrum—chemists can induce transformations at ambient temperatures, often without the need for harsh reagents or elevated pressures [36–39].

One of the most striking advantages of photochemical reactions is their ability to activate specific molecular orbitals through electronic excitation, enabling reactions like cycloadditions, radical-mediated rearrangements, and selective isomerizations. These processes are not only thermally forbidden but can also proceed with remarkable selectivity and efficiency when triggered by light [40–42].

Photochemical synthesis also aligns closely with green chemistry principles. Light acts as a reagent with zero chemical waste, and many photochemical reactions proceed in mild conditions—room temperature, benign solvents, and low energy input. This dramatically reduces the environmental footprint of chemical manufacturing. Furthermore, advancements in flow photochemistry have enabled continuous processing with LED-driven reactors, making these methods scalable and industrially viable [43–46].

The strategic value of photochemistry in synthesis lies in its precision and adaptability. Light intensity, wavelength, and catalyst design offer programmable control over reaction outcomes. As the field continues to evolve, photochemical methods are finding growing applications in pharmaceutical development, fluorinated compound synthesis, and eco-friendly manufacturing.

Building on our expertise in modern pharmaceutical development [47–52], with a particular focus on fluorine-containing therapeutics [53–61] and compounds derived from tailor-made amino acids [62–67], we actively pursue and evaluate innovative synthetic methodologies [68–74]. This strategic direction is reinforced by the fact that heterocyclic scaffolds and amino acid derivatives underpin approximately 85% and 35% of approved pharmaceutical agents, respectively. Accordingly, we prioritize advancements in these key synthetic domains [75–88]. Among them, heterocyclic compounds are especially vital in medicinal chemistry, owing to their remarkable biological activity and structural adaptability, which render them indispensable tools in rational drug design [89–92].

Recently, we provided a comprehensive overview of recent progress in the synthesis of fluorinated heterocyclic compounds, emphasizing emerging strategies such as carbon nanotube-mediated catalysis [93], the application of mechanochemical principles [94], and the integration of electrochemical methodolo-

gies [95]. In the present review, we build upon this foundation by advancing the discussion toward environmentally conscious and sustainable synthetic practices, with a detailed focus on photochemical approaches for constructing fluorinated heterocyclic scaffolds. Photochemistry continues to gain recognition as a dynamic and strategically valuable research area with considerable synthetic potential. In this review, we provide a systematic overview of studies published over the past decade concerning the photochemical synthesis of fluorine-containing heterocyclic compounds. The discussion is structured according to the number of reacting species, encompassing unimolecular, bimolecular, and trimolecular transformations. We anticipate that this compilation will serve not only as a practical reference but also as a source of inspiration for researchers and practitioners in synthetic and medicinal chemistry, particularly those pursuing environmentally sustainable methodologies.

Common transition metal photocatalysts.

Catalysis plays a central role in expanding the versatility of photochemical transformations. Photoredox catalysis, which uses visible light to toggle redox states via transition metal complexes or organic dyes, allows for a range of bond-forming reactions, including C–C, C–N, and C–O couplings. Dual catalysis strategies further integrate light with organocatalysis or transition metals to enable asymmetric synthesis, site-selective functionalizations, and late-stage modifications [96].

Most commonly used transition metal catalysts are presented in Fig. 1. $Ru(bpy)_3^{2+}$, or tris(2,2′-bipyridine)ruthenium(II), is a well-established photoredox catalyst widely used in synthetic chemistry. It absorbs visible light (around 450 nm) and reaches a long-lived excited state (~1 microsecond), enabling various single-electron transfer (SET) and energy transfer reactions. In its excited state, it acts as both a strong reductant and a strong oxidant, which allows it to drive a broad range of transformations. The complex is stable under air and moisture, operates under mild conditions, and facilitates C–C and C–X bond formation, dehalogenations, cycloadditions, and redox-neutral reactions. Its photochemical behavior aligns well with green chemistry goals: minimal energy input, reduced waste, and compatibility with flow systems. It is also explored for biological applications like photo-induced generation of reactive oxygen species (ROS) and targeted therapies. $Ru(bpy)_3^{2+}$ remains a cornerstone in both academic and industrial photochemistry thanks to its versatility, robustness, and responsiveness to visible light [97].

$Ir(bpy)_3(dtbbpy)^+$ is a heteroleptic iridium(III) polypyridyl complex used as a versatile photocatalyst in visible-light-promoted reactions. It consists of three bipyridine-type ligands, including dtbbpy (4,4'-di-*tert*-butyl-2,2'-bipyridine), which contributes to enhanced solubility and steric protection. Iridium is in the +3 oxidation state, and the complex carries an overall +1 charge. Upon irradiation with visible light, the complex enters a long-lived triplet metal-to-ligand charge transfer (MLCT) excited state, capable of engaging in single-electron transfer and energy transfer mechanisms. In its excited state, it acts as both a strong oxidant (around +1.21 V vs. SCE) and reductant (about –0.89 V vs. SCE), making it suitable for both oxidative and reductive photoredox cycles. $Ir(bpy)_3(dtbbpy)^+$ has been successfully applied in reactions such

as radical acylation, decarboxylative couplings, and C(sp^3)–H functionalization in dual catalytic systems (e.g., Ir/Ni). It is also explored in tandem photoredox cycles involving IrH^+ and IrH_3 intermediates, expanding its utility in multi-electron redox transformations [98].

The complex $Ir[dF(CF_3)bpy]_2(dtbbpy)^+$ is a highly efficient iridium(III) photocatalyst widely used in visible-light photoredox chemistry. It features two cyclometalated ligands—3,5-difluoro-2-(trifluoromethyl)pyridyl-phenyl ($dF(CF_3)ppy$)—and one ancillary ligand, 4,4'-di-*tert*-butyl-2,2'-bipyridine (dtbbpy), which enhances solubility and steric stability. This catalyst absorbs light around 380–450 nm and enters a long-lived triplet MLCT (metal-to-ligand charge transfer) excited state. In this state, it acts as both a strong oxidant (excited-state potential ≈ +1.21 V vs. SCE) and a competent reductant (≈ –0.89 V vs. SCE), making it suitable for both oxidative and reductive quenching cycles. $Ir[dF(CF_3)bpy]_2(dtbbpy)^+$ is particularly effective in radical acylation reactions, decarboxylative couplings, and tandem photoredox cycles. It can form reactive intermediates like IrH^+ and IrH_3 under multiphoton conditions, enabling sequential redox events. These properties make it valuable for constructing ketones, arylated products, and complex heterocycles under mild, sustainable conditions [99].

$Ir(dFppy)_3$, or tris(2-(2,4-difluorophenyl) pyridine)iridium(III), is a homoleptic cyclometalated iridium complex widely used in visible-light photocatalysis. It features three fluorinated phenylpyridine ligands, which enhance its photophysical properties by increasing the triplet state energy and blue-shifting its emission. This complex is air- and moisture-stable, absorbs light around 450 nm, and has a high triplet state energy (~60 kcal/mol), making it particularly effective for energy transfer reactions. Its excited-state redox potentials are relatively modest compared to other iridium complexes, which helps avoid undesired redox side reactions and makes it ideal for substrates sensitive to oxidation or reduction. $Ir(dFppy)_3$ is commonly used in [2+2] photocycloadditions, *E*/*Z* alkene isomerizations, and other transformations that rely on selective energy transfer rather than single-electron transfer. It has also been employed in synergistic dual photocatalyst systems, where it complements more redox-active catalysts by handling energy transfer steps. Overall, $Ir(dFppy)_3$ is a robust and selective photocatalyst, especially valuable in reactions requiring high triplet energy and minimal redox interference [100].

Finally, $(Cp^*RhCl_2)_2$, or pentamethylcyclopentadienyl rhodium(III) dichloride dimer, is a robust organometallic complex that has found increasing utility in photocatalysis, particularly in visible-light-driven transformations. While it is more traditionally known for thermal C–H activation chemistry, recent studies have explored its photochemical behavior and catalytic potential under light irradiation. This complex features two Rh(III) centers bridged by chloride ligands and stabilized by Cp^* (η^5-C_5Me_5) rings. It is air-stable, red in color, and soluble in organic solvents like dichloromethane and chloroform. Upon photoexcitation, it can participate in ligand-to-metal charge transfer (LMCT) and engage in catalytic cycles involving single-electron transfer or energy transfer, depending on the reaction conditions and substrates. $(Cp^*RhCl_2)_2$ has been used in mechanochemical and photochemical C–H bond functionalizations, halogenations, and annulation reactions. It can also be activated by silver

salts to form cationic Rh(III) species that are more reactive under light. In some systems, it has been incorporated into conjugated polymers or heterogenized frameworks to facilitate CO_2 photoreduction and other light-driven processes. Its versatility, stability, and compatibility with sustainable activation methods such as blue-light irradiation and electrocatalysis make it a promising candidate for expanding the scope of rhodium-based photocatalysis [101].

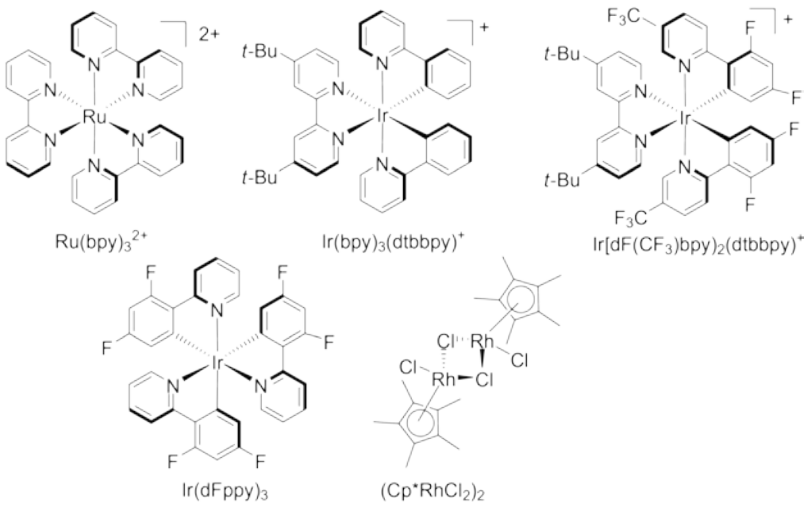

Fig. 1. Common Ru, Ir and Rh photocatalysts.

For these photocatalysts, the most commonly used counterions include PF_6^- (hexafluorophosphate), which is widely favored due to its low coordinating ability and excellent solubility in organic solvents. Chloride (Cl^-) is often found in commercially available salts such as tris(bipyridine)ruthenium(II) chloride. BF_4^- (tetrafluoroborate) offers a good balance of solubility and stability and is also commonly used. ClO_4^- (perchlorate) appears occasionally, although less frequently because of safety concerns. The choice of anion can influence key factors such as solubility, photophysical properties, and compatibility with different reaction environments. For photoredox catalysis in organic solvents, PF_6^- and BF_4^- are especially preferred due to their inert character and solvent compatibility. Additionally, these photocatalysts align well with the principles of green chemistry. They operate under mild conditions using visible light, support redox-neutral pathways, and are compatible with sustainable media, including aqueous-organic systems and flow chemistry setups. Their combination of chemical reactivity, operational stability, and environmental friendliness makes them valuable tools for advanced photochemical synthesis [102-104].

Unimolecular reactions.

Most of the unimolecular reactions discussed in this section involve photocatalytic cyclization. These transformations typically exhibit broad functional group tolerance across the starting materials, yet demonstrate limited generality with respect to the structural arrangement of reactive fragments. Successful cyclization requires precise geometric alignment of those

fragments, making structural predisposition a key determinant of reactivity.

Zhou *et al.* (Scheme 1) [105] reported a highly efficient cyclization protocol (yielding up to 90%) for the transformation of compounds **1**—synthesized from α-bromo acids and corresponding anilines or phenols—into fluorinated heterocycles **2**. Depending on the heteroatom (X), the products were identified as either (*Z*)-benzo[*b*]oxepin-2(3*H*)-ones (X = O) or (*Z*)-1*H*-benzo[*b*]azepin-2(3*H*)-ones (X = N-Alk). The reactions were carried out in dichloromethane (DCM) under an argon atmosphere at ambient temperature, with 2,6-lutidine (1.5 equiv.) as the base. Photochemical activation was achieved using LED irradiation in the presence of *fac*-Ir(ppy)$_3$ as the photocatalyst. The radical cyclization proceeded with remarkable regioselectivity, as no detectable byproducts were observed. This method enables the synthesis of heterocycles **2** bearing up to three fluorine atoms—one on the benzene moiety and up to two aliphatic fluorines positioned α to the carbonyl group on the seven-membered ring.

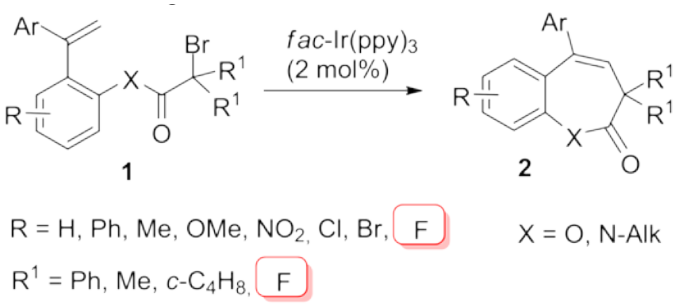

Scheme 1. Synthesis of fluorinated benzoxepines and benzazepines.

Li *et al.* (Scheme 2) [106] described the synthesis of fluorinated benzimidazoles **4** via cyclization of fluorine-containing *N*-phenylamidoxime esters **3**. The yields of the desired products **4** ranged from 20% to 77%. Reactions were carried out in methyl *tert*-butyl ether (MTBE) under an argon atmosphere at ambient temperature. Photochemical activation was achieved using 13 W white LEDs in the presence of Ir[dF(CF$_3$)ppy]$_2$(dtbbpy)PF$_6$ as the photocatalyst. The process was relatively slow, with optimal yields obtained after 36 hours of irradiation. Interestingly, the *para*-CF$_3$-benzoic acid moiety on the starting amidoxime esters **3** acted as a sacrificial unit, facilitating the initiation of the radical chain process.

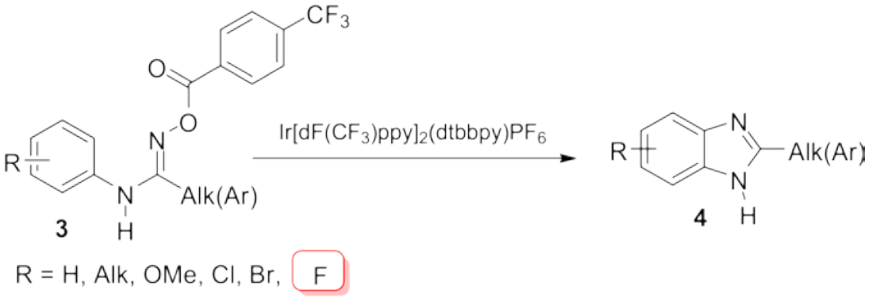

Scheme 2. Preparation of fluorinated benzimidazoles.

Fluorinated quinolinones and derivatives exhibit a wide spectrum of biological activities, making them valuable scaffolds in medicinal chemistry. Their bioactivity is largely attributed to the quinolinone core's ability to interact with diverse biological targets, and fluorine substitution enhances pharmacokinetic properties such as lipophilicity, metabolic stability, and membrane permeability [107-109].

González-Muñoz *et al.* (Scheme 3) [110] developed a photochemical protocol for the synthesis of trifluoromethyl-substituted tetrahydroquinolines **6** via intramolecular cyclization of aniline derivatives **5**. These precursors feature an iodine atom and an *N*-unsaturated moiety, enabling the formation of a six-membered heterocycle. The reactions were performed in acetonitrile at ambient temperature, using 2.5 equivalents of Hünig's base [111] under an inert atmosphere. Photochemical activation was achieved with 13 W white LEDs (visible light) in the presence of $Ir(ppy)_3$ as the photocatalyst. Cyclization proceeded efficiently, with completion times under 24 hours, affording the target tetrahydroquinolines **6** in moderate to good yields ranging from 40% to 80%.

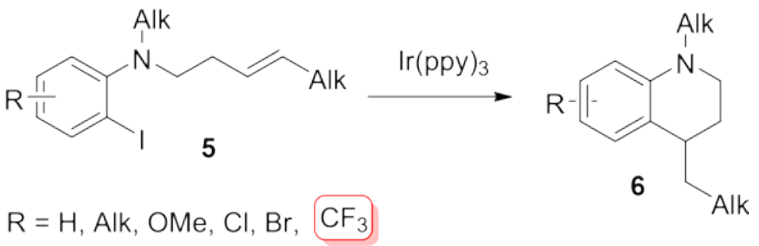

Scheme 3. Synthesis of trifluoromethyl-containing tetrahydroquinolines.

Fluorinated cinnamic acid derivatives are widely employed as electrophilic partners in Michael addition reactions, owing to their enhanced reactivity and utility as convenient building blocks for introducing aromatic fluorine into structurally complex, biologically active molecules [112–114]. Jovanovic *et al.* (Scheme 4) [115] reported a photochemical cyclization of enallenylamides **7**, derived from trifluoromethyl-substituted cinnamic acids, to afford sterically constrained bicyclic dihydropyridinones **8** in yields ranging from 40% to 88%. The transformation proceeds via a [2+2] cycloaddition pathway, catalyzed by $Ir(ppy)_3$ (1 mol%) under blue LED irradiation in dichloromethane at ambient temperature over 18 hours. The nitrogen substituent in the starting enallenylamides **7** can be an alkyl group or a hydrolyzable acyl or Boc moiety, allowing for facile deprotection and access to NH-functionalized products. This structural versatility broadens the scope of potential biological applications for the resulting dihydropyridinones.

Gore and Wang (Scheme 5) [116] reported a series of intramolecular cascade reactions that enable the synthesis of dihydroisochromenes **10** as central scaffolds within complex polycyclic architectures. These structures feature a bridged framework comprising six-, five-, and three-membered aliphatic rings fused to an aromatic system. The starting materials—fluorinated (*E*)-1-phenyl-3-[2-((*E*)-styryl) phenyl]prop-2-en-1-ones **9**—were subjected to visible-light irradiation (blue LEDs) in the presence of $Ir[dF(CF_3)ppy]_2(dtbbpy)PF_6$ as

the photocatalyst in DMSO at ambient temperature. The reactions proceeded efficiently over 7 hours, affording the polycyclic products **10** in excellent yields ranging from 65% to 93%. Mechanistic studies suggest that the transformation operates via an energy-transfer pathway, offering high selectivity and broad substrate tolerance. Notably, the methodology accommodates various fluorine substitutions on the aromatic ring, expanding its utility for the synthesis of structurally intricate, fluorinated frameworks with potential biological relevance.

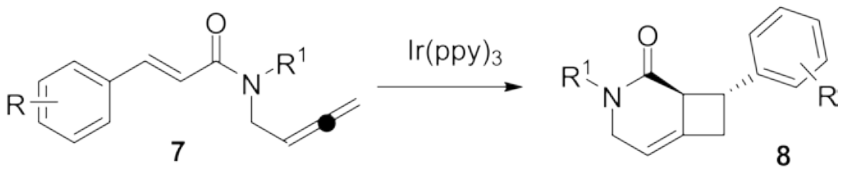

R = H, Alk, OMe, Cl, CF_3

R^1 = Alk, Ar, Bn, Ac, Boc

Scheme 4. Synthesis of trifluoromethyl-containing dihydropyridinones.

R = H, OMe, Cl, F ; R^1 = Alk, Ar; R^2 = H, Me, CN

Scheme 5. Synthesis of fluorinated polycyclic dihydroisochromenes.

Zhu *et al.* (Scheme 6) [117] reported another example of intramolecular cascade reactions yielding structurally intricate polycyclic frameworks. In this study, fluorinated indole derivatives **11** bearing *O*-substituted oximes (as *E*/*Z* mixtures) were subjected to photochemical conditions in dichloromethane at ambient temperature using 24 W blue LEDs in the presence of $Ir(dFppy)_3$ (1 mol%) as the photocatalyst. After 8 hours of irradiation, the reactions furnished indoline-fused azetidines **12**—comprising fused four-, five-, and six-membered rings—with yields ranging from 33% to 99%. This transformation proceeds via a [2+2] cycloaddition between the indole core and the unsaturated oxime moiety. Notably, when 3-substituted analogs **13** are employed as starting materials, the [2+2] pathway is inaccessible due to steric or electronic constraints. Nevertheless, the reaction still undergoes an intramolecular cascade via an alternative pathway, delivering indoline-fused piperidin-2-ones **14**. These reactions were conducted under identical photochemical conditions, yielding the corresponding bicyclic products **14** in good-to-excellent yields of 40% to 96%.

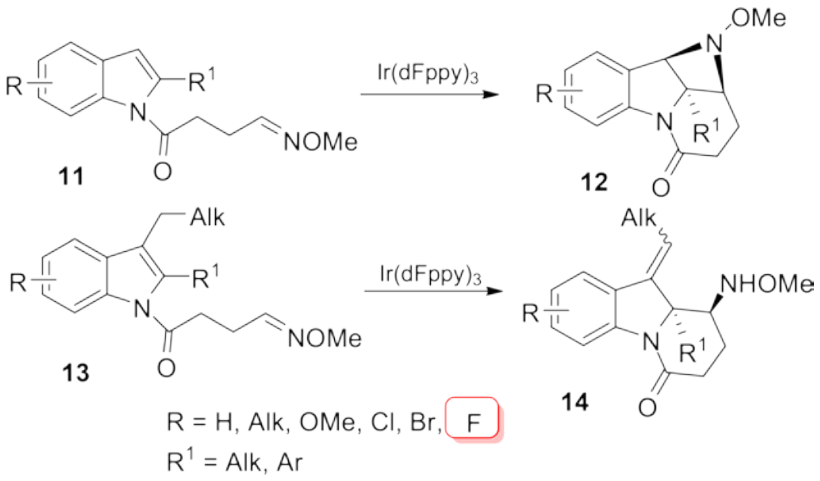

Scheme 6. Synthesis of indoline-fused azetidines and piperidinones.

Zhang *et al.* (Scheme 7) [118] described a photochemical strategy for the synthesis of indoline derivatives **16** featuring fused four- and five-membered rings. The transformation proceeds via an intramolecular [2+2] cycloaddition that simultaneously forms cyclobutene and pyrrolidine-type motifs with virtually complete stereoselectivity. In a representative procedure, fluorine-containing indole precursors **15** bearing an *N*-terminal olefinic moiety were irradiated with 30 W blue LEDs in trifluoroethanol at –30 °C for up to 36 hours, in the presence of $Ir(dFCF_3ppy)_2(dtbbpy)PF_6$ (1 mol%) as the photocatalyst. The resulting tetracyclic products **16** were isolated in yields ranging from 37% to 80%.

Notably, this approach exhibits excellent functional group tolerance and is amenable to late-stage diversification of bioactive molecules. For instance, tryptophan-based substrates [R^1 = H, $CH_2CH(NH_2)CO_2H$] are readily transformed into the corresponding polycyclic targets. Given tryptophan's central role in peptide folding and its function as a biosynthetic precursor to serotonin, melatonin, and niacin (vitamin B_3), the development of structurally complex derivatives of this essential amino acid continues to attract significant interest in both synthetic and medicinal chemistry [119-121].

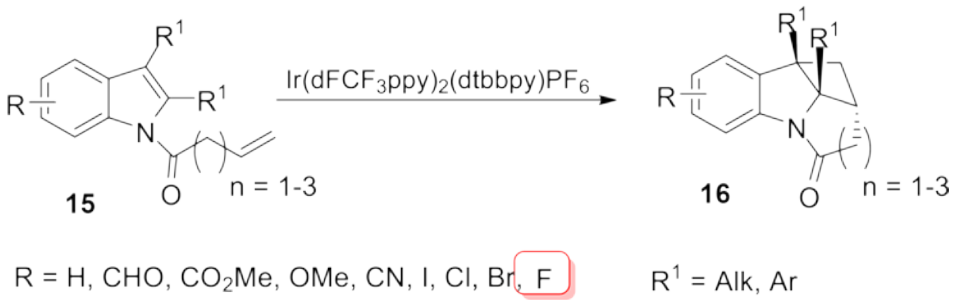

Scheme 7. Synthesis of polycyclic indolines.

Zhu *et al.* (Scheme 8) [122] reported a visible-light-induced intramolecular dearomatization of indole derivatives via a [2+2] cycloaddition, proceeding through an energy-transfer mechanism. This transformation enables direct access to highly strained, cyclobutane-fused angular tetracyclic spiroindolines**18**—architectures typically inaccessible under thermal conditions. The products **18** were obtained in high yields (up to 99%) with excellent diastereoselectivity (>20:1 dr) under mild reaction conditions. In a typical procedure, fluorinated indole substrates **17** were irradiated with 24 W blue LEDs in a CDM/acetonitrile mixture at ambient temperature for 48 hours, using $Ir(dFCF_3ppy)_2(dtbbpy)PF_6$ (4 mol%) as the photocatalyst. The method demonstrated broad functional group tolerance and was amenable to late-stage diversification of complex molecular targets. Fluorination was achieved through trifluoroacetic acid (TFA) protection of the indole nitrogen and aromatic substitution adjacent to the nitrogen, establishing a dual fluorinated motif conducive to biological relevance and synthetic versatility.

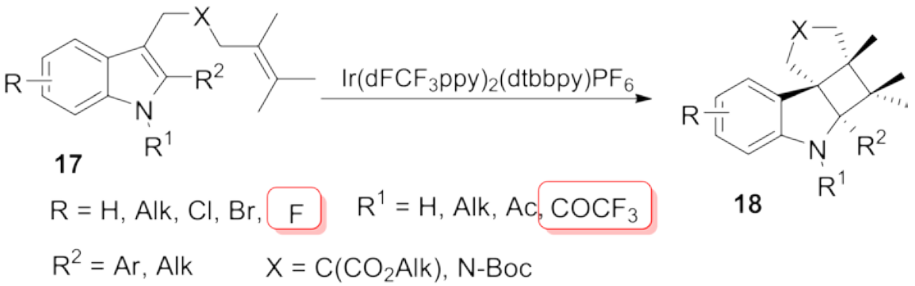

Scheme 8. Synthesis of polycyclic spiroindolines.

Guo *et al.* (Scheme 9) [123] reported an efficient photocatalytic strategy for the synthesis of isoquinolinone derivatives **20** via intramolecular carboamination of alkynes. Utilizing readily available propargyl alcohol derivatives **19**, this method demonstrates broad functional group tolerance and accommodates both terminal and alkyl-substituted alkynes. The reactions were performed in DMSO at 50 °C under irradiation with an 18 W compact fluorescent lamp (CFL) for 12 hours, employing *fac*-$Ir(ppy)_3$ (2 mol%) as the photocatalyst. The target polycyclic isoquinolinones **20** were obtained in yields ranging from 26% to 86%. Importantly, the protocol is operationally simple and readily scalable to gram quantities. Structural diversification was achieved by incorporating either fluorine atoms or trifluoromethyl groups on the aromatic ring of the starting materials **19**, enabling the synthesis of fluorinated oxazolidinone-fused isoquinolinones **20**. In addition to their biological potential, enantiomerically pure oxazolidinone derivatives serve as powerful stereocontrolling auxiliaries in asymmetric synthesis [124–126].

Ritu *et al.* (Scheme 10) [127] developed an efficient iridium–nickel dual photocatalytic protocol for the dehydrogenation of aliphatic *N*-heterocyclic compounds **21** into their corresponding aromatic analogs **22**. This acceptorless, redox-neutral transformation proceeds under mild conditions—at room temperature in ethyl acetate, under a nitrogen atmosphere—irradiated by 5 W 450 nm blue LEDs. Remark-

ably, the system employs only 0.004 mmol of $Ir(dFCF_3ppy)_2(dtbbpy)PF_6$ and 0.02 mmol of $NiBr_2(dtbbpy)$, achieving aromatic products **22** in yields ranging from 30% to 92%, with no evidence of overoxidation. The methodology is compatible with commercially available fluorinated *N*-heterocyclic alkanes and accommodates various functional groups. Importantly, this transformation enables direct access to fluorinated aromatic compounds of high synthetic and commercial relevance.

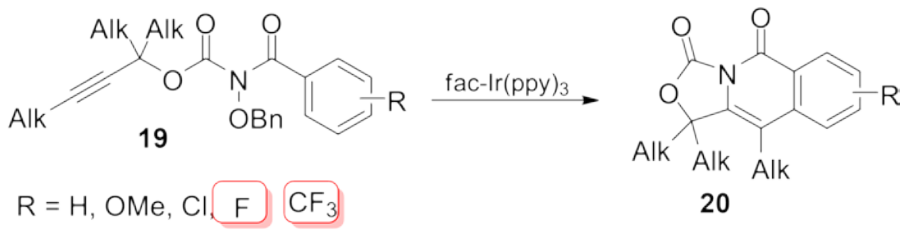

Scheme 9. Preparation of oxazolidinone-fused isoquinolinones.

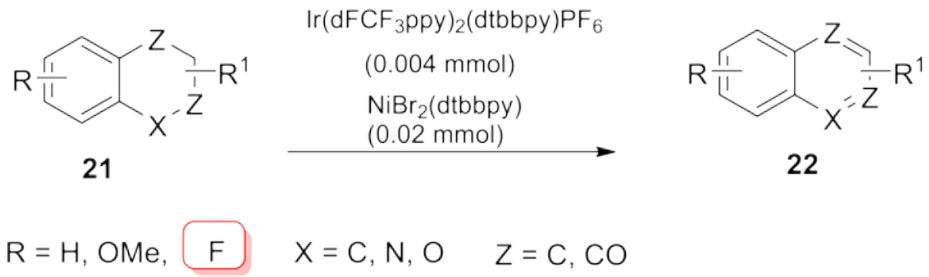

Scheme 10. Photocatalytic dehydrogenation of aliphatic heterocycles.

Bimolecular reactions.

Peng *et al.* (Scheme 11) [128] described a visible-light-promoted C3–H alkylation of 2*H*-indazoles **23** and indoles **24** using sulfoxonium ylides **25**. This protocol leverages readily available reagents and accommodates a broad scope of substrates, including structurally diverse 2*H*-indazoles, indoles, and sulfoxonium ylides, to afford alkylated products **26** and **27** under mild and operationally simple conditions. Reactions were carried out in a 1,2-dichloroethane (DCE)/acetonitrile mixture at 40 °C under an argon atmosphere, irradiated by blue LEDs (5 W) for 12 hours in the presence of *fac*-$Ir(ppy)_3$ (5 mol%) as the photocatalyst. The desired alkylation products **26** and **27** were obtained in isolated yields ranging from 38% to 90%. Fluorinated derivatives were synthesized via trifluoromethyl substitution on the six-membered aromatic rings of the corresponding indazoles and indoles, enabling structural diversification and enhancing the synthetic value of this transformation.

Ma *et al.* (Scheme 12) [129] developed an efficient visible-light-induced radical cascade trifluoromethylation/cyclization protocol for substrates **28** bearing –N=C and *N*-terminal alkene motifs. Using CF_3Br as the trifluoromethylating agent, this transformation enabled the synthesis of trifluoromethyl-containing polycyclic

quinazolinones, benzimidazoles, and indoles **29** under mild conditions. The reactions were conducted in *N*-methyl-2-pyrrolidone (NMP) at 40 °C under an argon atmosphere, irradiated with 5 W blue LEDs in the presence of LiCl (1 equiv.) and *fac*-Ir(ppy)$_3$ (5 mol%) as the photocatalyst. The polycyclic aza-heterocycles **29** were isolated in generally good yields—up to 80%—across a diverse array of substrates, demonstrating broad functional group tolerance and synthetic versatility. Fluorination in products **29** was introduced both via aliphatic –CF_3 groups and through aromatic fluorine or CF_3CO substituents on the aliphatic rings. The use of CF_3Br, a non-hygroscopic, non-corrosive, and industrially abundant reagent [130], further underscores the practicality and scalability of this method. Notably, trifluoromethyl ketones—present as key motifs in some products—are highly reactive toward nucleophilic addition at the carbonyl center. Beyond their biological significance, these intermediates serve as valuable synthetic handles for downstream functionalization [131–133].

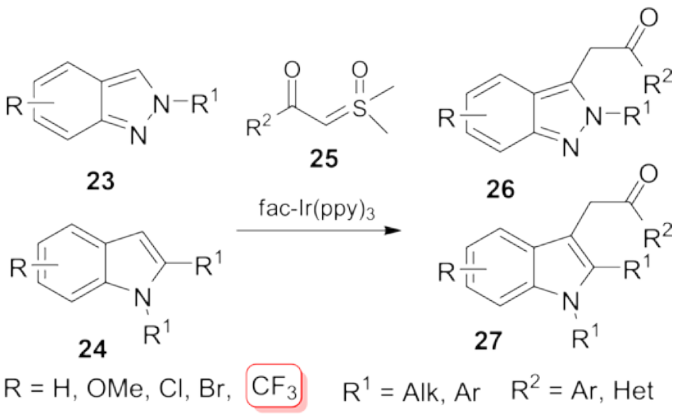

Scheme 11. Alkylation of indazoles and indoles with sulfoxonium ylides.

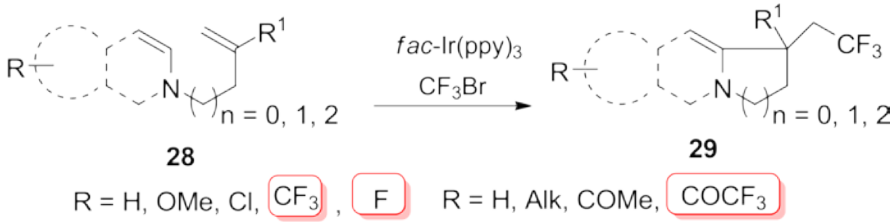

Scheme 12. Synthesis of trifluoromethyl-containing polycyclic quinazolinones, benzimidazoles, and indoles.

Shi *et al.* (Scheme 13) [134] developed a visible-light-induced deaminative [3+2] annulation strategy between *N*-aminopyridinium salts **30** and alkenes **31**, enabling the synthesis of functionalized γ-lactams **32** under mild conditions. The transformation proceeds with excellent diastereoselectivity and displays broad functional group tolerance. Reactions were performed in a DMSO/acetonitrile mixture under an inert nitrogen atmosphere,

irradiated by 15 W blue LEDs for 12 hours, in the presence of Na_2HPO_4 (2 equiv.) and fac-Ir(ppy)$_3$ (2 mol%) as the photocatalyst. The γ-lactam products **32** were isolated in 40% to 75% yields, demonstrating efficient annulation across various substrate combinations. Fluorination was incorporated via either monofluorinated or trifluoromethyl-substituted motifs on both precursors **30**, **31**, affording densely fluorinated products **32**. This dual representation of fluorine—both aliphatic and aromatic—enhances molecular complexity and contributes to the pharmacophoric potential of the resulting scaffolds. Formally, compounds **32** can be viewed as derivatives of tailor-made [135] γ-amino acids, underscoring the synthetic and biological relevance of fluorinated amino acid-inspired frameworks in the design of bioactive molecules [136, 137].

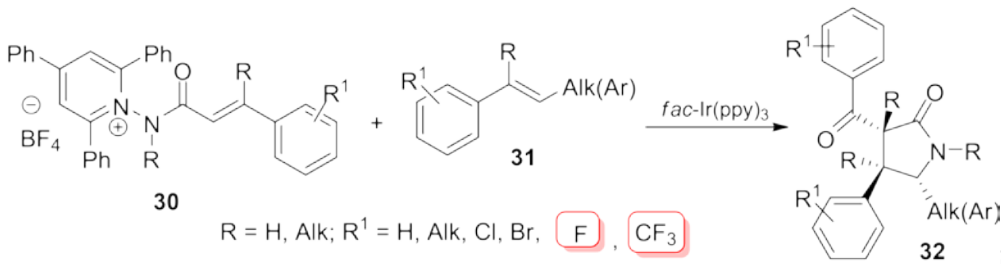

Scheme 13. Synthesis of fluorinated functionalized γ -lactams.

Liu and Patureau (Scheme 14) [138] reported a visible-light-induced photocatalytic protocol for the functionalization of quinoxalin-2(1*H*)-ones **33**, providing a mild, practical route to 3-substituted quinoxalin-2(1*H*)-ones **35** using ubiquitous and chemically benign precursors **33** and **34**. The method showcases broad substrate scope and good functional group tolerance, furnishing a wide array of functionalized heterocycles with strong potential in medicinal chemistry. The transformation was performed in acetonitrile under a nitrogen atmosphere at ambient temperature, irradiated by 40 W blue LEDs for 12 hours. The reaction employed Ir[dF(CF_3)ppy]$_2$(dtbpy)] PF_6 (2 mol%) as the photocatalyst, with triphenylphosphine and 1,4-diazabicyclo[2.2.2]octane (DABCO) as additives to facilitate reactivity. Target products **35** were isolated in yields of up to 88%, demonstrating operational simplicity and synthetic efficiency. Fluorination in the final compounds **35** arises from either aromatic fluorine or trifluoromethyl substitution, introduced through the quinoxalinone core **33** or the anhydride **34**. Notably, when $R^2 = CF_3$, the resulting product **35** structurally aligns with 2-amino-4,4,4-trifluorobutanoic acid—a privileged motif in drug design owing to its enhanced metabolic stability and bioactivity [139–141].

Samanta *et al.* (Scheme 15) [142] reported a photoredox-catalyzed direct arylation of quinoxalin-2(1*H*)-ones **36** using diaryliodonium triflates **37** as a convenient, stable, and cost-effective source of aryl groups. A diverse range of quinoxalin-2(1*H*)-ones was successfully coupled with structurally and electronically varied diaryliodonium salts, enabling efficient synthesis of pharmaceutically valuable 3-arylquinoxalin-2(1*H*)-ones **38**. The protocol is notable for its operational simplicity, ambient reaction conditions, broad substrate scope, excellent

functional group tolerance, and scalability. Reactions were conducted in acetonitrile at room temperature under blue LED irradiation for 24 hours, employing $Ru(bpy)_3Cl_2 \cdot 6H_2O$ (5 mol%) as the photocatalyst. Target arylated products **38** were obtained in yields ranging from 24% to 90%. Fluorination in products **38** is introduced via the aryl moiety of diaryliodonium triflates **37**, incorporating either a single fluorine atom, a trifluoromethyl group, or a trifluoromethoxy substituent. Notably, the aromatic trifluoromethoxy group has garnered increasing attention due to its prevalence in a growing number of successful pharmaceuticals and agrochemicals [143, 144], attributed to its unique electronic properties and favorable lipophilicity.

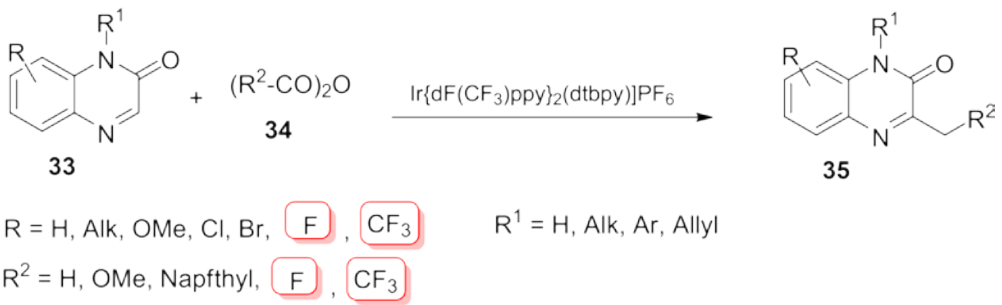

Scheme 14. Functionalization of fluorinated quinoxalin-2-(1*H*)-ones.

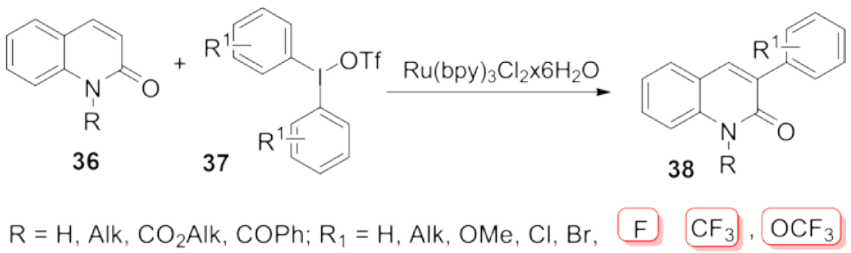

Scheme 15. Synthesis of fluorinated 3-arylquinoxalin-2-(1*H*)-ones.

Xie *et al.* (Scheme 16) [145] developed an efficient and sustainable strategy for the synthesis of 3-alkyl(aryl)quinoxalin-2(1*H*)-ones **41** via visible-light-induced decarboxylative alkylation/arylation of quinoxalin-2(1*H*)-ones **39** using phenyliodine(III) dicarboxylates **40** as alkyl/aryl sources. The reaction proceeds under ambient conditions in eco-friendly PEG-200, highlighting its green chemistry credentials. Employing $Ru(bpy)_3Cl_2 \cdot 6H_2O$ (1 mol%) as the photocatalyst and irradiating with 3 W blue LEDs, the process delivers a range of 3-substituted quinoxalin-2(1*H*)-ones **41** in yields of up to 93%, with reaction times varying between 6 and 12 hours. Notably, the ruthenium(II) catalytic system remains effective over five consecutive cycles without significant loss of activity. Fluorinated analogs were accessed through incorporation of aryl motifs bearing either a single fluorine atom or a trifluoromethyl group, reinforcing the method's relevance for medicinal chemistry applications.

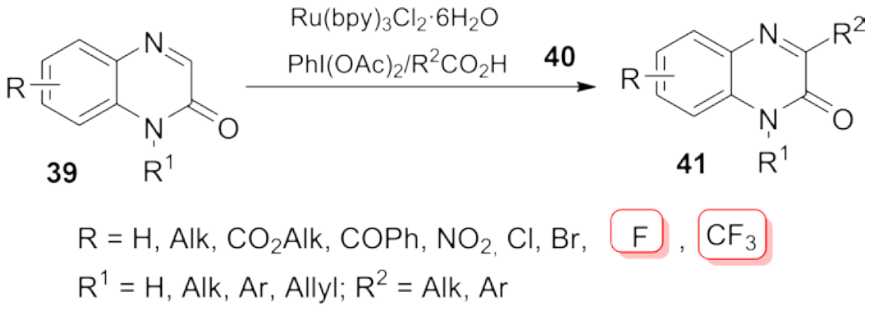

Scheme 16. Synthesis of 3-alkyl(aryl)quinoxalin-2(1*H*)-ones

Wang *et al.* (Scheme 17) [146] described a mild and efficient visible-light-induced atom transfer radical addition and cyclization of benzene-tethered 1,7-enynes **42** and nitrogen-tethered 1,6-enynes **45** with perfluoroalkyl halides **43**, yielding halo-perfluorinated 4-methylenequinolin-2(1*H*)-ones **44** and 3-methylenepyrrolidine derivatives **46**, respectively. Reactions were carried out in 1,4-dioxane at ambient temperature for 24 hours, utilizing K_3PO_4 (2 equiv.) as an additive, *fac*-Ir(ppy)$_3$ as the photocatalyst, and irradiation from 5 W blue LEDs. Products **44** and **46** were obtained in isolated yields ranging from 10% to 86% and 53% to 89%, respectively. This methodology enables the efficient incorporation of a broad spectrum of perfluoroalkyl groups—including *n*-C_3F_7, *n*-C_4F_9, *n*-C_6F_{13}, *n*-C_8F_{17}, and *n*-$C_{10}F_{21}$—into heterocyclic frameworks of pharmacological relevance. However, it is important to note that while some perfluorinated compounds find utility in life sciences and materials chemistry, many members of this class—commonly referred to as per- and polyfluoroalkyl substances (PFAS)—pose serious environmental hazards due to their persistence and bioaccumulative potential [147–149]. Accordingly, the synthesis and application of such substances should be approached with strict regulatory oversight and pursued only when no viable alternatives exist.

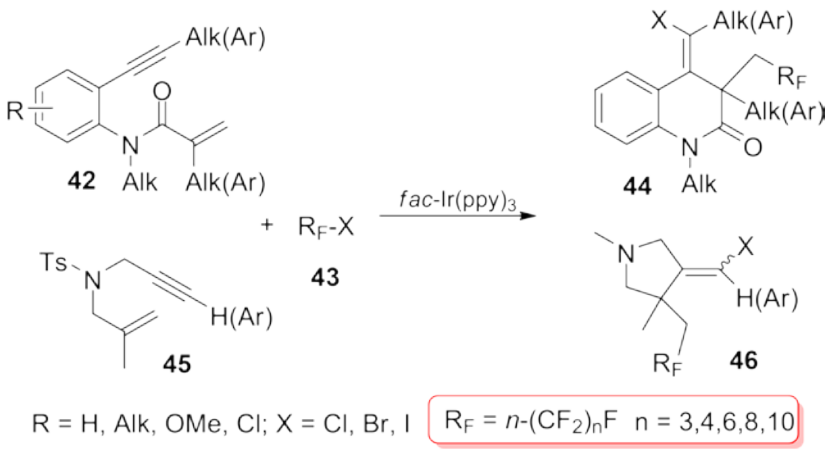

Scheme 17. Preparation of halo-perfluorinated 4-methylenequinolin-2(1*H*)-one and 3-methylenepyrrolidine derivatives.

Liu *et al.* (Scheme 18) [150] reported a practical visible-light-catalyzed tandem radical cyclization of *N*-propargylindoles **47** with acyl chlorides **48** to access 2-acyl-9*H*-pyrrolo[1,2-*a*] indoles **49**. The transformation involves a sequential mechanism: addition of the acyl radical to the carbon–carbon triple bond, intramolecular cyclization at the C2-position of the indole ring, followed by isomerization of the resulting carbon–carbon double bond. Reactions were performed in acetonitrile under an argon atmosphere at 100 °C for 20 hours, using triethylamine to neutralize the released HCl. Photocatalysis was enabled by $Ir(ppy)_3$ (1 mol%) under irradiation from 5 W blue LEDs. Target compounds **49** were obtained in yields of up to 86%. Fluorinated analogs were represented by the presence of aromatic fluorine substituents on the benzene ring in both the starting indoles **47** and the resulting products **49**, contributing to potential structural diversification relevant to medicinal chemistry.

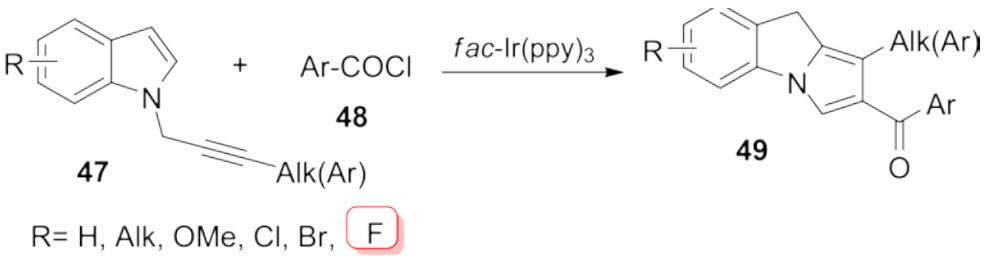

Scheme 18. Preparation of 2-acyl-9*H*-pyrrolo[1,2-*a*]indoles.

Santos *et al.* (Scheme 19) [151] reported a visible-light-induced radical cascade for the synthesis of 2-sulfenylindoles **52** via thiyl radical coupling with *ortho*-substituted arylisocyanides **50**, followed by intramolecular cyclization and aromatization. The key thiyl radicals are rapidly generated through a hydrogen atom transfer (HAT) event from thiol precursor **51**, enabling a redox-neutral transformation. The protocol exhibits broad substrate scope, excellent functional group tolerance, and proceeds under mild conditions. Notably, a continuous flow adaptation provides efficient scalability, with reduced residence time and process intensification advantages. Reactions were conducted in DMSO under an argon atmosphere at ambient temperature for over 3 hours using *p*-toluidine (0.5 equiv.) as an additive. $[Ru(bpy)_3](PF_6)_2$ (1 mol%) served as the photocatalyst, and irradiation was provided by 34 W blue LEDs. Desired sulfenylated products **52** were isolated in yields of up to 95%. Fluorinated derivatives were accessed via arylisocyanide precursors bearing aromatic fluorine substituents, which were retained in the final products. These fluorinated motifs contribute to structural diversification and enhance the relevance of this method for medicinal chemistry applications.

Zhu *et al.* (Scheme 20) [152] reported a reductive radical relay strategy for the synthesis of fused benzo[e]isoindole-1,3,5-triones **55** via the visible-light-mediated reaction of α-bromo ketones **53** with maleimides **54**, catalyzed by $Ir(ppy)_3$ under mild conditions. The transformation proceeds through a mechanistically elegant cascade involving $C(sp^3)$–Br/$C(sp^2)$–H functionalization, consecutive C–C bond for-

mations, and oxidative aromatization. Reactions were conducted in acetonitrile at ambient temperature for 20 hours under nitrogen, using K_2HPO_4 (1 equiv.) as an additive and 7.5 W blue LEDs as the light source. The photocatalyst $Ir(ppy)_3$ was employed at a loading of 2 mol%. Target products **55** were obtained in isolated yields ranging from 51% to 89%. Fluorinated derivatives were accessed using trifluoromethyl-substituted α-bromo ketones **53**, resulting in final products **55** bearing aromatic CF_3 groups. These fluorinated motifs enhance molecular lipophilicity and metabolic stability, underscoring the relevance of this strategy for fluorine-rich scaffold development in medicinal chemistry.

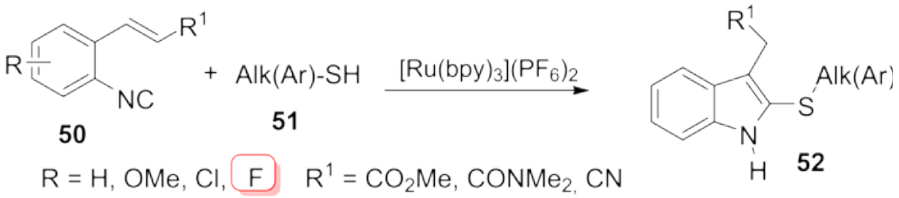

Scheme 19. Synthesis of 2-sulfenylindoles.

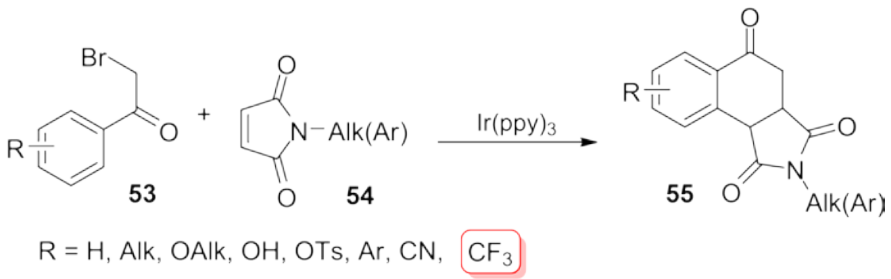

Scheme 20. Preparation of fused benzo[*e*]isoindole-1,3,5-triones.

Fan *et al.* (Scheme 21) [153] developed a visible-light-mediated approach for generating acyl radicals from oxime ester **57** via selective C–C bond activation. Upon irradiation with blue LEDs, a single-electron transfer (SET) occurs from *fac*-$Ir(ppy)_3$ (1 mol%) to oxime **57**, triggering rapid β-fragmentation to produce aliphatic acyl radicals. These intermediates are efficiently trapped by various Michael acceptors **56**, yielding fluorinated oxindoles **58** in 34% to 94% yields. The reactions proceed in 1,2-dichloroethane (DCE) under an argon atmosphere over 4 hours. The presence of fluorine on the aromatic ring in the oxindole products underscores the value of this protocol for the synthesis of fluorinated oxindoles, a scaffold of significant interest in medicinal chemistry [154].

The aza-Paternò–Büchi reaction is a [2+2]-cycloaddition between alkenes and imines that affords azetidines, four-membered nitrogen-containing heterocycles. To expand the synthetic utility of this transformation, Wearing *et al.* (Scheme 22) [155] demonstrated that appropriate matching of frontier molecular orbital energies between alkenes **59** and acyclic oximes **60** enables a visible-light-driven aza-Paternò–Büchi reaction via triplet energy transfer (EnT) catalysis. Under irradiation at 427 nm, the reaction proceeds in acetonitrile

for up to 24 hours, employing 1 mol% of Ir[dF(CF$_3$)ppy]$_2$(dtbpy)]PF$_6$ as photocatalyst. The methodology affords azetidines **61** in yields of up to 80%. Notably, the presence of fluorine on the aromatic rings of both the starting alkenes **59** and the azetidine products **61** highlights the relevance of this approach for constructing fluorinated nitrogen heterocycles, which are valuable in medicinal chemistry.

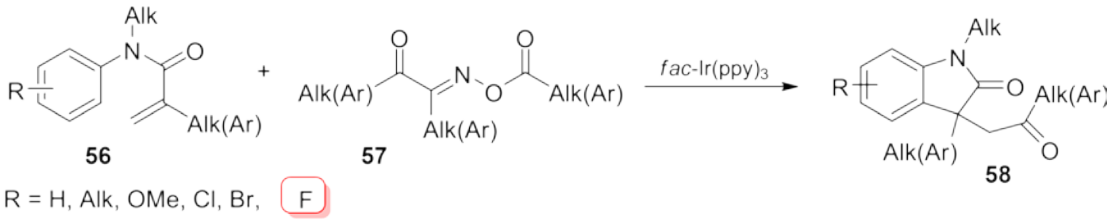

Scheme 21. Synthesis of fluorinated oxindoles.

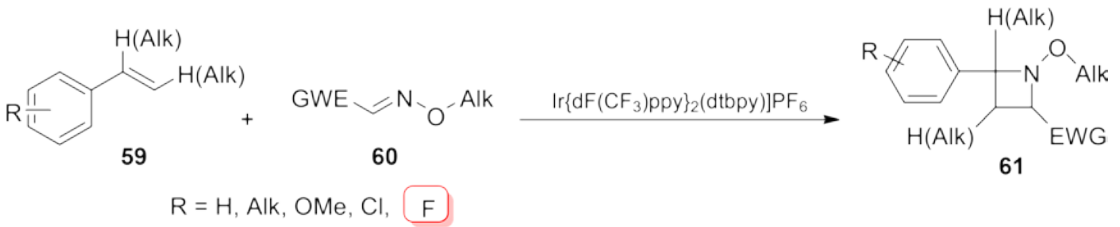

Scheme 22. Synthesis of fluorinated azetidines.

Yu *et al.* (Scheme 23) [156] reported a visible-light-enabled synthesis of tricyclic tetrahydrocarbazoles **64** via the reaction of indole-tethered alkenes **62** with arylsulfonyl chlorides **63** as sulfonyl surrogates. The transformation proceeds through a sequence involving photoreductive activation of the sulfonyl chloride, followed by sulfonylation and intramolecular cyclization. Under irradiation with blue LEDs for 3 hours, the reaction employs *fac*-Ir(ppy)$_3$ (1 mol%) as photocatalyst, Hünig's base (4 equiv.) to scavenge HCl, and CH_2Cl_2 as the solvent. This mild and operationally simple protocol delivers diverse multi-substituted tetrahydrocarbazoles **64** in yields of up to 83%, and is amenable to gram-scale synthesis. The incorporation of fluorine substituents on the aromatic rings of both starting materials allows for systematic modulation of fluorine patterns in the resulting products, enabling structure–activity relationship studies relevant to medicinal chemistry.

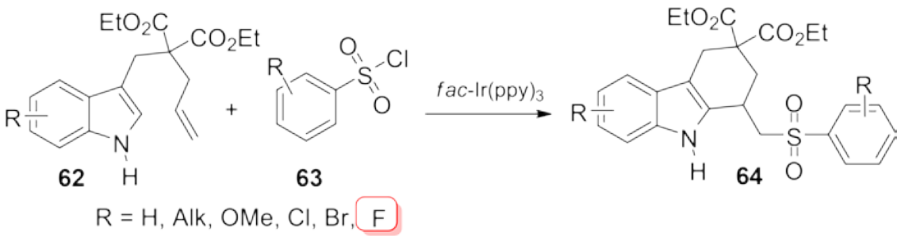

Scheme 23. Synthesis of fluorinated tetrahydrocarbazoles.

Hou *et al*. (Scheme 24) [157] reported a visible-light-induced chlorotrifluoromethylative cyclization strategy for synthesizing chlorotrifluoromethylated cyclic scaffolds. The method leverages photogenerated trifluoromethyl radicals to initiate a cascade involving radical addition, cyclization, and subsequent chlorination. Employing terminal alkene-derived enynes **65** and trifluoromethanesulfonyl chloride **66**, this protocol delivers regio- and stereoselective access to pyrrolidines and cyclopentanes **67** bearing trifluoromethyl group, with yields ranging from 70–75%. Reactions are performed in 1,2-dichloromethane (DCM) under an argon atmosphere at ambient temperature, using K_2HPO_4 (5 equiv.) as an additive and $Ru(bpy)_3Cl_2$ (5 mol%) as photocatalyst under 23 W fluorescent lamp irradiation. The resulting trifluoromethylated pyrrolidines are of significant biomedical interest and can be further derivatized via the embedded vinylchloride functionality, enabling downstream molecular elaboration.

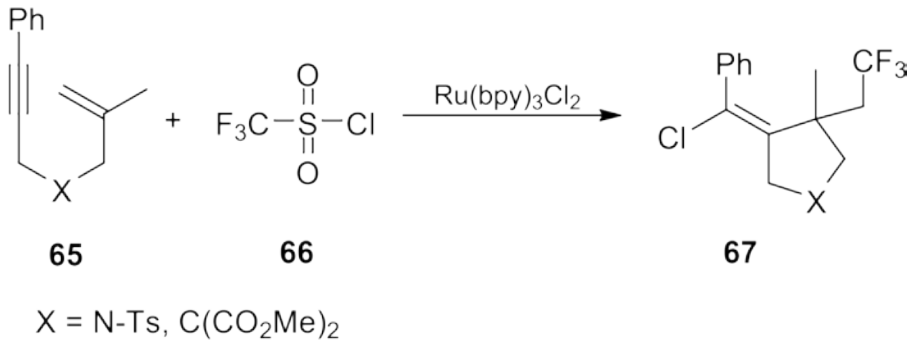

Scheme 24. Synthesis of trifluoromethyl-containing pyrrolidine and cyclopentane.

Cardinale *et al*. (Scheme 25) [158] reported a photocatalytic strategy for synthesizing 1,5-diaryl pyrazoles **70** via the reaction of arenediazonium salts **68** with cyclopropanols **69**. Conducted under mild conditions in acetonitrile at room temperature, the transformation proceeds within 20 minutes under blue LED irradiation using $Ru(bpy)_3Cl_2{\cdot}6H_2O$ (5 mol%) as photocatalyst. The protocol exhibits broad functional group tolerance, excellent regioselectivity, and delivers the desired pyrazoles in yields of up to 90%. Fluorinated motifs are well represented in both starting arenediazoniums **68** and the resulting heterocycles **70**, appearing as fluoro (F), trifluoromethyl (CF_3), or pentafluorosulfanyl (SF_5) substituents—underscoring the relevance of this method for constructing fluorinated pyrazole derivatives with potential medicinal applications.

Bromodifluoroacetate, along with its amide and phosphorus analogs, is a highly versatile reagent in synthetic organic chemistry due to its ability to introduce the difluoromethyl (CF_2) moiety under mild conditions [159]. Notably, its utility in the synthesis of tailor-made α- [160-162] and β-amino acids [163-165] is well documented. Under photochemical conditions, bromodifluoroacetate can also serve as a precursor to reactive intermediates via radical formation—a reactivity showcased in the examples that follow.

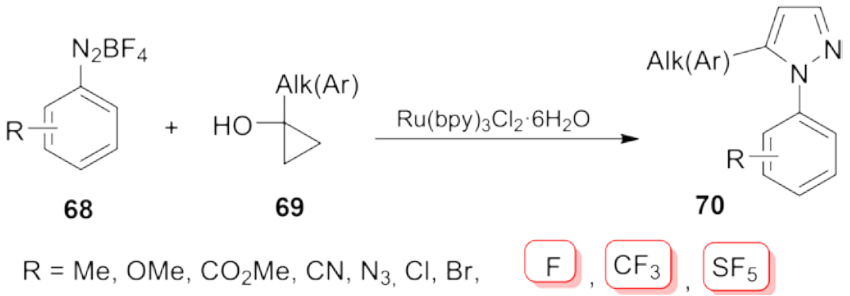

Scheme 25. Synthesis of fluorinated 1,5-disubstituted pyrazoles.

Mei *et al.* (Scheme 26) [166] described an efficient visible-light-promoted cascade reaction for the synthesis of tetracyclic tetrahydrocarbazoles **73** from alkene-tethered indoles **71** and bromodifluoroacetate esters **72**. The transformation involves the formation of two carbon–carbon bonds and one carbon–nitrogen bond, proceeding through a reactive tetrahydrocarbazole intermediate via dual cyclization. Conducted under mild conditions, the protocol accommodates a broad substrate scope and affords the desired products in yields of up to 84%. Its synthetic utility was further highlighted through successful gram-scale synthesis and post-reaction reduction of the tetracyclic framework. The typical reaction is carried out in dimethylformamide (DMF) with *N*,*N*,*N*',*N*'-tetramethylethylenediamine (TMEDA) as an additive, employing *fac*-Ir(ppy)$_3$ as the photocatalyst under blue LED irradiation. In addition to the difluoromethylene unit introduced by bromodifluoroacetate esters **72**, the products **73** also feature aromatic fluorination on the benzene ring, enabling tunable fluorine content with relevance to medicinal and biological applications.

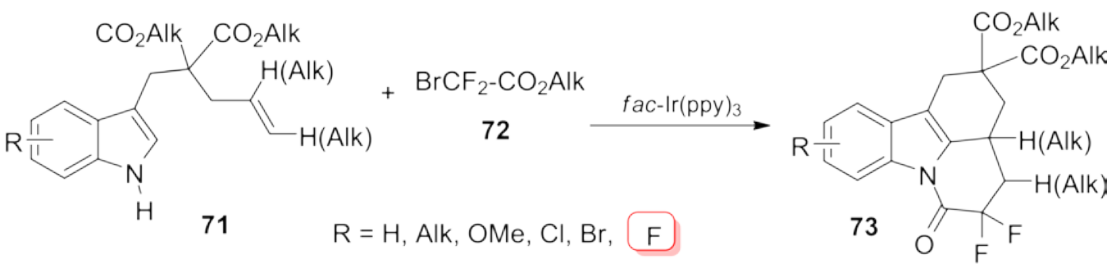

Scheme 26. Synthesis of fluorinated tetracyclic tetrahydrocarbazoles.

Mei *et al.* (Scheme 27) [167] designed a series of indole-derived alkenes **74** and applied them in a photocatalytic cascade reaction with bromodifluoroacetate esters **72**, resulting in the formation of a previously unreported class of tetracyclic tetrahydro-γ-carboline derivatives **75** in yields of up to 90%. Mechanistic studies indicate that the transformation proceeds via a key tetrahydro-γ-carboline intermediate formed through sequential cyclization. The reaction exhibits broad substrate tolerance, offering an efficient and modular approach to constructing tetracyclic tetrahydro-γ-carboline frameworks. In addition to

the difluoromethylene unit introduced by the bromodifluoroacetate esters, the products also incorporate aromatic fluorine substituents on the benzene ring, enabling the fine-tuning of fluorine content for applications in medicinal and biological contexts. The reaction is typically performed in dioxane with TMEDA as base, under a nitrogen atmosphere at room temperature for two hours. Photocatalysis is facilitated by *fac*-Ir(ppy)$_3$ under irradiation from a 4.5 W blue LED source.

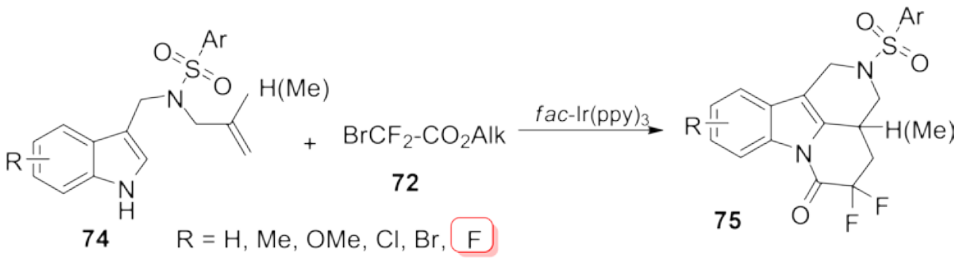

Scheme 27. Synthesis of fluorinated tetrahydro-γ-carbolines.

Zhou *et al.* (Scheme 28) [168] reported a visible-light-mediated difluoroalkylation of 1-(allyloxy)-2-(1-arylvinyl)benzenes and 1-(1-arylvinyl)-2-(vinyloxy)benzenes **76** using bromodifluoroacetate esters **72** to access *bis*-difluoroalkylated benzoxepines and 2*H*-chromenes **77** in yields of up to 73%. The transformation proceeds under mild conditions, exhibiting excellent regioselectivity, broad substrate scope, good functional-group tolerance, and compatibility with late-stage functionalization. Mechanistic studies suggest that the CF_2CO_2Et radical preferentially adds to the aryl-adjacent double bond. Reactions are conducted at room temperature in acetonitrile under an argon atmosphere, employing NaOAc (2 equiv.) to neutralize the liberated hydrogen bromide. Photocatalysis is facilitated by *fac*-Ir(ppy)$_3$ under irradiation from a 12 W blue LED source.

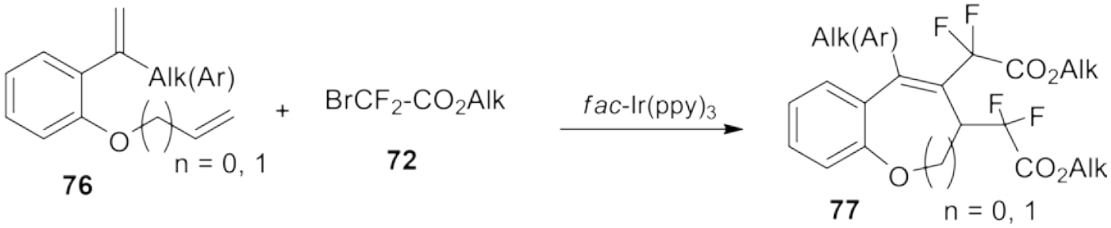

Scheme 28. Preparation of *bis*-difluoroalkylated benzoxepines and2*H*-chromenes.

Lian *et al.* (Scheme 29) [169] reported a photoredox-catalyzed cascade reaction for the synthesis of fluorinated pyrrolo[1,2-*d*]benzodiazepine derivatives **79** under mild conditions. The process is initiated by single-electron transfer (SET) from the excited-state photocatalyst *fac*-Ir(ppy)$_3$ (2 mol%) to ethyl bromodifluoroacetate **72**, generating a reactive radical species that undergoes regioselective addition to a diverse array of 2-(1*H*-pyrrol-1-yl)anilines **78**. A subsequent SET event triggers intramolecular amidation, forming the desired

tetracyclic scaffold. Reactions are conducted in dichloromethane at room temperature under an argon atmosphere, with triethylamine as base, and irradiated using a 23 W compact fluorescent lamp (CFL) over 30 hours. In addition to the difluoromethylene moiety introduced by reagent **72**, the final products feature additional fluorine substitution, either as monofluoro or trifluoromethyl (CF_3) groups—enhancing their relevance for medicinal and structural exploration.

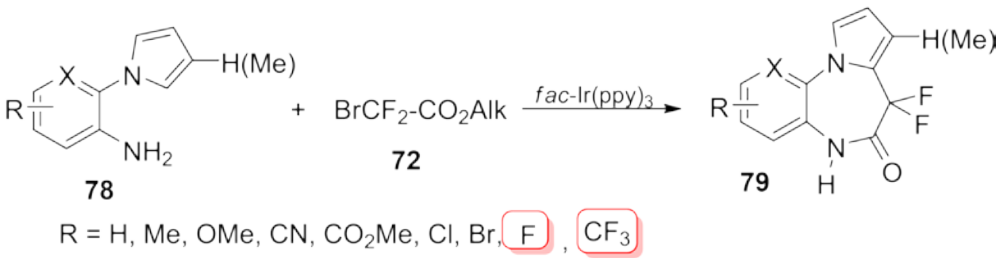

Scheme 29. Preparation of fluorinated pyrrolo[1,2-*d*]benzodiazepine.

Hydroxanthones have garnered significant attention for their roles in organic synthesis and medicinal chemistry, yet efficient methods for their construction remain limited. Wang *et al.* (Scheme 30) [170] reported a photoredox-enabled synthesis of tetrahydroxanthone derivatives **82** via radical cyclization of chromone-tethered alkenes **80** and bromodifluoroacetamide or bromodifluoroacetate reagents **81**. The transformation proceeds under visible-light irradiation through the generation of either difluoroacetate radicals or alkene radical cations, facilitated by *fac*-Ir(ppy)$_3$ or $[Ru(bpy)_3](PF_6)_2$ as photocatalysts. Conducted in tetrahydrofuran (THF) at room temperature under an argon atmosphere, the reaction employs K_3PO_4 as base and a 4.5 W blue LED light source. This protocol provides access to functionalized tetrahydroxanthones in yields of up to 85%, showcasing broad substrate scope and synthetic utility. Beyond enabling efficient construction from readily available building blocks, this strategy enriches the chemistry of heteroarene-tethered alkenes and expands the toolkit for designing fluorinated polycyclic scaffolds.

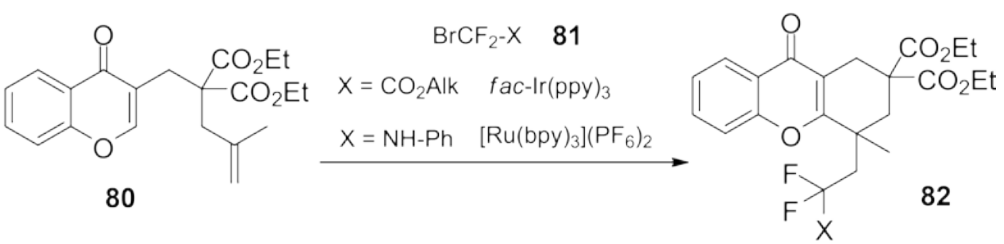

Scheme 30. Synthesis of fluorinated tetrahydroxanthones.

Stefanoni and Wilhelm (Scheme 31) [171] reported a mild, scalable, and highly chemoselective photocatalytic method for the direct functionalization of indolizines **83** using

N-[(trifluoromethyl)thio]saccharin **84** as a trifluoromethylthiolation reagent. The reaction proceeds smoothly in acetone at room temperature under an argon atmosphere, employing $[Ru(bpy)_3](PF_6)_2$ as the photocatalyst and 3 W blue LEDs (455 nm) for 3 hours. The protocol exhibits broad functional-group tolerance and affords the SCF_3-substituted products **85** in yields of approximately 70%. Incorporation of the trifluoromethylthio (SCF_3) group is particularly valuable in drug development, as it enhances the metabolic stability and membrane permeability of bioactive compounds.

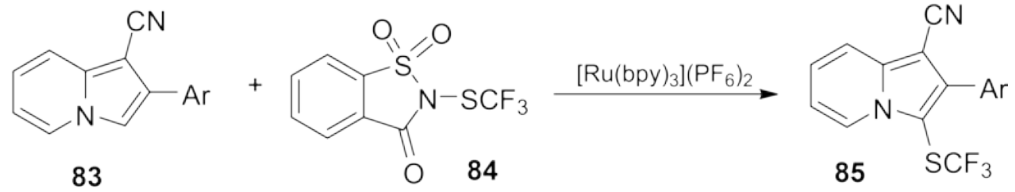

Scheme 31. Synthesis of (trifluoromethyl)thio-modified indolizines.

Fluorine-containing benzoimidazoles and quinazolines [172, 173] exhibit a wide range of properties valuable to medicinal chemistry and molecular design. In a notable contribution, Jiang *et al.* [174] (Scheme 32) reported a visible-light photoredox-catalyzed radical cascade cyclization involving 2-phenyl-1*H*-benzo[*d*]imidazole-1-carbonitriles **86** and simple ethers. This strategy enables sequential inert $C(sp^3)$-H and $C(sp^2)$-H functionalizations, initiated by the intermolecular addition of oxyalkyl radicals to *N*-cyano groups. The process proceeds via in situ generation and intramolecular cyclization of iminyl radicals, incorporating C-2 aryl substituents. The transformation affords tetracyclic benzo[4,5]imidazo[1,2-*c*]quinazolines **87** in 65–86% yield under ambient conditions. Key reaction parameters include 2 equivalents of di-*tert*-butyl peroxide (DTBP) and irradiation with 25 W blue LEDs for 14 hours, using $Ir[dFppy]_2(dtbbpy)]PF_6$ (1 mol%) as the photoredox catalyst. Fluorination is represented by the presence of aromatic fluorine atoms and trifluoromethyl groups, enhancing the structural diversity and potential bioactivity of the products.

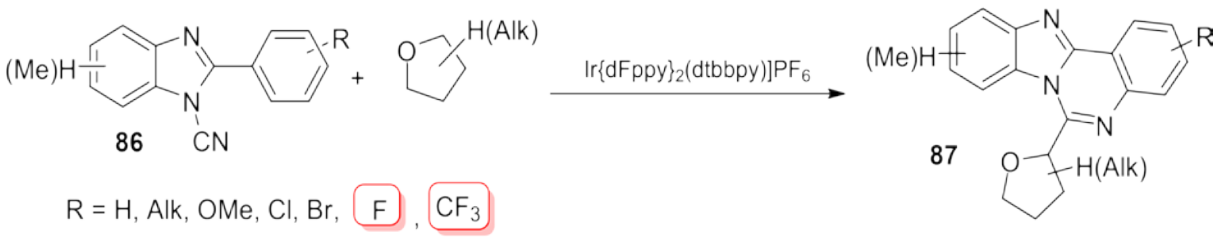

Scheme 32. Synthesis of benzo[4,5]imidazo[1,2-c]quinazolines.

Zhang *et al.* (Scheme 33) [175] reported a visible-light-induced ring-opening $C(sp^3)$–C bond coupling between quinoxalin-2(1*H*)-ones **88** and cyclobutanone oxime esters to access

cyanoalkyl-substituted quinoxalin-2(1*H*)-ones **89**. The transformation proceeds under sunlight or blue LED irradiation at room temperature, without requiring additional additives, and delivers a range of functionalized alkylnitrile derivatives in moderate to excellent yields. The reaction protocol is operationally simple, displays broad functional-group tolerance, and is amenable to scale-up. Mechanistic investigations revealed the involvement of a cyanoalkyl radical intermediate in the key bond-forming step. Reactions are conducted in dichloromethane under an argon atmosphere, employing *fac*-Ir(ppy)$_3$ as the photocatalyst and 6 W blue LEDs as the light source. Fluorinated products **89**, featuring aromatic fluorine atoms on the benzene ring, were obtained in isolated yields ranging from 30% to 67%.

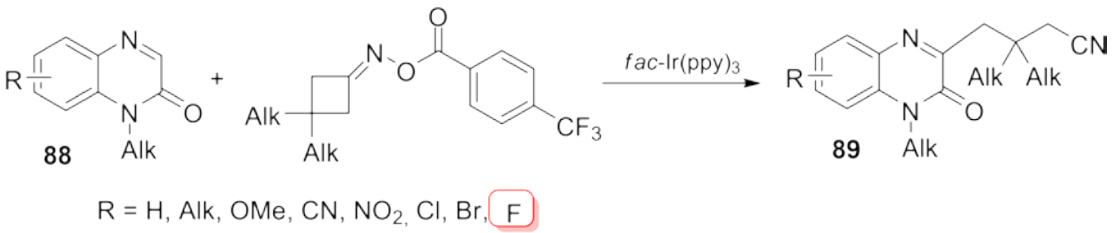

Scheme 33. Synthesis of cyanoalkyl-substituted quinoxalin-2(1*H*)-ones.

Mao *et al.* (Scheme 34) [176] developed an efficient and straightforward visible-light-mediated tandem difluoromethylation–cyclization of alkenyl aldehydes **90** using the air-stable and readily accessible reagent $[Ph_3PCF_2H]^+Br^-$ as a source of the CF_2H group. This transformation enables the synthesis of CF_2H-functionalized chroman-4-one scaffolds and related heterocycles—including chromen-4-ones, quinolin-4(1H)-ones, and thiochromen-4-ones **91**—with moderate to excellent yields (30–90%) and outstanding chemoselectivity under mild conditions. The reaction is typically performed in DMSO at ambient temperature, employing 2,6-lutidine to scavenge the liberated HBr. Photochemical activation is achieved using *fac*-Ir(ppy)$_3$ (2 mol%) under blue LED irradiation for 24 hours. In addition to introducing an aliphatic difluoromethyl group, the resulting heterocyclic products **91** frequently incorporate aromatic fluorination on the benzene ring. This dual fluorine pattern facilitates the generation of compound libraries with diverse fluorine substitution profiles—highly relevant for molecular design and medicinal chemistry applications.

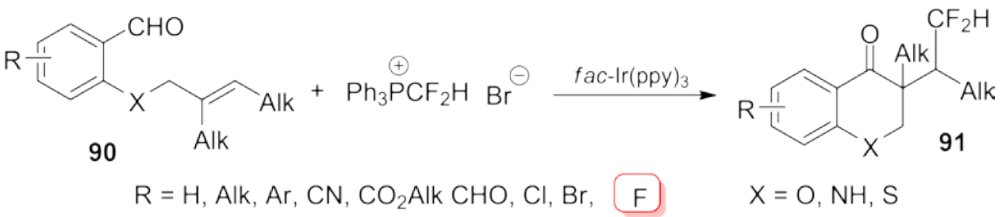

Scheme 34. Synthesis of difluoromethyl-substituted chromen-4-ones, quinolin-4(1*H*)-ones and thiochromen-4-ones.

Meng *et al.* (Scheme 35) [177] reported a visible-light-induced fluoroalkylation–cycloisomerization cascade involving ene-substrates **92** and either ethyl iododifluoroacetate or perfluoroalkyl iodides **93**. This transformation affords fluorinated pyrrolidine derivatives **94** in moderate to excellent yields (23–93%) under mild conditions, while demonstrating broad functional group tolerance. Mechanistic studies suggest a radical chain pathway, initiated under visible-light irradiation, as central to the formation of the heterocyclic scaffolds. Reactions are typically conducted in dioxane under an argon atmosphere at room temperature, using *fac*-Ir(ppy)$_3$ (5 mol%) as the photocatalyst and 30 W blue LEDs as the irradiation source over 12 hours. In addition to the incorporation of aliphatic fluoroacetic or perfluoroalkyl chains, the products also feature aromatic fluorination on the benzene ring, resulting in a dual fluorine motif. This structural versatility enables the design of compound libraries with varied fluorine substitution patterns—highly relevant for medicinal chemistry and molecular property tuning. Beyond their bioactive potential, chiral pyrrolidine frameworks are recognized as privileged scaffolds in asymmetric synthesis [178–180], further underscoring the synthetic utility of this methodology.

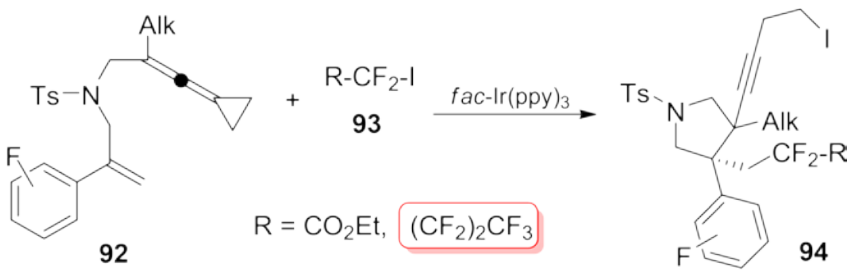

Scheme 35. Synthesis of fluorinated pyrrolidines.

Liang *et al.* (Scheme 36) [181] reported a visible-light-driven, photoredox-catalyzed radical cyclization between isocyanides **92** and thiols **93**, furnishing 2-thioquinoline derivatives **94** in an efficient and regioselective manner from readily available starting materials. Mechanistic studies suggest that the reaction may proceed via the *in situ* generation of either a sulfide radical cation or an α-thioalkyl radical, which undergoes addition to the isocyanide moiety, followed by intramolecular cyclization and/or intermolecular nucleophilic substitution to form the quinoline core. Reactions are performed in tetrahydrofuran (THF) with 2 equivalents of 1,8-diazabicyclo[5.4.0]undec-7-ene (DBU) as base, under ambient conditions. Photochemical activation is achieved using Ru(bpy)$_3$(PF$_6$)$_2$ (5 mol%) as the photocatalyst and blue LED irradiation, with reaction times ranging from 16 to 32 hours. The methodology delivers 2-thioquinoline products **94** in yields of 42–97%, depending on substrate variation. Notably, both the isocyanide precursors and the final products feature mono-fluorine substitution on the benzene ring, contributing to the structural diversity and potential utility of this protocol in fluorine-rich heterocyclic library construction.

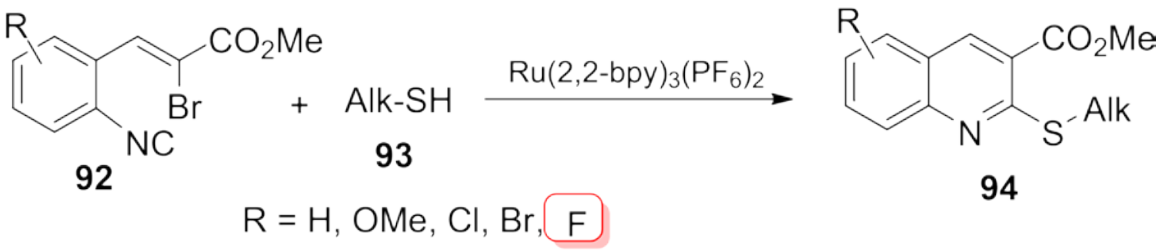

Scheme 36. Synthesis of 2-thioquinolines.

Liu *et al.* (Scheme 37) [182] disclosed a visible-light-promoted strategy for the synthesis of α-trifluoromethylamines **97** and *N*-trifluoroethylamine derivatives **98** via C,N-selective heteroarylation of *N*-trifluoroethyl hydroxylamine reagents **96** with quinoxalin-2(1*H*)-ones **95** under ambient conditions. The reaction's chemoselectivity—favoring either trifluoroalkylation or *N*-trifluoroethylamination—is readily modulated by the structural design of the hydroxylamine substrate. In particular, the protecting group on the nitrogen atom plays a pivotal role by governing the 1,2-hydrogen shift of the in situ-generated *N*-trifluoroethyl radical. This methodology features mild reaction conditions, operational simplicity, high selectivity, and broad functional group tolerance. More importantly, the resulting trifluoroalkylated products can be efficiently elaborated into diverse analogs with promising applications in pharmaceutical development. Reactions are conducted in acetonitrile with K_3PO_4 as additive, using *fac*-Ir(ppy)$_3$ (2 mol%) as the photocatalyst under 24 W purple LED irradiation for 36 hours. Products **97** and **98** are isolated in yields of up to 97%. Beyond the incorporation of an aliphatic trifluoromethyl group, the synthesized heterocyclic amine derivatives also display aromatic fluorination, enabling access to compound libraries with varied fluorine substitution patterns—a feature of high relevance for medicinal chemistry and biological profiling.

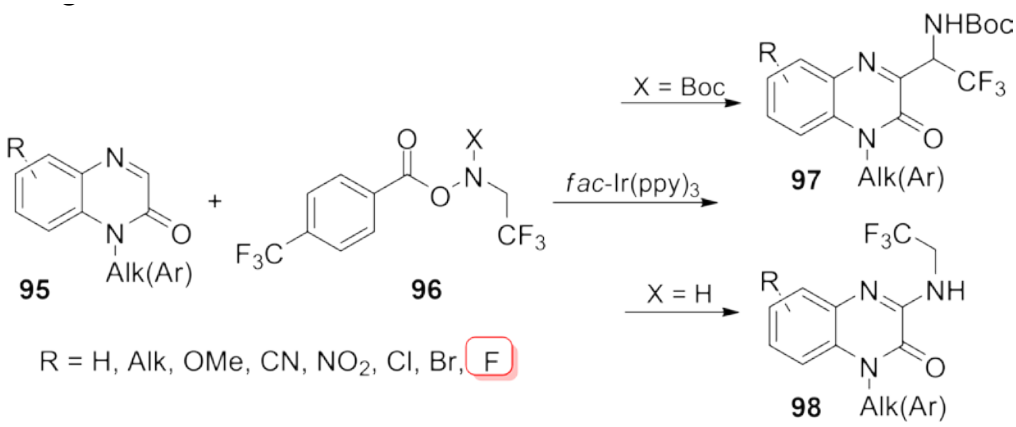

Scheme 37. Synthesis of fluorinated quinoxalin-2(1*H*)-ones.

ISSN 2708-129X. Укр. хім. журн., 2026

It is worth noting that the α-trifluoromethyl amino compounds discussed above can be conveniently accessed from corresponding aldehydes and ketones via a biomimetic transamination pathway [183-185], commonly referred to as a [1,3]-proton shift reaction [186-188]. Specifically, 2,2,2-trifluoroethylamine, employed in reagent **96**, can be synthesized through a double [1,3]-proton shift sequence starting from trifluoroacetic acid and benzylamine, as illustrated in Scheme 38 [189].

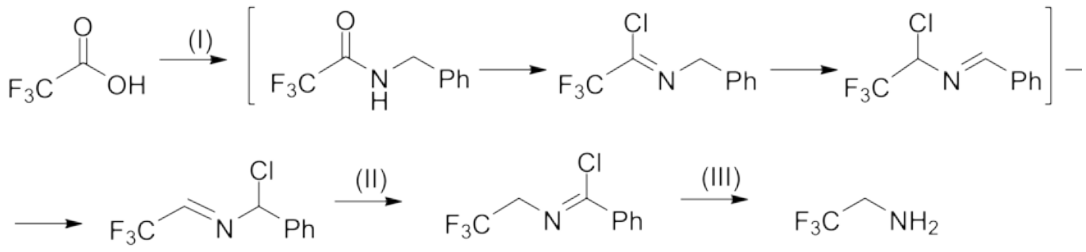

Key: (I) $BnNH_2$ (1 eq), Ph_3P (4 eq)/CCl_4 (4 eq), TEA (1.5 eq), $CHCl_3$ reflux, 40 min.; (II) TEA (3 eq)/H_2O; (III) MeOH/HCl (conc), reflux, 24 hr

Scheme 38. Synthesis of 2,2,2-trifluoroethylamine via [1,3]-proton shift reaction.

Coumarin (2*H*-1-benzopyran-2-one) and its derivatives exhibit a broad spectrum of pharmacological activities, including anti-inflammatory, antibacterial, antiviral, antioxidant, antithrombotic, anti-Alzheimer, and anticancer properties [190]. In this context, Tan *et al.* (Scheme 39) [191] reported a visible-light-induced, photoredox-catalyzed tandem radical addition/cyclization of 2-alkenylphenols **99** with carbon tetrabromide (CBr_4) to access a variety of 4-arylcoumarins **100** in a one-pot fashion. The reaction proceeds under mild, redox-neutral conditions and demonstrates good functional-group tolerance, operational simplicity, and scalability. Preliminary mechanistic studies confirm the radical nature of the process and highlight the essential role of water as an additive. The transformation is typically conducted in CH_2Cl_2 at ambient temperature with water (5 equiv.) and K_2CO_3 (1.5 equiv.), using *fac*-Ir(ppy)$_3$ (2 mol%) as photocatalyst and 7 W blue LEDs for irradiation. The desired coumarin derivatives **100** are isolated in yields ranging from 52% to 95%. Importantly, fluorination in the final products **100** may be introduced on both aromatic rings, either as monofluorinated substituents or in combination with trifluoromethyl groups, offering considerable structural diversity. This enables the design of fluorinated coumarin derivatives with enhanced medicinal relevance and tunable physicochemical profiles.

Fluorinated indoles are widely recognized as valuable end products due to their potent bioactivity. However, they also serve as versatile synthetic intermediates for accessing more complex molecular architectures with desirable biological and physicochemical properties [192]. In this context, Wu *et al.* (Scheme 40) [193] developed a visible-light-driven oxidative cyclization protocol utilizing fluorinated 3-alkenylindoles **101** and styrene **102** to construct carbazole derivatives **103**. The transformation is enabled by Ir(dtbbpy)(ppy)$_2$PF$_6$

(2 mol%) under aerobic conditions, where the substrate pair undergoes a tandem [2+2] cycloaddition followed by rearrangement, delivering the targeted carbazole frameworks in good to excellent yields (50–79%). Mechanistic studies reveal that the process proceeds through photoinduced energy transfer, subsequently followed by electron transfer, establishing a dual activation pathway. Reactions are performed in a CH_2Cl_2/DMSO solvent system under blue LED irradiation at ambient temperature for 12 hours.

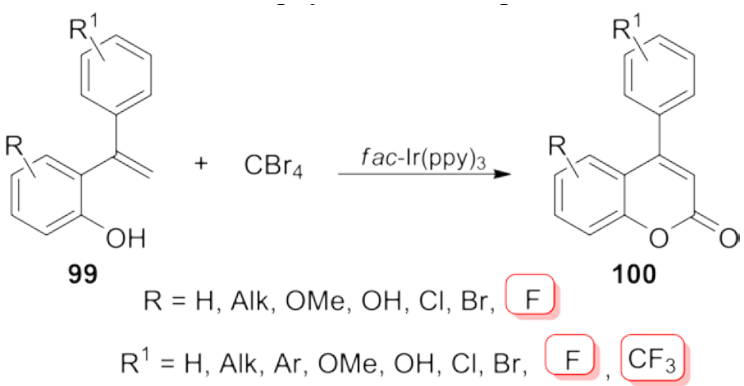

Scheme 39. Synthesis of fluorinated 4-arylcoumarins.

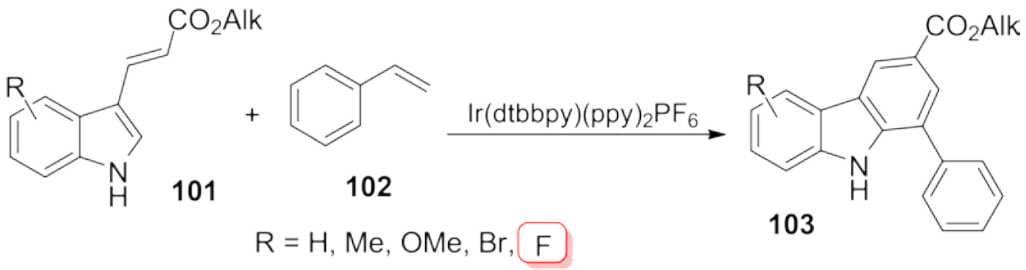

Scheme 40. Synthesis of fluorinated carbazoles.

Chen *et al.* (Scheme 41) [194] reported a visible-light-induced alkoxycarbonyl-radical-triggered cascade cyclization of 1,7-enynes **104** using alkyloxalyl chlorides **105** as esterifying agents, enabling the efficient synthesis of benzo[*j*]phenanthridine derivatives **106**. The methodology demonstrates broad compatibility with diverse alkoxycarbonyl radical precursors and achieves selective incorporation of ester functionalities into polycyclic frameworks. This radical cascade exhibits mild reaction conditions, excellent functional group tolerance, and yields ranging from 52% to 95%. The transformation is typically conducted in acetonitrile at 40–50 °C for 36 hours, employing 2,6-lutidine as a base to neutralize evolving HCl. Photochemical activation is accomplished using $Ir(ppy)_3$ (2 mol%) under blue LED irradiation. Importantly, the protocol allows strategic fluorine incorporation—either a single fluorine atom or a trifluoromethyl group—on both aromatic rings adjacent to the

alkyne moiety in the starting enynes **104**, and correspondingly in the final products **106**. This structural flexibility enhances the method's utility for constructing fluorine-rich polycyclic compounds, supporting the development of tailored molecular scaffolds for medicinal chemistry and bioactivity profiling.

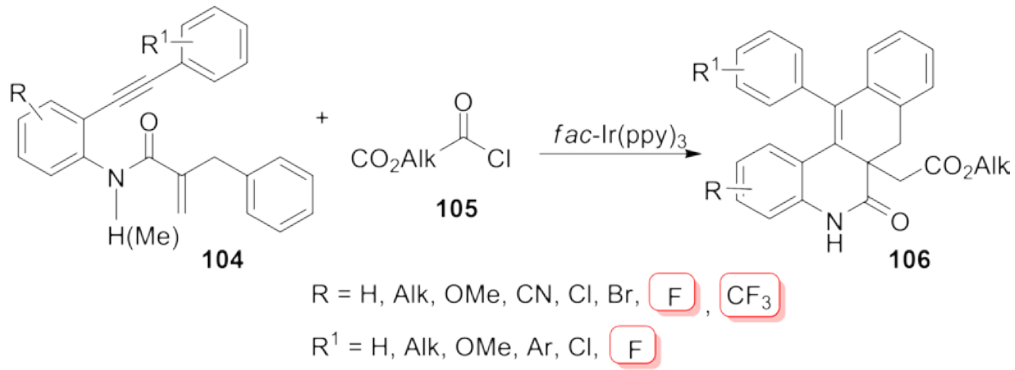

Scheme 41. Synthesis of ester-substituted benzo[*j*]phenanthridines.

Cyclopropane α-amino acids represent a compelling class of sterically constrained amino acid derivatives, with both naturally occurring and synthetic examples attracting sustained interest in medicinal chemistry and drug discovery [52, 195]. Their rigid three-membered ring imparts unique conformational properties, making them valuable scaffolds for modulating biological activity and metabolic stability. Of particular significance are fluorinated cyclopropane α-amino acids, which are being intensively investigated as key structural motifs in the design of highly potent inhibitors targeting the hepatitis C virus (HCV) NS3/4A protease [196–198]. These fluorinated analogs contribute to improved lipophilicity, binding affinity, and resistance to enzymatic degradation—features critical to antiviral therapeutic development. In this context, Huang *et al.* (Scheme 42) [199] reported an efficient strategy for the synthesis of cyclopropane-fused indolines **109** via a photoredox-catalyzed dearomative cyclopropanation of indole derivatives **107** with reagent **108**. The methodology accommodates a broad array of functionalized indoles and proceeds under mild conditions, delivering the desired products in moderate to excellent yields. To demonstrate the synthetic utility, reactions were successfully scaled to 5 mmol and product derivatizations were performed, highlighting the versatility of the approach. The transformation is conducted in DMSO at ambient temperature using $Ir[dF(CF_3)ppy]_2(dtbbpy)]PF_6$ (3 mol%) as photocatalyst under 3 W blue LED irradiation for 24 hours. The resulting cyclopropane amino acid-fused indolines **109** are obtained in 30–93% yields depending on substrate variation. Importantly, fluorination is introduced through various fluorine substituents positioned on the aromatic rings of both the starting indoles **107** and the final products **109**. This flexible fluorine incorporation expands the structural diversity of the indoline scaffolds and supports the construction of fluorinated compound libraries for medicinal chemistry and molecular optimization studies.

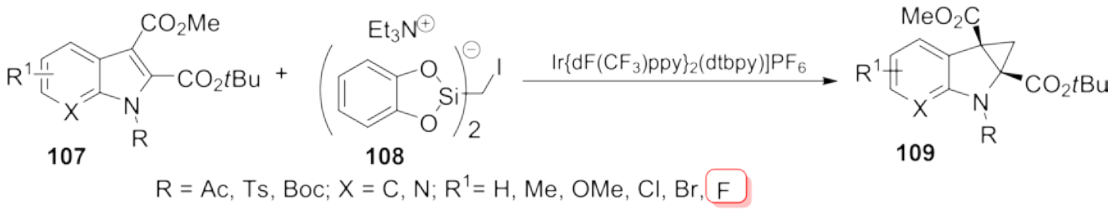

Scheme 42. Preparation of cyclopropane fused indolines.

Xie *et al.* (Scheme 43) [200] reported a visible-light-induced radical cascade reaction between 2-alkynylarylethers **110** and sodium sulfinates **111**, enabling the efficient synthesis of sulfonyl-functionalized dihydrobenzofurans **112**. The transformation proceeds via an intramolecular 1,5-hydrogen atom transfer (1,5-HAT) mechanism, followed by C–C bond formation that constructs the dihydrobenzofuran core in a streamlined manner. The protocol demonstrates broad substrate scope, accommodating various substituents on both 2-alkynylarylethers **110** and sodium sulfinates **112** and affords the target products **112** in moderate to good yields (20–78%). Reactions are performed in a mixture of acetic acid and water under a nitrogen atmosphere for 24 hours. Photochemical activation is achieved using $Ir(ppy)_2(dtbbpy)]PF_6$ (2 mol%) as the catalyst, with 30 W blue LEDs serving as the light source. Fluorination is incorporated through either mono-fluorine atoms or trifluoromethyl groups positioned on the aromatic ring of the starting materials **110** and retained in the final dihydrobenzofuran products **112**. This versatility supports the generation of fluorinated heterocycles with potential relevance for medicinal chemistry, structure–activity exploration, and property tuning.

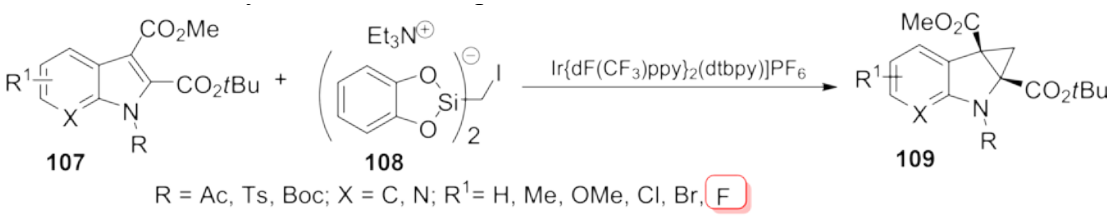

Scheme 43. Synthesis of dihydrobenzofurans.

Zhang *et al.* (Scheme 44) [201] reported a mild and efficient protocol for the synthesis of substituted quinazolines **115** via visible-light-induced benzylic C–H functionalization, employing benzophenones **113** and benzylamines **114** as starting materials. The transformation proceeds under a nitrogen atmosphere at room temperature, using *tert*-butyl peroxybenzoate (TBPB) (4 equiv.) as the radical initiator and Li_2CO_3 (3 equiv.) as a base, with $Ir(ppy)_3$ (1 mol%) as the photocatalyst and blue LED irradiation for 12 hours. The reaction exhibits high chemoselectivity and affords the quinazoline products **115** in yields

ranging from 45% to 85%. Fluorine incorporation is achieved using trifluoromethyl-substituted benzylamines **114**, which translate into trifluoromethylphenyl motifs in the final quinazoline products **115**, enhancing their potential for medicinal chemistry applications.

It is worth noting that both starting materials are readily available and synthetically versatile.

Ortho-amino benzo- and acetophenones **113** are widely utilized in the synthesis of benzodiazepines [202] and in the design of tridentate ligands for asymmetric synthesis of tailor-made amino acids [203–206]. Trifluorobenzylamines **114** have found application in biomimetic transamination strategies, contributing to the synthesis of fluorinated amines and bioactive scaffolds [207–209].

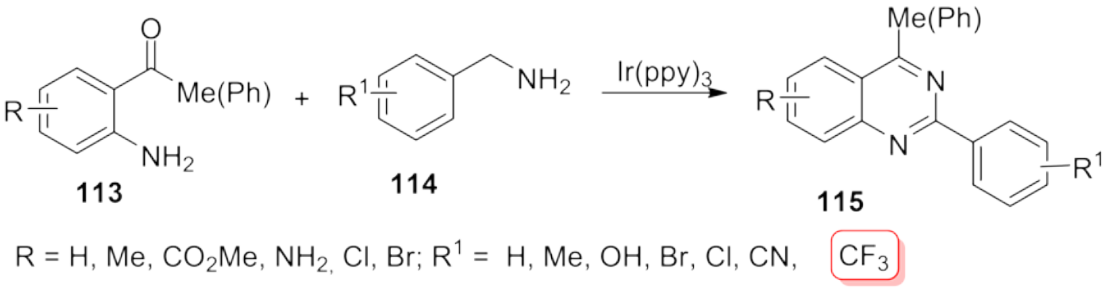

Scheme 44. Synthesis of 2-arylquinazolines.

Wang *et al.* (Scheme 45) [210] reported a visible-light-accelerated C–H annulation strategy catalyzed by $[Cp^*RhCl_2]_2$ (2.5 mol%), enabling the synthesis of bridged tetrahydrobenzocarbazoles **118** from aromatic amines **116** and bicyclic alkenes **117**. This transformation leverages the synergistic effect of rhodium catalysis and visible-light irradiation (40 W blue LEDs), allowing diverse **116** substrates to react efficiently with azabicyclic alkenes **117** under ambient conditions. The reactions are typically performed in 1,2-dichloroethane (DCE) under an argon atmosphere at room temperature for 12 hours, affording the desired bridged oxa- or aza-tetrahydrobenzocarbazoles **118** in good to excellent yields (53–98%). Fluorination is introduced via the starting anilines **116**, which may bear either a monofluorine substituent or a trifluoromethyl group, contributing to the structural diversity and potential pharmacological relevance of the final products **118**.

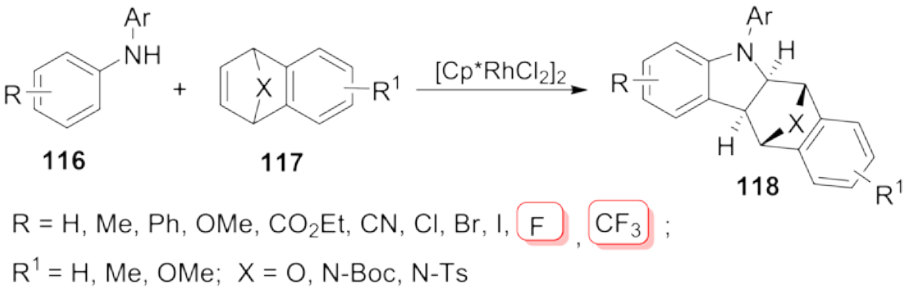

Scheme 45. Synthesis of tetrahydro benzocarbazoles.

Indoles represent a cornerstone scaffold in drug design, prized for their broad-spectrum biological activity and ability to engage diverse molecular targets. Found extensively in both natural products and synthetic pharmaceuticals, indole-based compounds play pivotal roles in anticancer, antimicrobial, anti-inflammatory, and neuroprotective therapies. Their structural flexibility allows medicinal chemists to fine-tune potency, selectivity, and bioavailability, making indoles indispensable in contemporary drug discovery efforts [211–214].

A wide array of synthetic strategies has been developed for the construction of indole derivatives [215–218], including those bearing fluorine substituents, which enhance metabolic stability and target specificity [219–222]. In this work, we have already discussed several methodologies for the preparation of indole-based compounds. The following sections will further expand on the application of indoles and their derivatives as both starting materials and products in a variety of innovative photochemical transformations, highlighting their continued relevance in synthetic and medicinal chemistry.

Fluorine-containing tryptophans are biologically significant compounds with intrinsic pharmacological relevance [223–225]. Their use as starting materials is particularly attractive, as they enable the construction of indole-based scaffolds bearing pharmacophoric units, thereby expanding the chemical space for drug discovery. In this context, Li *et al.* (Scheme 46) [226] reported a facile and efficient synthesis of multi-substituted *trans*-fused hexahydrocarbazoles **121** via a stereoselective intermolecular radical cascade reaction between readily available substituted tryptophans **119** (including fluorinated variants) and acrylamides **120**. The transformation is enabled by visible-light-induced photoredox catalysis, delivering the target products in up to 82% yield with >20:1 diastereoselectivity, and forming four stereocenters, including two quaternary centers. Interestingly, when the reaction is conducted under ambient air, the major products shift toward tetrahydrocarbazoles, suggesting oxygen influences the radical pathway. Preliminary mechanistic studies indicate a sequence involving radical addition cascades followed by radical–polar crossover events. The reactions are performed in DMA at 30 °C under an argon atmosphere, using Na_2CO_3 (3 equiv.) as a base. Photochemical activation is achieved with $Ir[dF(CF_3)ppy]_2(dtbbpy)]PF_6$ (1 mol%) under blue LED irradiation. Fluorination is introduced through multiple vectors: the trifluoromethyl group on the starting 2-(trifluoromethyl)acrylamides **120** and fluorine atoms on the aromatic rings of both **119** and **120**, resulting in multi-fluorinated hexahydrocarbazole products **121** with enhanced structural and physicochemical diversity.

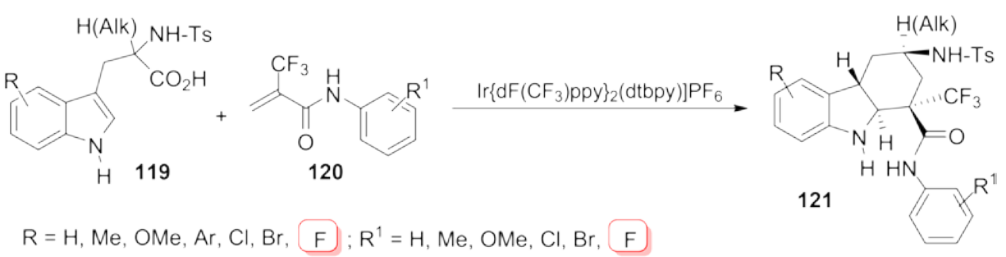

Scheme 46. Synthesis of fluorinated hexahydrocarbazoles.

The stereochemical outcome of these reactions warrants particular emphasis. The simultaneous formation of four stereogenic centers with exceptional diastereoselectivity (>20:1) is a remarkable achievement, underscoring the stereocontrolling influence of the trifluoromethyl group [227, 228]. Such high-level stereochemical precision is rarely observed in radical cascade processes and highlights the strategic value of fluorinated motifs in stereoselective synthesis. Moreover, the 2-(trifluoromethyl) acrylamides **120** employed in these transformations are exceptionally reactive Michael acceptors, owing to the strong electron-withdrawing nature of the CF_3 group. Their reactivity has been successfully harnessed in the synthesis of trifluoromethylated derivatives of glutamic acid and related analogs, expanding their utility in the construction of fluorine-rich bioactive frameworks [229–231].

Kim *et al.* (Scheme 47) [232] reported a direct C–H functionalization/cyclization of acetanilides **122** with alkyne derivatives **123**, enabled by a dual catalytic system involving photoredox and transition-metal catalysis. The reaction employed a readily available photoredox catalyst, $[Ru(dtbbpy)_2(bpy)]PF_6$ (1 mol%), in combination with $[RhCp^*Cl_2]_2$ (2 mol%), a well-established catalyst for C–H activation. Under irradiation with an 11 W compact fluorescent lamp (CFL), the transformation proceeded smoothly to furnish indoles **124** in good yields (33–88%). Mechanistic investigations revealed that each catalyst operates independently, contributing distinct roles to the overall transformation. The reactions were carried out in chlorobenzene at 120 °C for 12 hours, with $AgSbF_6$ (8 mol%) as an additive to facilitate catalyst activation. Fluorinated motifs were incorporated both as fluorine atoms and trifluoromethyl groups on the starting anilines **122**, and these substituents were retained on the benzene ring of the resulting indoles **124**, highlighting the method's compatibility with fluorinated substrates.

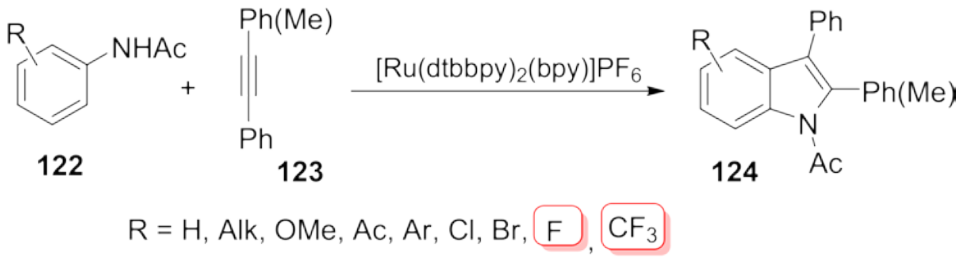

Scheme 47. Synthesis of fluorinated indoles.

Lin *et al.* (Scheme 48) [233] reported a mild and efficient protocol for the visible-light-induced radical cascade difluoromethylation/cyclization of indoles bearing unactivated alkenes **125**. The transformation utilizes a bench-stable and readily accessible difluoromethyltriphenylphosphonium bromide **126** as a precursor for the $-CF_2H$ group, enabling the synthesis of CF_2H-substituted polycyclic indole derivatives **127** in moderate to good yields (50–90%). This strategy is notable for its ability to construct $C(sp^3)–CF_2H$ and C–C bonds under additive-free conditions, with simple operational setup, ambient temperature, and a broad

substrate scope. Mechanistic investigations confirm the involvement of a difluoromethyl radical pathway as central to the transformation. Reactions are performed in acetonitrile at room temperature for 16 hours, using *fac*-Ir(ppy)$_3$ (2 mol%) as the photocatalyst under 5 W blue LED irradiation. Fluorine substituents are incorporated both on the aromatic rings of the starting indoles **125** and retained in the final polycyclic products **127**, contributing to the structural and physicochemical diversity of the resulting compounds.

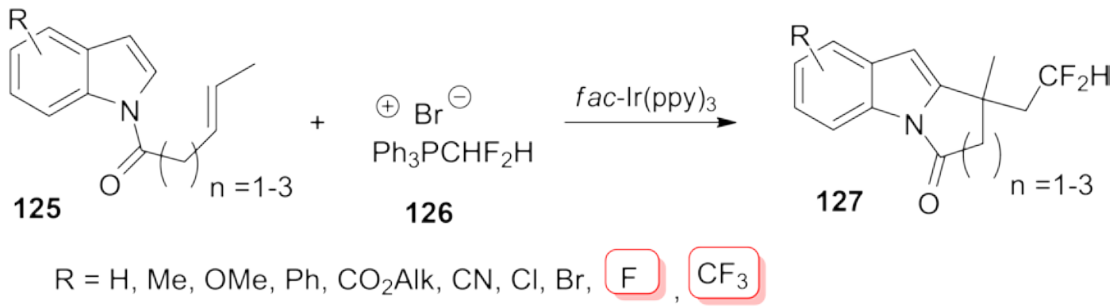

Scheme 48. Preparation of difluoromethyl-containing indoles.

Owing to the strong electron-withdrawing effect of fluorine, fluorinated benzaldehydes exhibit high reactivity, particularly in asymmetric aldol addition reactions [234–236]. Leveraging this reactivity, Liu *et al.* (Scheme 49) [237] developed a visible-light-induced dual acylation strategy involving fluorobenzaldehydes tethered to alkenes **128** for the synthesis of 3-substituted chroman-4-ones **130**. The transformation proceeds via a radical tandem cyclization, initiated by carbon–carbon bond cleavage of oxime esters **129** through a nitrogen-centered radical pathway. This method enables the efficient construction of chroman-4-one frameworks, delivering a series of 3-substituted chroman-4-ones **130** in yields up to 86%. Reactions are typically conducted in acetone at 80 °C for 24 hours, using 2,6-lutidine (1 equiv.) as a base. Photochemical activation is achieved with Ir(ppy)$_3$ as the photocatalyst under 5 W blue LED irradiation. Fluorine substituents, either as single fluorine atoms or trifluoromethyl groups, are incorporated on the aromatic rings of the final chromanone products **130**, contributing to their electronic diversity and potential bioactivity.

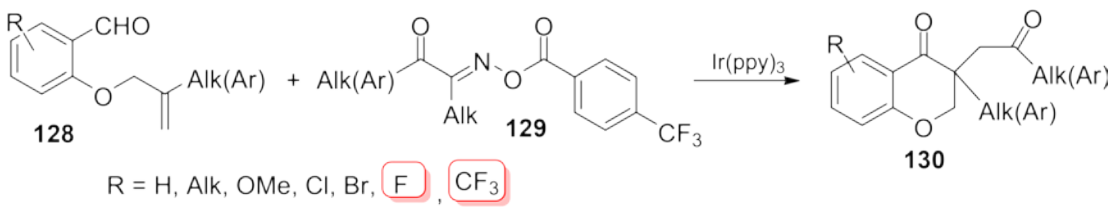

Scheme 49. Synthesis of 3-substituted chroman-4-ones.

Fluorinated imines are versatile intermediates in organic synthesis, widely employed as precursors for the construction of fluorine-containing amines and amino acids [238–240]. In this context, the photochemical protocol reported by Li and Zhou (Scheme 50) [241] presents a mechanistically intriguing transformation, wherein the fluorine pattern of the starting imine differs from that of the final product. Specifically, the reaction involves the loss of one fluorine atom and a conversion from aliphatic to aromatic fluorination, representing a rare synthetic event. The methodology utilizes vinyldiazo reagents **132** as radical acceptors in a visible-light-promoted sequential radical cyclization, enabling a [3+3] cyclization pathway that is mechanistically distinct from conventional annulation strategies. Starting from *N*-aryl chlorodifluoromethyl alkynyl ketoimines **131**, the reaction facilitates the construction of acridine frameworks **133**, incorporating a fluorine atom into the acridine core during the simultaneous formation of both pyridine and benzene rings from acyclic precursors. The resulting 4-fluoroacridines **133** exhibit pronounced solid-state fluorescence, underscoring their potential utility in materials science and photonic applications. Reactions are typically conducted in dichloromethane (DCM) at ambient temperature for 18 hours, using Hünig's base (3 equiv.) to scavenge acidic byproducts. Photochemical activation is achieved with $Ru(bpy)_3Cl_2$ (1 mol%) under 5 W blue LED irradiation, affording mono-fluorinated acridines in yields ranging from 37% to 79%.

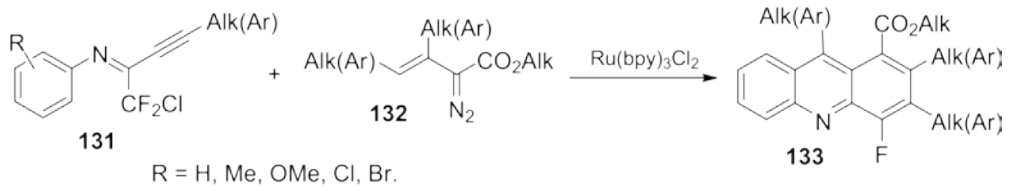

Scheme 50. Synthesis of 4-fluoroacridines.

Xue *et al*. (Scheme 51) [242] reported a sustainable and efficient protocol for the synthesis of *O*-heterocycle spiro-fused cyclopentaquinolinone derivatives **136** via a visible-light-driven radical cascade reaction between *N*-(*o*-ethynylaryl)acrylamides **134** and *O*-heterocycles **135**. Mechanistic studies revealed that the transformation is initiated by visible-light-induced radical generation from the *O*-heterocycle, followed by regioselective radical addition onto the acrylamide moiety. This triggers a cascade involving 6-*exo*-*dig* and 5-*endo*-*trig* radical annulations, which are terminated by single-electron oxidation and proton elimination to furnish the spirocyclic products. The protocol features broad substrate scope, extremely mild reaction conditions, excellent atom economy, high efficiency, and good compatibility with diverse functional groups. Reactions are performed under an argon atmosphere using TBPB (2 equiv.) as a radical initiator, *fac*-$Ir(ppy)_3$ as the photocatalyst, and 8 W blue LED irradiation for 18 hours. The desired spiro-fused cyclopentaquinolinones **136** are obtained in yields of up to 96%. Fluorination is introduced via mono-fluorine substitution on the aromatic ring of the starting acrylamides **134** and is retained in the final products **136**, contributing to their electronic and structural diversity.

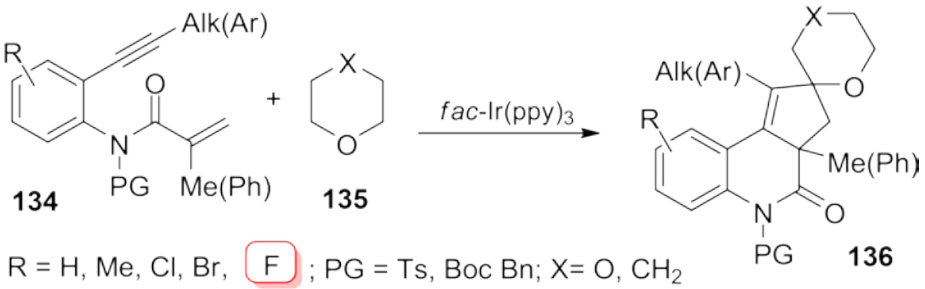

Scheme 51. Synthesis of *O*-heterocycle spiro-fused cyclopentaquinolinones.

Trimolecular reactions.

Trimolecular photochemical reactions are extremely rare. A true trimolecular reaction involves the simultaneous collision of three reactant species in a single elementary step. In the context of photochemistry, this would require three molecules to interact under light activation to form products directly, without intermediates. The rarity of such processes arises from several fundamental constraints. One major limitation is the low probability of three-body collisions. The likelihood of three molecules colliding simultaneously, with the correct orientation and sufficient energy, is less than 0.1% compared to bimolecular collisions. This statistical improbability makes trimolecular elementary steps kinetically unfavorable under typical reaction conditions. Another critical factor is the distribution of energy and momentum during such collisions. Even if three molecules do collide, the energy must be partitioned in a way that allows bond formation without immediate dissociation. Often, a third molecule is required to absorb excess energy, but this typically occurs in stepwise mechanisms rather than true trimolecular elementary reactions. Mechanistic complexity further limits the feasibility of trimolecular photochemical reactions. Most reactions that appear trimolecular are actually pseudo-trimolecular, proceeding through the formation of a binary intermediate that subsequently reacts with a third species. In photochemistry, excited states typically undergo unimolecular or bimolecular transformations. The involvement of three species in a concerted photochemical event is both kinetically and spectroscopically difficult to observe or validate. Additionally, the radical nature of many photochemical reactions introduces further challenges. Radicals are highly reactive and can follow multiple competing pathways, making it difficult to orchestrate a trimolecular process that proceeds selectively through a single route. As a result, successful examples of trimolecular photochemical reactions are exceedingly rare and represent significant theoretical and practical interest in reaction design and mechanistic exploration [243,244].

Liang *et al.* (Scheme 52) [245] reported a visible-light-driven strategy for the synthesis of valuable perfluoroalkylated dihydrobenzoxazines **140** via a perfluoroalkyl radical-mediated cascade reaction. The transformation involves the reaction of *N*-tosyl-2-vinylanilines **137**, Umemoto's reagents **138**, and aldehydes **139** under photoredox conditions. The reactions are carried out in dichloromethane (CH_2Cl_2) at 5 °C in the presence of sodium acetate (NaOAc) as a base additive. Photochemical ac-

tivation is achieved using $Ir(ppy)_2(dtbbpy)PF_6$ (2 mol%) as the photocatalyst under 3 W blue LED irradiation for 4 hours. The method affords perfluoroalkylated dihydrobenzoxazines **140** in good to excellent yields, ranging from 54% to 80%. Notably, the transformation is enabled by the radical reactivity of Umemoto's reagents **138**, which serve as perfluoroalkyl group donors. Fluorination is further represented by mono-fluorine and trifluoromethyl substituents on the aromatic rings of the starting *N*-tosyl-2-vinylanilines **137**. These fluorine motifs are retained in the final products **140**, allowing for structural diversity with one to three fluorine atoms per molecule. This modular approach enables the synthesis of fluorinated heterocycles with potential applications in agrochemicals and pharmaceuticals, owing to the physicochemical properties imparted by the perfluoroalkyl groups.

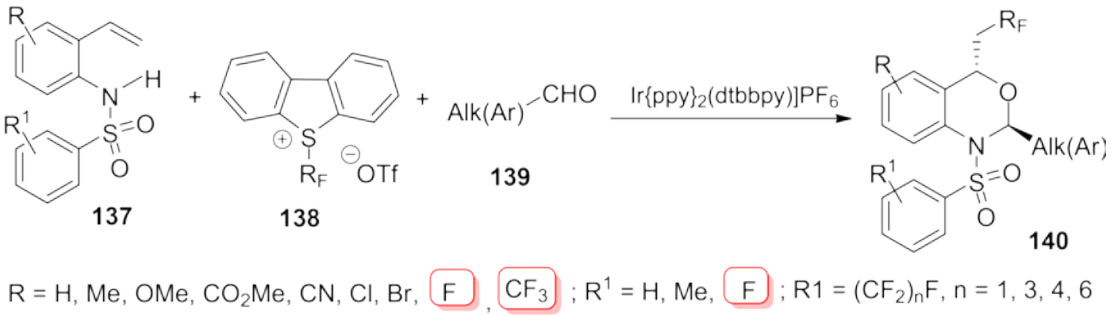

Scheme 52. Synthesis of fluorinated dihydrobenzoxazines.

However, it is crucial to recognize that while certain perfluorinated compounds have found valuable applications in life sciences and materials chemistry, a significant subset—collectively known as per- and polyfluoroalkyl substances (PFAS)—pose substantial environmental and public health risks. These "forever chemicals" are characterized by extreme persistence, bioaccumulative behavior, and mobility in ecosystems, leading to widespread contamination of soil, water, and biota. Their resistance to degradation and tendency to biomagnify through food webs have prompted increasing regulatory scrutiny and calls for safer alternatives [147–149].

Geng *et al.* (Scheme 53) [246] developed a visible-light-driven three-component cyclization that enables the direct synthesis of pyrimido[1,2-*b*]indazole derivatives **144** through the in situ trapping of a 1,3-vinylimine ion intermediate. The reaction proceeds under mild conditions from bromodifluoroacetic acid derivatives **141**, enaminones **142**, and 3-aminoindazoles **143**. Notably, this robust methodology allows for the efficient incorporation of aliphatic substituents and demonstrates excellent compatibility with structurally complex bioactive molecules. This transformation represents the first example of a photoinduced multicomponent reaction employing bromodifluoroacetic acid derivatives as a C1 synthon. The reactions were carried out in DMSO at room temperature using *fac*-$Ir(ppy)_3$ (2 mol%) as the photocatalyst under blue LED irradiation for five hours. The desired pyrimido[1,2-*b*]indazole products **144** were obtained in moderate to good yields, ranging from 40% to 79%. Despite their initial fluorinated structure, both

fluorine atoms from the bromodifluoroacetic acid derivatives **141** are lost during the course of the reaction. Nevertheless, fluorination is retained through aromatic substitution on the 3-aminoindazole starting materials **143**, which is preserved in the final heterocyclic products **144**. The resulting pyrimido[1,2-*b*]indazoles **144** offer structural diversity and potential relevance in medicinal chemistry due to their fused heterocyclic architecture and tunable fluorine content.

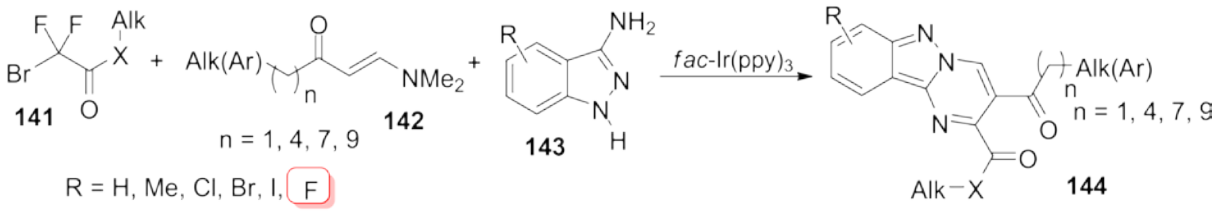

Scheme 53. Preparation of pyrimido[1,2-*b*]indazole derivatives.

Manna and Prabhu (Scheme 54) [247] reported a visible-light-mediated three-component difunctionalization of activated alkynes **145** using boronic acids **146** and hypervalent iodine reagents **147**, enabling the synthesis of 3-alkylated coumarins **148**. The *para*-substituent on the aryl ring of the aryl alkynoate was found to be crucial for directing selective chain alkylation, facilitating coumarin formation under mild conditions. Reactions were performed in 1,2-dichloroethane (DCE) at room temperature over 8–12 hours, employing $Ru(bpy)_3Cl_2$ (0.5 mol%) as the photocatalyst under visible-light irradiation. The desired coumarin products **148** were obtained in yields of up to 60%. Fluorinated motifs were incorporated via mono-fluoro or trifluoromethyl substitutions on the aromatic ring or within the ester/amide fragments of the starting alkynes **145**, showcasing the method's compatibility with fluorinated substrates.

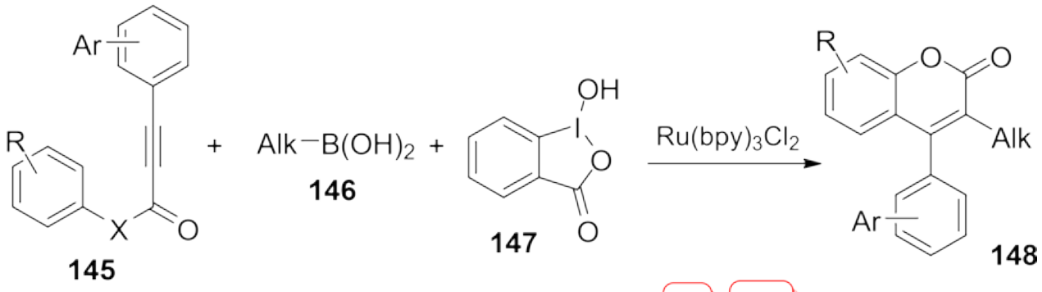

Scheme 54. Synthesis of coumarins.

ISSN 2708-129X. Укр. хім. журн., 2026

CONCLUSIONS.

In sum, photochemistry reimagines light not as a passive illuminator but as a precise and sustainable reagent—unlocking synthetic possibilities with elegance and minimal environmental cost. It is no exaggeration to state that many of the reactions described in this review would be inaccessible under conventional thermal, acid–base, or redox conditions. Photochemical activation enables unique reactivity patterns, particularly through radical pathways, that allow for the rapid construction of complex molecular architectures.

That said, photochemistry is not universally applicable. Certain structural targets and reactivity types remain beyond theirreach, and the approach carries inherent limitations. One key challenge lies in the architectural design of starting materials: the spatial arrangement and positioning of reactive functional groups must be meticulously orchestrated to ensure productive radical engagement. This requirement stems from the mechanistic nature of photochemical reactions, which often proceed through highly selective and transient radical intermediates. Another limitation is the labor-intensive optimization process. Small changes in reaction parameters—such as photocatalyst identity, light source, solvent, or additives—can dramatically affect the outcome. The search for ideal conditions can be extensive, yet when successful, photochemical methods offer unmatched efficiency, functional group tolerance, and scalability. Most reactions proceed under ambient conditions and require only catalytic amounts of photocatalyst, typically around 1 mol%, simplifying product isolation and purification. Fluorination plays a prominent role in many of these transformations. Fluorine is introduced in diverse forms, including mono-fluoro, trifluoromethyl, perfluoroalkyl, trifluoromethoxy, and pentafluorosulfanyl groups. Fluorinated reagents are frequently employed, and multiple fluorine substitutions are often retained in the final products. This versatility makes photochemical synthesis particularly valuable for constructing fluorinated heterocycles with relevance to medicinal chemistry and pharmaceutical development. Notably, asymmetric photochemical transformations remain underexplored. The scarcity of enantioselective protocols suggests that this field is still in its early stages. Given the importance of chiral fluorinated compounds in drug design, future research is expected to focus on enantiocontrolled photochemical methodologies for fluorinated heterocyclic scaffolds. Overall, photochemistry represents a vibrant and rapidly evolving area of synthetic research, offering vast potential for innovation. As the field continues to expand, we anticipate exciting developments that will further redefine the boundaries of molecular construction.

AUTHORS' CONTRIBUTION. All authors have read the research results and approved the final version of the manuscript.

CONFLICT OF INTEREST. The authors declare no conflict of interest.

ACKNOWLEDGMENTS. We gratefully acknowledge the financial support from IKERBASQUE, Basque Foundation for Science (for Soloshonok). The authors acknowledge the assistance of Microsoft Copilot and Google Gemini for their support in translating to Ukrainian.

ОСТАННІ ДОСЯГНЕННЯ У ФОТОХІМІЧНИХ ПІДХОДАХ ДЛЯ ОТРИМАННЯ ФТОРОВМІСНИХ ГЕТЕРОЦИКЛІВ (огляд)

Аліція Взорек,[1] Таїзо Оно,[2] Даніель Беккер,[3] Вей Чжан,[4] Вадим А. Солошонок,[5]*

[1] Хімічний інститут, Університет Яна Кохановського в Кельці, вул. Університетська 7, 25-406 Кельце, Польща;
[2] Національний інститут передової науки та технологій (AIST), 2266-98, Анагахора, Шімошідамі, район Моріяма, Нагоя, 463-8560, Японія;
[3] Відділ фармацевтичної та лікарської хімії, Фармацевтичний інститут, Вільний університет Берліна, Кьонігін-Луїзе-Штрасе 2+4, 14195 Берлін, Німеччина;
[4] Хімічний факультет, Університет Массачусетса в Бостоні, Бостон, Массачусетс 02125, Сполучені Штати Америки;
[5] ІКЕРБАСКЕ, Баскська наукова фундація, вул. Марія Діас де Харо 3, Площа Бізкая, 48013 Більбао, Іспанія,
e-mail: vadimsoloshonok@gmail.com

Анотація: Фторовмісні гетероцикли займають центральне місце у фармацевтиці, агрохімії та матеріалознавстві завдяки своїм унікальним фізико-хімічним властивостям та широкій функціональній значущості. Прагнення до ефективних та екологічно стійких методів синтезу сприяло появі фотохімії як переконливої альтернативи традиційним підходам на основі термічної, кислотно-лужної чи окисно-відновної реакцій. Дійсно, багато із трансформацій, висвітлених у цьому огляді, були б недосяжними за звичайних умов, що підкреслює виняткову реакційну здатність, яку забезпечують процеси, що приводяться в рух світлом.

Цей огляд вивчає ключові досягнення за останнє десятиліття у фотохімічному синтезі фторованих гетероциклічних сполук. Він починається з огляду фундаментальних фотохімічних принципів і фотокаталізаторів, які використовують найчастіше. Потім обговорення продовжується, розподіляючи реакції на унімолекулярні, бімолекулярні та тримолекулярні класи. Унімолекулярні реакції, як правило, включають циклізацію стратегічно розроблених субстратів, здатних утворювати гетероциклічні структури після фотоактивації. Бімолекулярні реакції є найпоширенішим класом, де дві окремі компоненти надають взаємодоповнюючі фрагменти для побудови цільового гетероциклу. Натомість тримолекулярні фотохімічні реакції є надзвичайно рідкісними через властиві механістичні, кінетичні та просторові обмеження, пов'язані з тритільними взаємодіями в фотохімічних умовах.

Для кожної обговорюваної трансформації ми детально описуємо використаний фотокаталізатор, джерело опромінення, умови реакції та специфічний введений патерн фторування. Фотохімія переосмислює світло не просто як джерело енергії, а як точний і стійкий реагент, що відкриває синтетичні шляхи зі зручністю, селективністю та мінімальним впливом на довкілля.

Ця робота має на меті слугувати всебічним ресурсом для дослідників і практиків, які прагнуть використовувати фотохімічні

стратегії для синтезу фторованих гетероциклів, з акцентом на каталітичну ефективність, структурну різноманітність та екологічну відповідальність.

Ключові слова: хімія фтору, гетероцикли, органофтористі сполуки, фото-редокс каталіз, структурне різноманіття, зелена хімія, сталий синтез, вплив на довкілля.

REFERENCES

[1] Mai S., González L. Molecular photochemistry: recent developments in theory. *Angew. Chem. Internat. Ed.* 2020. **59**(39): 16832–16846. doi.org/10.1002/anie.201916381.

[2] George C., Ammann M., D'Anna B. *et al.* Heterogeneous photochemistry in the atmosphere. *Chem. Rev.* 2015. **115**(10): 4218–58. doi.org/10.1021/cr500648z.

[3] Szaciłowski K., Macyk W., Drzewiecka-Matuszek A. *et al.* Bioinorganic photochemistry: frontiers and mechanisms. *Chem. Rev.* 2005. 105(6): 2647–2694. doi.org/10.1021/cr030707e.

[4] Ashfold M.N., King G.A., Murdock D. *et al.* πσ* excited states in molecular photochemistry. *Phys. Chem. Chem. Phys*. 2010. **12**(6): 1218–1238. doi.org/10.1039/B921706A.

[5] Balzani V., Bergamini G., Campagna S., Puntoriero F. Photochemistry and photophysics of coordination compounds: overview and general concepts. Springer Berlin Heidelberg; 2007.

[6] Goti G., Manal K., Sivaguru J., Dell'Amico L. The impact of UV light on synthetic photochemistry and photocatalysis. *Nature Chem*. 2024. **16**(5): 684-692. doi.org/10.1038/s41557-024-01472-6.

[7] Öberg K.I. Photochemistry and astrochemistry: Photochemical pathways to interstellar complex organic molecules. *Chem Rev*. 2016. **116**(17): 9631–9663. doi.org/10.1021/acs.chemrev.5b00694.

[8] Gal J. Louis Pasteur, language, and molecular chirality. I. Background and dissymmetry. *Chirality*. 2011. **23**(1): 1–6. doi.org/10.1002/chir.20866.

[9] Brosseau C. Polarization and coherence optics: historical perspective, status, and future directions. Prog. Optics. 2010. **54**: 149–208. doi.org/10.1016/S0079-6638(10)05408-9.

[10] Panyala N.R., Peña-Méndez E.M., Havel J. Gold and nano-gold in medicine: overview, toxicology and perspectives. *J. Appl. Biomedic*. 2009. **7**(2): 75–91.

[11] Rabitz H., de Vivie-Riedle R., Motzkus M., Kompa K. Whither the future of controlling quantum phenomena? *Science*. 2000. **288**(5467): 824–828. DOI: 10.1126/science.288.5467.824.

[12] Thrush B.A. The genesis of flash photolysis. *Photochem. Photobiol. Scien*. 2003. **2**(5): 453–454. doi.org/10.1039/B212614C.

[13] Charlson R.J., Harrison H., Hardwick R. Efficient flash photolysis system. *Rev. Sci. Instr.* 1960. **31**. doi.org/10.1063/1.1716789.

[14] Windsor M.W. Flash photolysis and triplet states and free radicals in solution. *Photochem. Photobiol. Scien*. 2003. **2**(5): 455–458. doi.org/10.1039/B300213F.

[15] Song P.S., Tapley K.J. Photochemistry and photobiology of psoralens. *Photochem. Photobiol*. 1979. **29**(6): 1177–1197. doi.org/10.1111/j.1751-1097.1979.tb07838.x.

[16] Ciamician G. The photochemistry of the future. *Science*. 1912. **36**(926): 385–394. DOI: 10.1126/science.36.926.385.

[17] Watanabe K., Menzel D., Nilius N., Freund H. J. Photochemistry on metal nanoparticles. *Chem. Rev*. 2006. **106**(10): 4301–4320. doi.org/10.1021/cr050167g.

[18] Casasanta G., Falcini F., Garra R. Beer–Lambert law in photochemistry: A new approach. *J. Photochem. Photobiol*. 2022. **432**: 114086. doi.org/10.1016/j.jphotochem.2022.114086.

[19] Parnis J.M., Oldham K.B. Beyond the Beer–Lambert law: The dependence of absorbance

on time in photochemistry. *J. Photochem. Photobiol*. 2013. **267**: 6–10. doi.org/10.1016/j.jphotochem.2013.06.006.

[20] Mayerhöfer T.G., Pahlow S., Popp J. The Bouguer-Beer-Lambert law: Shining light on the obscure. *ChemPhysChem*. 2020. **21**(18): 2029–2046. doi.org/10.1002/cphc.202000464.

[21] Kisch H., Bahnemann D. Best practice in photocatalysis: comparing rates or apparent quantum yields? *J. Phys. Chem. Lett*. 2015. **6**(10): 1907–1910. doi.org/10.1021/acs.jpclett.5b00521.

[22] Stadler E., Eibel A., Fast D. *et al*. A versatile method for the determination of photochemical quantum yields via online UV-Vis spectroscopy. *Photochemi. Photobiol. Scien*. 2018. **17**: 660–669. doi.org/10.1039/c7pp00401j.

[23] Ishida H., Tobita S., Hasegawa Y. *et al*. Recent advances in instrumentation for absolute emission quantum yield measurements. *Coordin. Chem. Rev*. 2010. **254**(21-22): 2449–2458. doi.org/10.1016/j.ccr.2010.04.006.

[24] Daniel C. Photochemistry and photophysics of transition metal complexes: Quantum chemistry. *Coordin. Chem. Rev*. 2015. **282**: 19–32. doi.org/10.1016/j.ccr.2014.05.023.

[25] Hoffmann N. Photochemical reactions as key steps in organic synthesis. *Chem. Rev*. 2008. **108**(3): 1052–1103. doi.org/10.1021/cr0680336.

[26] Beeler A.B. Introduction: Photochemistry in organic synthesis. *Chem. Rev*. 2016. **116**(17): 9629–9630. doi.org/10.1021/acs.chemrev.6b00378.

[27] Liu J., Lu L., Wood D., Lin S. New redox strategies in organic synthesis by means of electrochemistry and photochemistry. *ACS Centr. Scien*. 2020. **6**(8): 1317–1340. doi.org/10.1021/acscentsci.0c00549.

[28] Hidaka M., Kojima M., Nakahata M., Sakai S. Visible light-curable chitosan ink for extrusion-based and vat polymerization-based 3D bioprintings. *Polymers*. 2021. **13**(9): 1382. doi.org/10.3390/polym13091382.

[29] Schneider O.D., Stepuk A., Mohn D. *et al*. Light-curable polymer/calcium phosphate nanocomposite glue for bone defect treatment. *Acta Biomaterialia*. 2010. **6**(7): 2704–2710. doi.org/10.1016/j.actbio.2010.01.033.

[30] Singh R., Unni K. N., Solanki A. Improving the contrast ratio of OLED displays: An analysis of various techniques. *Optical Mater*. 2012. **34**(4): 716–723. doi.org/10.1016/j.optmat.2011.10.005.

[31] Salehi A., Fu X., Shin D. H., So F. Recent advances in OLED optical design. *Adv. Func. Mater*. 2019. **29**(15): 1808803. doi.org/10.1002/adfm.201808803.

[32] Sinha R.P., Häder D.P. UV-induced DNA damage and repair: a review. *Photochem. Photobiol. Scien*. 2002. **1**(4): 225–236. doi.org/10.1039/B201230H.

[33] Braun A. M., Peschl G. H., Oliveros E. Industrial photochemistry. InCRC Handbook of Organic Photochemistry and Photobiology, Third Edition-Two Volume Set 2019 Apr 5 (pp. 1–19). CRC Press.

[34] Protti S., Manzini S., Fagnoni M., Albini A. The contribution of photochemistry to green chemistry. *Eco-friend. ly Synt. Fine Chem*. 2009. **17**: 80–111. DOI:10.1002/9780470988305.

[35] Protti S., Dondi D., Fagnoni M., Albini A. Photochemistry in synthesis: Where, when, and why. *Pure Appl. Chem*. 2007. **79**(11): 1929–1938. doi.org/10.1351/pac200779111929.

[36] Griesbeck A.G., Mattay J. Synthetic organic photochemistry. In Synthetic Organic Photochemistry 2004. Nov 30 (pp. 13-22). CRC press.

[37] Buglioni L., Raymenants F., Slattery A. *et al*. Technological innovations in photochemistry for organic synthesis: flow chemistry, high-throughput experimentation, scale-up, and photoelectrochemistry. *Chem. Rev*.

2021. **122**(2): 2752–2906. doi.org/10.1021/acs.chemrev.1c00332.

[38] Yoon T.P., Ischay M.A., Du J. Visible light photocatalysis as a greener approach to photochemical synthesis. *Nature Chem*. 2010. **2**(7): 527–532. doi.org/10.1038/nchem.687.

[39] Bach T, Hehn J.P. Photochemical reactions as key steps in natural product synthesis. *Angew. Chem. Intern. Ed.* 2011. **50**(5): 1000–1045. doi.org/10.1002/anie.201002845.

[40] Oelgemoller M. Solar photochemical synthesis: from the beginnings of organic photochemistry to the solar manufacturing of commodity chemicals. Chem. Rev. 2016. **116**(17): 9664–9682. doi.org/10.1021/acs.chemrev.5b00720.

[41] Karkas M.D., Porco J.A., Stephenson C.R. Photochemical approaches to complex chemotypes: applications in natural product synthesis. *Chem. Rev*. 2016. **116**(17): 9683–9747. doi.org/10.1021/acs.chemrev.5b00760.

[42] Prier C.K., Rankic D.A., MacMillan D.W. Visible light photoredox catalysis with transition metal complexes: applications in organic synthesis. *Chem. Rev*. 2013. **113**(7): 5322–5363. doi.org/10.1021/cr300503r

[43] Rehm T.H. Flow photochemistry as a tool in organic synthesis. *Chem. Eur. J*. 2020. **26**(71): 16952–16974. doi.org/10.1002/chem.202000381.

[44] Cambie D., Bottecchia C., Straathof N.J. *et al*. Applications of continuous-flow photochemistry in organic synthesis, material science, and water treatment. *Chem. Rev*. 2016, **116**(17): 10276–10341. doi.org/10.1021/acs.chemrev.5b00707.

[45] Gilmore K., Seeberger P. H. Continuous flow photochemistry. *Chem. Record*. 2014. **14**(3): 410–418. doi.org/10.1002/tcr.201402035.

[46] Politano F., Oksdath-Mansilla G. Light on the horizon: current research and future perspectives in flow photochemistry. *Org. Proc. Res. Devel*. 2018. **22**(9): 1045–1062. doi.org/10.1021/acs.oprd.8b00213.

[47] Mei H., Han J., White S. *et al.* Tailor-made amino acids and fluorinated motifs as prominent traits in modern pharmaceuticals. *Chem.—Eur. J.* 2020. **26**(50): 11349–11390. doi: 10.1002/chem.202000617.

[48] Liu J., Han J., Izawa K. *et al.* Cyclic tailor-made amino acids in the design of modern pharmaceuticals. *Eur. J. Med. Chem.* 2020. **208**: 112736. doi: 10.1016/j.ejmech.2020.112736.

[49] Han J., Konno H., Sato T., Soloshonok V.A., Izawa K. Tailor-made amino acids in the design of small-molecule blockbuster drugs. *Eur. J. Med. Chem.* 2021. **220**: 113448. doi: 10.1016/j.ejmech.2021.113448.

[50] Han J., Remete A.M., Dobson L.S. *et al.* Next generation organofluorine containing blockbuster drugs. *J. Fluor. Chem*. 2020. **239**: 109639. doi.org/10.1016/j.jfluchem.2020.109639.

[51] Han J., Konno H., Sato T. *et al.* Peptidomimetics and Peptide-Based Blockbuster Drugs. *Curr. Org. Chem.* 2021. **25**(14): 1627–1658. doi: 10.2174/1385272825666210610155047.

[52] Wzorek A., Han J., Ono T. *et al*. Cutting-Edge Strategies in the Asymmetric Synthesis of α-Aminocyclopropyl Carboxylic Acids: Essential Scaffolds for Drug Discovery. *Ukr. Chem. J*. 2025. **91**(10): 27–71.

[53] Mei H., Han J., Fustero S. *et al.* Fluorine-Containing Drugs Approved by the FDA in 2018. *Chem.—Eur. J.* 2019. **25**(51): 11797–11819. doi: 10.1002/chem.201901840.

[54] Wang Q., Bian Y., Dhawan G. *et al.* FDA approved fluorine-containing drugs in 2023. *Chin. Chem. Lett*. 2024. **35**(11): 109780. doi: 10.1016/j.cclet.2024.109780.

[55] Mei H., Remete A.M., Zou Y. *et al.* Fluorine-containing drugs approved by the FDA in 2019. *Chin. Chem. Lett.* 2020. **31**(9): 2401–2413. doi: 10.1016/j.cclet.2020.03.050.

[56] Yu Y., Liu A., Dhawan G. *et al.* Fluorine-containing pharmaceuticals approved by the FDA in 2020: Synthesis and biological

activity. *Chin. Chem. Lett.* 2021. **32**(11): 3342–3354.
doi: 10.1016/j.cclet.2021.05.042.

[57] He J., Li Z., Dhawan G. *et al.* Fluorine-containing drugs approved by the FDA in 2021. *Chin. Chem. Lett.* 2023. **34**(1): 107578.
doi: 10.1016/j.cclet.2022.06.001.

[58 Du Y., Bian Y., Baecker D. *et al.* Fluorine in the Pharmaceutical Industry: FDA-Approved Fluorine-Containing Drugs in 2024. *Chem. Eur. J.* 2025, e202500662.
doi.org/10.1002/chem.202500662.

[59] Han J., Wzorek A., Ono T. *et al.* MODERN PHARMACEUTICAL DRUGS FEATURING ALIPHATIC FLUORINE-CONTAINING GROUPS. *Ukr. Chem. J.* 2025. **91**(6): 15–54.

[60] Han J., Wzorek A., Dhawan G. *et al.* Chiral, Fluorine-containing Pharmaceuticals. *Ukr. Chem. J.* 2025. **91**(2): 55–90.
doi.org/10.33609/2708-129X.91.2.2025.55-90.

[61] Wzorek A., Han J., Ono T. *et al.* Synthesis of Tailor-Made Amino Acids Containing C(sp2)–F bonds. *Ukr. Chem. J.* 2025. **91**(8): 36–64.

[62] Han J., Wzorek A. Dhawan G. *et al.* New drugs on the pharmaceutical market containing fluorine and residues of tailor-made amino acids. *Ukr. Chem. J.* 2024. **90**(9): 31–56.
doi: 10.33609/2708-129X.90.9.2024.31-56.

[63] Han J., Wzorek A., Dhawan G. *et al.* New drugs appearing on the market in 2023: molecules containing fluorine and fragments of tailor-made amino acids. *Ukr. Bioorg. Acta.* 2024. **19**(1): 3–20.
doi: 10.15407/bioorganica2024.01.003.

[64] Wang Q., Han J., Sorochinsky A. *et al.* The Latest FDA-Approved Pharmaceuticals Containing Fragments of Tailor-Made Amino Acids and Fluorine. *Pharmaceuticals.* 2022. **15**(8): 999.
doi.org/10.3390/ ph150809991847558.

[65] Liu A., Han J., Nakano A. *et al.* New pharmaceuticals approved by FDA in 2020: Small-molecule drugs derived from amino acids and related compounds. *Chirality.* 2022. **34**(1): 86–103. doi: 10.1002/chir.23376.

[66] Yin Z., Hu W., Zhang W. *et al.* Tailor-made amino acid-derived pharmaceuticals approved by the FDA in 2019. *Amino Acids.* 2020. **52**(9): 1227–1261.
doi: 10.1007/s00726-020-02887-4.

[67] Wang N., Mei H., Dhawan G. *et al.* New Approved Drugs Appearing in the Pharmaceutical Market in 2022, Featuring Fragments of Tailor-Made Amino Acids and Fluorine. *Molecules.* 2023. **28**(9): 3651.
doi: 10.3390/molecules28093651.

[68] Wzorek A., Sorochinsky A.E., Klika K.D. *et al.* Asymmetric synthesis of chi-constrained glutamic acids and related compounds via Michael addition reactions. *Ukr. Chem. J.* 2024. **90**(8): 83–108.
doi: 10.33609/2708-129X.90.8.2024.83-108.

[69] Han J., Liu H., Wang J. *et al.* Hamari's contribution to the asymmetric synthesis of tailor-made amino acids. *Ukr. Chem. J.* 2024. **90**(10): 88–134.
doi: 10.33609/2708-129X.90.10.2024.88-134.

[70] Ellis T.K., Hochla V.M., Soloshonok V.A. Efficient synthesis of 2-aminoindane-2-carboxylic acid via dialkylation of nucleophilic glycine equivalent. *J. Org. Chem.* 2003. **68**(12): 4973–4976. doi.org/10.1021/jo030065v.

[71] Soloshonok V.A., Ohkura H., Yasumoto M. Operationally convenient asymmetric synthesis of (*S*)- and (*R*)-3-amino-4,4,4-trifluorobutanoic acid: Part II. Enantioselective biomimetic transamination of 4,4,4-trifluoro-3-oxo-*N*-[(*R*)-1-phenylethyl)butanamide. *J. Fluor. Chem.* 2006. **127**(7): 930–935.
doi: 10.1016/j.jfluchem.2006.04.004.

[72] Cai C., Soloshonok V.A., Hruby V.J. Michael Addition Reactions between Chiral Ni(II) Complex of Glycine and 3-(*trans*-Enoyl)oxazolidin-2-ones. A Case of Electron Donor–Acceptor Attractive Interaction-Controlled

Face Diastereoselectivity. *J. Org. Chem.* 2001. **66**(4): 1339–1350. doi: 10.1021/jo0014865.

[73] Bravo P., Farina A., Kukhar V.P. *et al.* Stereoselective Additions of a-Lithiated Alkyl *p*-Tolylsulfoxides to *N*-PMP Fluoroalkyl Aldimines. An Efficient Approach to Enantiomerically Pure Fluoro-Amino Compounds. *J. Org. Chem*. 1997. **62**(11): 3424–3425. doi.org/10.1021/jo970004v.

[74] Qiu W., Gu X., Soloshonok V.A. *et al.* Stereoselective synthesis of conformationally constrained reverse turn dipeptide mimetics. *Tetrahedron Lett.* 2001. **42**(2): 145–148. doi: 10.1016/S0040-4039(00)01864-5.

[75] Soloshonok V.A., Kirilenko A.G., Fokina N.A. *et al.* Biocatalytic Resolution of b-Fluoroalkyl-b-Amino Acids, *Tetrahedron: Asymm*. 1994. **5**(6): 1119-1126. doi.org/10.1016/0957-4166(94)80063-4.

[76] Rizzo C., Amata S., Pibiri I. *et al.* FDA-approved fluorinated heterocyclic drugs from 2016 to 2022. *Int. J. Mol. Sci.* 2023. **24**(9): 7728. doi.org/10.3390/ijms24097728.

[77] He J., Wang C., Mei H. *et al.* Visible-light-promoted cyclization of 3-indolylallylamides enabling synthesis of tetrahydrocarbolinones. *Tetrahedron.* 2024. **150**: 133776. doi.org/10.1016/j.tet.2023.133776.

[78] Du Y., Mei H., Makarem A. *et al.* Copper-catalyzed multicomponent reaction of β-trifluoromethyl β-diazo esters enabling the synthesis of β-trifluoromethyl *N*,*N*-diacyl-β-amino esters. *Beilstein J. Org. Chem.* 2024. **20**(1): 212–219. doi.org/10.3762/bjoc.20.21.

[79] Javahershenas R., Mei H., Koley M. *et al.* Recent advances in the multicomponent synthesis of heterocycles using 5-aminotetrazole. *Synthesis.* 2024. **56**(16): 2445–2461. doi: 10.1055/s-0042-1751526.

[80] Turcheniuk K.V., Poliashko K.O., Kukhar V.P. *et al.* Efficient asymmetric synthesis of trifluoromethylated β-aminophosphonates and their incorporation into dipeptides. *Chem. Commun*. 2012. **48**(94): 11519–11521. DOI: 10.1039/c2cc36702e.

[81] Abbas A.A., Farghaly T.A., Dawood K.M. Recent progress in therapeutic applications of fluorinated five-membered heterocycles and their benzo-fused systems. *RSC Adv.* 2024. **14**(46): 33864–33905. doi: 10.1039/D4RA05697C.

[82] Yamada T., Okada T., Sakaguchi K. *et al.* Efficient asymmetric synthesis of novel 4-substituted and configurationally stable analogues of thalidomide. *Org. Lett.* 2006. **8**(24): 5625–5628. doi: 10.1021/ol0623668.

[83] Soloshonok V.A., Gerus I.I., Yagupolskii Y.L., Kukhar V.P. Fluorine-containing amino acids. III. α-Trifluoromethyl-α-amino acids. *Zh Org Khim*. 1987. **23**: 2308-2313.

[84] Takeda R., Kawamura A., Kawashima A. *et al.* Chemical dynamic kinetic resolution and *S*/*R* interconversion of unprotected α-amino acids. *Angew. Chem., Int. Ed.* 2014. **53**(45): 12214–12217. doi.org/10.1002/anie.201407944.

[85] Taylor S.M., Yamada T., Ueki H., Soloshonok V.A. Asymmetric synthesis of enantiomerically pure 4-aminoglutamic acids via methylenedimerization of chiral glycine equivalents with dichloromethane under operationally convenient conditions. *Tetrahedron* Lett. 2004. **45**(50): 9159–9162. doi.org/10.1016/j.tetlet.2004.10.111.

[86] Wang Y., Song X., Wang J. *et al.* Recent approaches for asymmetric synthesis of α-amino acids via homologation of Ni(II) complexes. *Amino Acids.* 2017. **49**(9): 1487–1520. doi: 10.1007/s00726-017-2458-6.

[87] Soloshonok V.A., Yasumoto M. Catalytic asymmetric synthesis of α-(trifluoromethyl) benzylamine via cinchonidine derived base-catalyzed biomimetic 1,3-proton shift reaction. *J. Fluor. Chem*. 2007. **128**(3): 170–173. doi.org/10.1016/j.jfluchem.2006.11.011.

[88] Nian Y., Wang J., Zhou S. *et al.* Recyclable ligands for the non-enzymatic dynamic kinetic resolution of challenging α-amino acids. *Angew. Chem., Int. Ed.* 2015. **54**(44): 12918–12922. doi.org/10.1002/anie.201507273.

[89] Grygorenko O.O., Volochnyuk D.M., Vashchenko B.V. Emerging Building Blocks for Medicinal Chemistry: Recent Synthetic Advances. *Eur. J. Org. Chem.* 2021. **2021**(47): 6478–6510. doi.org/10.1002/ejoc.202100857.

[90] Leśniewska A., Przybylski P. Seven-membered *N*-heterocycles as approved drugs and promising leads in medicinal chemistry as well as the metal-free domino access to their scaffolds. *Eur. J. Med. Chem.* 2024. **275**: 116556. doi.org/10.1016/j.ejmech.2024.116556.

[91] Kumar N., Goel N. Heterocyclic compounds: importance in anticancer drug discovery. *Anticancer Agents Med. Chem.* 2022. **22**(19): 3196–3207. doi.org/10.2174/1871520622666220404082648.

[92] Rusu A., Moga I.M., Uncu L., Hancu G. The role of five-membered heterocycles in the molecular structure of antibacterial drugs used in therapy. *Pharmaceutics.* 2023. **15**(11): 2554. doi.org/10.3390/pharmaceutics15112554.

[93] Lyutenko N.V., Han J., Wzorek A. *et al.* Carbon nanotubes-catalyzed synthesis of fluorine-containing heterocycles. *Ukr. Chem. J.* 2024. **90**(6): 71–86. doi: 10.33609/2708-129X.90.6.2024.71-86.

[94] Han J., Wzorek A., Ono T. *et al.* Mechanochemical Synthesis of Fluorine-Containing Heterocycles via Ball Milling. *Ukr. Chem. J.* 2025. **91**(7): 35–55.

[95] Wzorek A., Ono T., Baecker D. *et al.* Electrochemical Synthesis of Fluorinated Heterocyclic Compounds. *Ukr. Chem. J.* 2025. **91**(11): 35–62.

[96] Skubi K.L., Blum T.R., Yoon T.P. Dual catalysis strategies in photochemical synthesis. *Chem. Rev.* 2016. **116**(17): 10035–10074. doi.org/10.1021/acs.chemrev.6b00018.

[97] Medlycott E.A., Hanan G.S. Synthesis and properties of mono-and oligo-nuclear Ru (II) complexes of tridentate ligands: The quest for long-lived excited states at room temperature. *Coordin. Chem. Rev.* 2006. **250**(13–14): 1763–1782. doi.org/10.1016/j.ccr.2006.02.015.

[98] Mills I.N., Porras J.A., Bernhard S. Judicious design of cationic, cyclometalated Ir (III) complexes for photochemical energy conversion and optoelectronics. *Acc. Chem. Res.* 2018. **51**(2): 352–364. doi.org/10.1021/acs.accounts.7b00375.

[99] Monos T.M., Stephenson C.R. Photoredox Catalysis of Iridium (III)-Based Photosensitizers. Iridium (III) in *Optoelectronic and Photonics Applications*. 2017, 541–581. doi.org/10.1002/9781119007166.ch11.

[100] Monti F., Baschieri A., Sambri L., Armaroli N. Excited-state engineering in heteroleptic ionic iridium (III) complexes. *Acc. Chem. Res.* 2021. **54**(6): 1492–1505. doi.org/10.1021/acs.accounts.0c00825.

[101] Hua R., Jiang J.L. Recent development of rhenium-catalyzed organic synthesis. *Curr. Org. Syn.* 2007. **4**(2): 151–174. doi.org/10.2174/157017907780598907.

[102] Michelin C., Hoffmann N. Photocatalysis applied to organic synthesis–A green chemistry approach. *Curr. Opin. Green Sustain. Chem.* 2018. **10**: 40–5. doi.org/10.1016/j.cogsc.2018.02.009.

[103] Ravelli D., Dondi D., Fagnoni M., Albini A. Photocatalysis. A multi-faceted concept for green chemistry. *Chem. Soc. Rev.* 2009. **38**(7): 1999–2011. doi.org/10.1039/B714786B.

[104] Williams J.D., Kappe C.O. Recent advances toward sustainable flow photochemistry. *Curr. Opini. Green Sustain. Chem.* 2020. **25**:100351. doi.org/10.1016/j.cogsc.2020.05.001.

[105] Zhou N., Zhao F., Wang L. *et al.* Visible-Light-Induced Regioselective Cascade Radical Cyclization of α-Bromocarbonyls: Access to Benzazepine Derivatives. *J. Org, Chem*. 2024. **89**(4): 2238–2246. doi.org/10.1021/acs.joc.3c02184.

[106] Li G., He R., Liu Q. *et al*. Formation of Amidinyl Radicals via Visible-Light-Promoted Reduction of N-Phenyl Amidoxime Esters and Application to the Synthesis of 2-Substituted Benzimidazoles. *J. Org, Chem.* 2019. **84**(13): 8646–8660. doi.org/10.1021/acs.joc.9b01158.

[107] Sun X., Yu W., Min L. *et al*. Synthesis, structural determination, and antifungal activity of novel fluorinated quinoline analogs. *Molecules*. 2023. **28**(8): 3373. doi.org/10.3390/molecules28083373

[108] El-mrabet A., Haoudi A., Kandri-Rodi Y., Mazzah A. An Overview of Quinolones as Potential Drugs: Synthesis, Reactivity and Biological Activities. *Organics*. 2025. **6**(2): 16. doi.org/10.3390/org6020016

[109] Berbasov D.O., Soloshonok V.A. Chemoselectivity in the reactions between ethyl 4, 4, 4-trifluoro-3-oxobutanoate and anilines: Improved synthesis of 2-trifluoromethyl-4-and 4-trifluoromethyl-2-quinolinones. *Synthesis*. 2003. (13): 2005–2010. DOI: 10.1055/s-2003-41043.

[110] González-Muñoz D., Nova-Fernández J.L., Martinelli A. *et al*. Visible light photocatalytic synthesis of tetrahydroquinolines under batch and flow conditions. *Eur. J. Org. Chem*. 2020. (37): 5995–5999. doi.org/10.1002/ejoc.202001018.

[111] Moore J.L., Taylor S.M., Soloshonok V.A. An efficient and operationally convenient general synthesis of tertiary amines by direct alkylation of secondary amines with alkyl halides in the presence of Huenig's base. *Arkivoc*. 2005. **6**(iv): 287–292. doi.org/10.3998/ark.5550190.0006.624.

[112] Soloshonok V.A., Cai C., Hruby V.J. Asymmetric Michael addition reactions of chiral Ni (II)-complex of glycine with (*N*-trans-enoyl) oxazolidines: improved reactivity and stereochemical outcome. *Tetrahedron: Asymm*. 1999. **10**(22): 4265–4269. doi.org/10.1016/S0957-4166(99)00483-8.

[113] Soloshonok V.A., Ueki H., Tiwari R. *et al*. Virtually complete control of simple and face diastereoselectivity in the Michael addition reactions between achiral equivalents of a nucleophilic glycine and (*S*)-or (*R*)-3-(*E*-enoyl)-4-phenyl-1,3-oxazolidin-2-ones: practical method for preparation of β-substituted pyroglutamic acids and prolines. *J. Org. Chem*. 2004. **69**(15): 4984–4990. doi.org/10.1021/jo0495438.

[114] Soloshonok V.A., Ueki H., Ellis T.K. *et al*. Application of modular nucleophilic glycine equivalents for truly practical asymmetric synthesis of β-substituted pyroglutamic acids. *Tetrahedron Lett*. 2005. **46**(7): 1107–1110. doi.org/10.1016/j.tetlet.2004.12.093.

[115] Jovanovic M., Jovanovic P., Tasic G. *et al*. Regio-and Stereoselective, Intramolecular [2+2] Cycloaddition of Allenes, Promoted by Visible Light Photocatalysis. *Adv. Syn. Cat*.. 2023. **365**(15): 2516–2523. doi.org/10.1002/adsc.202300301.

[116] Gore B.S., Wang J.J. Visible-light-induced oxidant/additive-free atom-economic synthesis of multifunctionalized cyclopropanes via energy transfer. *Chem. Commun*. 2023. **59**(39): 5878–5881.

[117] Zhu M., Zhang X., Zheng C., You S.L. Visible-light-induced dearomatization via [2+2] cycloaddition or 1,5-hydrogen atom transfer: divergent reaction pathways of transient diradicals. *ACS Cat*. 2020. **10**(21): 12618–12626. doi.org/10.1021/acscatal.0c03808.

[118] Zhang Z., Yi D., Zhang M. *et al*. Photocatalytic intramolecular [2+2] cycloaddition of indole derivatives via energy transfer: a method for late-stage skeletal transformation. *ACS Cat*. 2020. **10**(17): 10149–10156.

doi.org/10.1021/acscatal.0c01841.

[119] Zou Y., Takeda R., Han J. *et al*. Asymmetric Synthesis of *N*-Fmoc-(*S*)-7-aza-tryptophan via Alkylation of Chiral Nucleophilic Glycine Equivalent. *Eur. J. Org. Chem*. 2021. (21): 2962–2965. DOI: 10.1002/ejoc.202100485.

[120] Han J., Lyutenko N.V., Sorochinsky A.E. *et al*. Tailor-Made Amino Acids in Pharmaceutical Industry: Synthetic Approaches to Aza-Tryptophan Derivatives. *Chem.– Eur. J*. 2021. **27**(70): 17510–17528. doi.org/10.1002/chem.202102485.

[121] Monnie C.M., Hernández I., Meléndez-Pacheco R. *et al*. Synthesis of 4,6-Difluoro-Tryptophan as a Probe for Protein ^{19}F NMR. *Adv. Syn. Cat*. 2024. **366**(16): 3417–3422. doi.org/10.1002/adsc.202400031.

[122] Zhu M., Zheng C., Zhang X., You S.L. Synthesis of cyclobutane-fused angular tetracyclic spiroindolines via visible-light-promoted intramolecular dearomatization of indole derivatives. *J. Am. Chem. Soc*. 2019. **141**(6): 2636–2644. doi.org/10.1021/jacs.8b12965.

[123] Guo Q., Lu D., Mao Y., Lu Z. Visible-light promoted intramolecular carboamination of alkynes for the synthesis of oxazolidinone-fused isoquinolinones. *Chem. Commun*. 2023. **59**(14): 1979–1982. DOI: 10.1039/D2CC06542H.

[124] Soloshonok V.A., Cai C., Hruby V.J. Toward design of a practical methodology for stereocontrolled synthesis of χ-constrained pyroglutamic acids and related compounds. Virtually complete control of simple diastereoselectivity in the Michael addition reactions of glycine Ni (II) complexes with *N*-(enoyl) oxazolidinones. *Tetrahedron Lett*. 2000. **41**(2): 135–139. doi.org/10.1016/S0040-4039(99)02018-3.

[125] Soloshonok V.A., Cai C., Hruby V.J. A unique case of face diastereoselectivity in the Michael addition reactions between Ni (II)-complexes of glycine and chiral 3-(*E*-enoyl)-1, 3-oxazolidin-2-ones. *Tetrahedron Lett*. 2000. **41**(49): 9645–9649. doi.org/10.1016/S0040-4039(00)01737-8.

[126] Soloshonok V.A., Cai C., Hruby V.J. (*S*)-or (*R*)-3-(*E*-Enoyl)-4-phenyl-1, 3-oxazolidin-2-ones: ideal Michael acceptors to afford a virtually complete control of simple and face diastereoselectivity in addition reactions with glycine derivatives. *Org. Lett*. 2000. **2**(6): 747–750. doi.org/10.1021/ol990402f.

[127] Ritu, Das S, Tian Y.M. *et al*. Photocatalyzed dehydrogenation of aliphatic N-heterocycles releasing dihydrogen. *ACS Cat*. 2022. **12**(16): 10326–10332. doi.org/10.1021/acscatal.2c02830.

[128] Peng Y., Wang Y., Wang K. *et al*. Visible-light photocatalyzed C3–H alkylation of 2 *H*-indazoles/indoles with sulfoxonium ylides via diversified mechanistic pathways. *ACS Cat*. 2024. **14**(2): 1193–1204. doi.org/10.1021/acscatal.3c04729.

[129] Ma R., Ren Y., Deng Z. *et al*. Visible Light Promotes Cascade Trifluoromethylation/Cyclization, Leading to Trifluoromethylated Polycyclic Quinazolinones, Benzimidazoles and Indoles. *Molecules*. 2022. **27**(23): 8389. doi.org/10.3390/molecules27238389.

[130] Soloshonok V.A., Mikami K., Yamazaki T., Welch J.T., Honek J.F. Eds. Current fluoroorganic chemistry: new synthetic directions, technologies, materials, and biological applications. ACS Symposium Series #949; Oxford University Press, 2007. doi: 10.1021/bk-2007-0949.

[131] Xie C., Wu L., Mei H. *et al*. Generalized access to fluorinated β-keto amino compounds through asymmetric additions of α,α-difluoroenolates to CF_3-sulfinylimine. *Org. Biomol. Chem*. 2014. **12**(39): 7836–7843. doi: 10.1039/C4OB01575D.

[132] Soloshonok V.A., Kirilenko A.G., Kukhar V.P., Resnati G. A practical route to fluoroalkyl-and fluoroarylamines by base-catalyz-

ed [1,3]-proton shift reaction. *Tetrahedron Lett*. 1994. **35**(19): 3119–3122. doi.org/10.1016/S0040-4039(00)76845-6.

[133] Wu L., Xie C., Mei H. *et al*. Synthesis of trifluoromethyl-containing vicinal diamines by asymmetric decarboxylative Mannich addition reactions. *J. Org. Chem*. 2015. **80**(6): 3187–3194. doi.org/10.1021/acs.joc.5b00124.

[134] Shi C., Guo L., Gao H. *et al*. Highly Diastereoselective Synthesis of γ-Lactams Enabled by Photoinduced Deaminative [3+2] Annulation Reaction. *Org. Lett*. 2022. **24**(24): 4365–4370. doi.org/10.1021/acs.orglett.2c01565.

[135] Soloshonok V.A, Cai C., Hruby V.J. *et al*. Stereochemically defined C-substituted glutamic acids and their derivatives. 1. An efficient asymmetric synthesis of (2*S*,3*S*)-3-methyl-and-3-trifluoromethylpyroglutamic acids. *Tetrahedron*. 1999. **55**(41): 12031–12044. doi.org/10.1016/S0040-4020(99)00711-5.

[136] Mei H., Han J., Klika K.D. et al. Applications of fluorine-containing amino acids for drug design. *Eur. J. Med. Chem*. 2020. **186**: 111826. doi.org/10.1016/j.ejmech.2019.111826.

[137] Kukhar V.P., Sorochinsky A.E., Soloshonok V.A. Practical synthesis of fluorine-containing α-and β-amino acids: recipes from Kiev, Ukraine. *Future Med. Chem*. 2009. **1**(5): 793–819. doi.org/10.4155/fmc.09.70.

[138] Liu D., Patureau F.W. Visible-Light-Induced Photocatalytic Deoxygenative Benzylation of Quinoxalin-2-(1*H*)-ones with Carboxylic Acid Anhydrides. *Org. Lett*. 2024. **26**(32): 6841–6846. doi.org/10.1021/acs.orglett.4c02316.

[139] Wang J., Lin D., Zhou S. *et al*. Asymmetric synthesis of sterically and electronically demanding linear ω-trifluoromethyl containing amino acids via alkylation of chiral equivalents of nucleophilic glycine and alanine. *J. Org. Chem*. 2011. **76**(2): 684–687. doi.org/10.1021/jo102031b.

[140] Mei H., Hiramatsu T., Takeda R. *et al*. Expedient asymmetric synthesis of (*S*)-2-amino-4,4,4-trifluorobutanoic acid via alkylation of chiral nucleophilic glycine equivalent. *Org. Proc. Res. Devel*. 2019. **23**(4): 629–634. DOI: 10.1021/acs.oprd.8b00404

[141] Han J., Takeda R., Liu X. *et al*. Preparative Method for asymmetric synthesis of (*S*)-2-amino-4,4,4-trifluorobutanoic acid. *Molecules*. 2019. **24**(24): 4521. doi:10.3390/molecules24244521.

[142] Samanta R.K., Meher P., Murarka S. Visible Light Photoredox-Catalyzed Direct C–H Arylation of Quinoxalin-2 (1*H*)-ones with Diaryliodonium Salts. *J. Org. Chem*. 2022. **87**(16): 10947–10957. doi.org/10.1021/acs.joc.2c01234.

[143] Wang Q., Zhang X., Sorochinsky A.E. *et al*. Advances in the development of trifluoromethoxylation reagents. *Symmetry*. 2021. **13**(12): 2380. doi.org/10.3390/sym13122380.

[144] Liu J., Lin W., Sorochinsky A.E. *et al*. Successful trifluoromethoxy-containing pharmaceuticals and agrochemicals. *J. Fluor. Chem*. 2022. **257**: 109978. doi.org/10.1016/j.jfluchem.2022.109978.

[145] Xie L.Y., Jiang L.L., Tan J.X. *et al*. Visible-light-initiated decarboxylative alkylation of quinoxalin-2 (1*H*)-ones with phenyliodine (III) dicarboxylates in recyclable ruthenium (II) catalytic system. *ACS Sustain. Chem. Eng*. 2019. **7**(16): 14153–14160. doi.org/10.1021/acssuschemeng.9b02822.

[146] Wang S.W., Yu J., Zhou Q.Y. *et al*. Visible-light-induced atom transfer radical addition and cyclization of perfluoroalkyl halides with enynes. *ACS Sustain. Chem. Eng*. 2019. **7**(11): 10154–10162. doi.org/10.1021/acssuschemeng.9b02178.

[147] Sonne C., Bank M.S., Jenssen B.M. *et al*. PFAS pollution threatens ecosystems worldwide. *Science*. 2023. **379**(6635): 887–888. DOI: 10.1126/science.adh093.

[148] Renfrew D., Pearson T.W. The social life of the "forever chemical": PFAS pollution legacies

and toxic events. *Environ. Soc*. 2021. **12**(1): 146–163. doi.org/10.3167/ares.2021.120109.

[149] Han J., Kiss L., Mei H. *et al*. Chemical aspects of human and environmental overload with fluorine. *Chem. Rev*. 2021. **121**(8): 4678–4742. doi.org/10.1021/acs.chemrev.0c01263.

[150] Liu Y., Chen Z., Wang Q.L. *et al*. Visible light-catalyzed cascade radical cyclization of *N*-propargylindoles with acyl chlorides for the synthesis of 2-acyl-9*H*-pyrrolo [1,2-*a*] indoles. *J. Org. Chem*. 2020. **85**(4): 2385–2394. doi.org/10.1021/acs.joc.9b03090.

[151] Santos M.S., Betim H.L., Kisukuri C.M. *et al*. Photoredox Catalysis toward 2-Sulfenylindole Synthesis through a Radical Cascade Process. *Org. Lett*. 2020. **22**(11): 4266–4271. doi.org/10.1021/acs.orglett.0c01297.

[152] Zhu J.N., Wang W.K., Zhu Y. *et al*. Cascade Functionalization of C (sp3)–Br/C (sp2)–H Bonds: Access to Fused Benzo [*e*] isoindole-1,3,5-trione via Visible-Light-Induced Reductive Radical Relay Strategy. *Org. Lett*. 2019. **21**(16): 6270–6274. doi.org/10.1021/acs.orglett.9b02153.

[153] Fan X., Lei T., Chen B. *et al*. Photocatalytic C–C bond activation of oxime ester for acyl radical generation and application. *Org. Lett*. 2019. **21**(11): 4153–4158. doi.org/10.1021/acs.orglett.9b01338.

[154] Zhu Y., Mao Y., Mei H. *et al.* Palladium-Catalyzed Asymmetric Allylic Alkylations of Colby Pro-Enolates with MBH Carbonates: Enantioselective Access to Quaternary C–F Oxindoles. *Chem.—Eur. J*. 2018. **24**(36): 8994–8998. doi.org/10.1002/chem.201801670.

[155] Wearing E.R., Yeh Y.C., Terrones G.G. *et al*. Visible light–mediated aza Paternò–Büchi reaction of acyclic oximes and alkenes to azetidines. *Science*. 2024. **384**(6703): 1468–1476. DOI: 10.1126/science.adj6771.

[156] Yu Y., Liu A., He J. *et al*. Visible-light-irradiated tandem sulfonylation/cyclization of indole tethered alkenes for the synthesis of tetrahydrocarbazoles. *Chin. Chem. Lett*. 2022. **33**(11): 4886–4890. doi.org/10.1016/j.cclet.2022.03.038.

[157] Hou H., Tang D., Li H. *et al*. Visible-light-driven chlorotrifluoromethylative and chlorotrichloromethylative cyclizations of enynes. *J. Org. Chem*. 2019. **84**(11): 7509–7517. doi.org/10.1021/acs.joc.9b00842.

[158] Cardinale L., Neumeier M., Majek M. *et al*. Aryl pyrazoles from photocatalytic cycloadditions of arenediazonium. *Org. Lett*. 2020. **22**(18): 7219–7224. doi.org/10.1021/acs.orglett.0c02514.

[159] David E., Couve-Bonnaire S., Jubault P., Pannecoucke X. Ethyl dibromofluoroacetate: a versatile reagent for the synthesis of fluorinated molecules. *Tetrahedron*. 2013. **69**(52): 11039–11055. doi.org/10.1016/j.tet.2013.10.048.

[160] Tokairin Y., Soloshonok V.A., Konno H. *et al*. Convenient synthesis of racemic 4,4-difluoro glutamic acid derivatives via Michael-type additions of Ni (II)-complex of dehydroalanine Schiff bases. *J. Fluor. Chem*. 2019. **227**: 109376. doi.org/10.1016/j.jfluchem.2019.109376.

[161] Tokairin Y., Shigeno Y., Han J. *et al*. Asymmetric Synthesis of 4,4-(Difluoro) glutamic Acid via Chiral Ni (II)-Complexes of Dehydroalanine Schiff Bases. Effect of the Chiral Ligands Structure on the Stereochemical Outcome. *ChemistryOpen*. 2020. **9**(1): 93–96. doi.org/10.1002/open.201900343.

[162] Tokairin Y., Konno H., Noireau A. *et al* Asymmetric synthesis of the two enantiomers of β-phosphorus-containing α-amino acids via hydrophosphinylation and hydrophosphonylation of chiral Ni (II)-complexes. *Org. Chem. Front*. 2021. **8**(10): 2190–2195. doi.org/10.1039/D1QO00159K.

[163] Soloshonok V.A., Ohkura H., Sorochinsky A. *et al*. Convenient, large-scale asymmetric synthesis of β-aryl-substituted α, α-dif-

luoro-β-amino acids. *Tetrahedron Lett*. 2002. **43**(31): 5445–5448. doi.org/10.1016/S0040-4039(02)01103-6.

[164] Sorochinsky A., Voloshin N., Markovsky A. *et al*. Convenient asymmetric synthesis of β-substituted α,α-difluoro-β-amino acids via Reformatsky reaction between Davis' *N*-Sulfinylimines and ethyl bromodifluoroacetate. *J. Org. Chem*. 2003. **68**(19): 7448–7454. doi.org/10.1021/jo030082k.

[165] Xie C., Zhang L., Mei H. *et al*. New Chiral Reagent for Installation of Pharmacophoric (*S*)-or (*R*)-2-(Alkoxyphosphono)-1-amino-2,2-difluoroethyl Groups. *Chem.–Europ. J*. 2016. **22**(21): 7036–7040. DOI: 10.1002/chem.201600758.

[166] Mei H., Yu Y., Wang C. *et al*. Assembly of tetracyclic tetrahydrocarbazoles via a visible-light promoted cascade process. *Org. Chem. Front*. 2022. **9**(9): 2516–2521. doi.org/10.1039/D2QO00247G.

[167] Mei H., Liu A., He J. *et al*. Visible-light-irradiated cascade reaction of indole-tethered alkenes to access tetracyclic tetrahydro-γ-carbolines. *Org. Lett*. 2022. **24**(14): 2630–2635. doi.org/10.1021/acs.orglett.2c00626.

[168] Zhou N., Xia Z., Kuang K. *et al*. Visible-Light-Induced Difluoroalkylation of 1-(Allyloxy)-2-(1-arylvinyl) benzenes and 1-(1-Arylvinyl)-2-(vinyloxy) benzenes: Synthesis of *Bis*-Difluoroalkylated Benzoxepines and 2*H*-Chromenes. *Org. Lett*. 2022. **24**(31): 5791–5796. doi.org/10.1021/acs.orglett.2c02314.

[169] Lian G., Li J., Liu P., Sun P. Photoredox-catalyzed radical cascade reaction to synthesize fluorinated pyrrolo [1,2-*d*] benzodiazepine derivatives. *J. Org. Chem*. 2019. **84**(14): 9322–9329. doi.org/10.1021/acs.joc.9b00937.

[170] Wang C., He J., Mei H. *et al*. Visible-Light-Triggered Difluoroacetylation/Cyclization of Chromone-Tethered Alkenes Enabling Synthesis of Tetrahydroxanthones. *J. Org. Chem*. 2024. **89**(8): 5619–5633. doi.org/10.1021/acs.joc.4c00129.

[171] Stefanoni K.K., Wilhelm R. Access to SCF_3-Substituted Indolizines via a Photocatalytic Late-Stage Functionalization Protocol. *Org. Lett*. 2025. doi.org/10.1021/acs.orglett.5c02079.

[172] Mei H., Xie C., Wu L. *et al*. Asymmetric Mannich reactions of imidazo [2,1-*b*] thiazole-derived nucleophiles with (S_S)-*N*-*tert*-butanesulfinyl (3,3,3)-trifluoroacetaldimine. *Org. Biomol. Chem*. 2013. **11**(46): 8018–8021. DOI: 10.1039/c3ob41785a.

[173] Imai T., Niijima E., Terada S. *et al*. Chirality-dependent halogen bonds in axially chiral quinazolin-4-one derivatives bearing *ortho*-halophenyl groups. *CrystEngComm*. 2019. **21**(22): 3385–3389. DOI: 10.1039/C9CE00320G.

[174] Jiang S., Tian X.J., Feng S.Y. *et al*. Visible-light photoredox catalyzed double C–H functionalization: Radical cascade cyclization of ethers with benzimidazole-based cyanamides. *Org. Lett*. 2021. **23**(3): 692–696. doi.org/10.1021/acs.orglett.0c03853.

[175] Zhang W., Pan Y.L., Yang C. *et al*. Ring-opening C (sp 3)–C coupling of cyclobutanone oxime esters for the preparation of cyanoalkyl containing heterocycles enabled by photocatalysis. *Org. Chem. Front*. 2019. **6**(15): 2765–2770. doi.org/10.1039/C9QO00625G.

[176] Mao L.L., Zhou A.X., Zhu X.H. *et al*. Visible-Light-Mediated Tandem Difluoromethylation/Cyclization of Alkenyl Aldehydes toward CF_2H-Substituted Chroman-4-one Derivatives. *J. Org. Chem*. 2022. **87**(18): 12414–12423. doi.org/10.1021/acs.joc.2c01689.

[177] Meng Z., Zhang X., Shi M. Visible-light mediated cascade cyclization of ene-vinylidenecyclopropanes: access to fluorinated heterocyclic compounds. *Org. Chem. Front*. 2021. **8**(14): 3796–3801. doi.org/10.1039/D1QO00540E.

[178] Romoff T.T., Ignacio B.G., Mansour N.

et al. Large-scale synthesis of the glycine Schiff base Ni (II) complex derived from (*S*)-and (*R*)-N-(2-benzoyl-4-chlorophenyl)-1-[(3,4-dichlorophenyl) methyl]-2-pyrrolidinecarboxamide. *Org. Proc. Res. Devel*. 2020. **24**(2): 294–300. doi.org/10.1021/acs.oprd.9b00399.

[179] Ellis T.K., Ueki H., Tiwari R., Soloshonok V.A. Michael addition reactions between various nucleophilic glycine equivalents and (*S*, *E*)-1-enoyl-5-oxo-*N*-phenylpyrrolidine-2-carboxamide, an optimal type of chiral Michael acceptor in the asymmetric synthesis of β-phenyl pyroglutamic acid and related compounds. *Tetrahedron: Asymm*. 2009. **20**(22): 2629–2634. doi.org/10.1016/j.tetasy.2009.10.006.

[180] Romoff T.T., Palmer A.B., Mansour N. *et al*. Scale-up Synthesis of (*R*)-and (*S*)-*N*-(2-Benzoyl-4-chlorophenyl)-1-(3,4-dichlorobenzyl) pyrrolidine-2-carboxamide Hydrochloride, A Versatile Reagent for the Preparation of Tailor-Made α-and β-Amino Acids in an Enantiomerically Pure Form. *Org. Proc. Res. Devel*. 2017. **21**(5): 732–739. doi.org/10.1021/acs.oprd.7b00055.

[181] Liang Y.X., Gong Y., Xu X.C. *et al*. Visible light-induced radical cyclization of *o*-alkenyl aromatic isocyanides with thioethers: direct synthesis of 2-thioquinolines. *Org. Chem. Front*. 2024. **11**(7): 2033–2039. doi.org/10.1039/D3QO02055J.

[182] Liu Y., Zhou T., Xuan L. *et al*. Visible-Light-Driven C, N-Selective Heteroarylation of *N*-Fluoroalkyl Hydroxylamine Reagents with Quinoxalin-2 (1*H*)-ones. *Org. Lett*. 2023. **25**(48): 8693–8699. doi.org/10.1021/acs.orglett.3c03594.

[183] Soloshonok V.A., Kukhar V.P. Biomimetic transamination of α-keto perfluorocarboxylic esters. An efficient preparative synthesis of β,β,β-trifluoroalanine. *Tetrahedron*. 1997. **53**(25): 8307–8314. doi.org/10.1016/S0040-4020(97)00517-6.

[184] Soloshonok V.A., Kirilenko A.G., Fokina N.A. *et al*. Chemo-enzymatic approach to the synthesis of each of the four isomers of α-alkyl-β-fluoroalkyl-substituted β-amino acids. *Tetrahedron: Asymmetry*. 1994. **5**(7): 1225–1228. doi.org/10.1016/0957-4166(94)80163-0.

[185] Soloshonok V.A, Kukhar V.P. Biomimetic base-catalyzed [1, 3]-proton shift reaction. A practical synthesis of β-fluoroalkyl-β-amino acids. *Tetrahedron*. 1996. **52**(20): 6953–6964. doi.org/10.1016/0040-4020(96)00300-6.

[186] Yasumoto M., Ueki H., Soloshonok V.A. Thermal 1,3-proton shift reaction and its application for operationally convenient and improved synthesis of α-(trifluoromethyl) benzylamine. *J. Fluor. Chem*. 2007. **128**(7): 736–739. doi.org/10.1016/j.jfluchem.2007.02.008.

[187] Soloshonok V.A., Ono T., Soloshonok I.V. Enantioselective biomimetic transamination of β-keto carboxylic acid derivatives. an efficient asymmetric synthesis of β-(fluoroalkyl) β-amino acids. *J. Org. Chem*. 1997. **62**(22): 7538–7539. doi.org/10.1021/jo9710238.

[188] Soloshonok V.A., Soloshonok I.V., Kukhar V.P., Svedas V.K. Biomimetic transamination of α-alkyl β-keto carboxylic esters. Chemoenzymatic approach to the stereochemically defined α-alkyl β-fluoroalkyl β-amino acids. *J. Org. Chem*. 1998. **63**(6): 1878–1884. doi.org/10.1021/jo971777m.

[189] Soloshonok V.A., Ohkura H., Uneyama K. Biomimetic reductive amination of perfluoroalkylcarboxylic acids to α,α-dihydroperfluoroalkylamines. *Tetrahedron Lett*. 2002. **43**(31): 5449–5452. doi.org/10.1016/S0040-4039(02)01104-8.

[190] Koley M., Han J., Soloshonok V.A. *et al*. Latest developments in coumarin-based anticancer agents: Mechanism of action and structure–activity relationship studies. *RSC Med. Chem*. 2024. **15**(1): 10–54. DOI: 10.1039/D3MD00511A.

[191] Tan L.P., Liang D., Cheng Y. *et al.* Visible-light-induced tandem radical addition/cyclization of 2-alkenylphenols and CBr_4 for the synthesis of 4-arylcoumarins. *Org. Chem. Front*. 2021. **8**(18): 5052–5057. doi.org/10.1039/D1QO00831E.

[192] Wu L., Xie C., Mei H. *et al.* Asymmetric Friedel–Crafts Reactions of *N-tert*-Butylsulfinyl-3,3,3-trifluoroacetaldimines: General Access to Enantiomerically Pure Indoles Containing a 1-Amino-2,2,2-trifluoroethyl Group. *J. Org. Chem.* 2014. **79**(16): 7677–7681. doi.org/10.1021/jo5012009.

[193] Wu C.J., Cao W.X., Chen B. *et al.* Tandem [2+2] Cycloaddition/Rearrangement toward Carbazoles by Visible-Light Photocatalysis. *Org. Lett*. 2021. **23**(6): 2135–2139. doi.org/10.1021/acs.orglett.1c00290

[194] Chen J.Q., Luo X., Chen M. *et al.* Visible-light-induced 1,7-enyne dicyclization: synthesis of ester-substituted benzo [*j*] phenanthridines. *Org. Lett*. 2023. **25**(11): 1978–1983. doi.org/10.1021/acs.orglett.3c00544

[195] Sato T., Izawa K., Aceña J.L. *et al.* Tailor-made α-amino acids in the pharmaceutical industry: synthetic approaches to (1*R*,2*S*)-1-amino-2-vinylcyclopropane-1-carboxylic acid (vinyl-ACCA). *Europ. J. Org. Chem*. 2016. (16): 2757–2774. DOI: 10.1002/ejoc.201600112

[196] Wang S., Wang Y., Wang J. *et al.* The second-generation of highly potent hepatitis C virus (HCV) NS3/4A protease inhibitors: Evolutionary design based on tailor-made amino acids, synthesis and major features of bio-activity. *Curr. Pharm. Design*. 2017. **23**(30): 4493–4554. DOI: 10.2174/1381612823666170522122424

[197] Kawashima A., Xie C., Mei H. *et al.* Asymmetric synthesis of (1*R*,2*S*)-1-amino-2-vinylcyclopropanecarboxylic acid by sequential S_N2–S_N2' dialkylation of (*R*)-*N*-(benzyl) proline-derived glycine Schiff base Ni (ii) complex. *RSC Adv*. 2015. **5**(2): 1051–1058. DOI: 10.1039/C4RA12658K

[198] Kawashima A., Shu S., Takeda R. *et al.* Advanced asymmetric synthesis of (1*R*,2*S*)-1-amino-2-vinylcyclopropanecarboxylic acid by alkylation/cyclization of newly designed axially chiral Ni (II) complex of glycine Schiff base. *Amino Acids*. 2016. **48**(4): 973–986. DOI: 10.1007/s00726-015-2138-3

[199] Huang X.L., Cheng Y.Z., You S.L. Visible-light enabled synthesis of cyclopropane-fused indolines via dearomatization of indoles. *Org. Chem. Front*. 2022. **9**(20): 5463–5468. doi.org/10.1039/D2QO01174C.

[200] Xie S., Li Y., Liu P., Sun P. Visible light-induced radical addition/annulation to construct phenylsulfonyl-functionalized dihydrobenzofurans involving an intramolecular 1, 5-hydrogen atom transfer process. *Org. Lett*. 2020. **22**(22): 8774–8779. doi.org/10.1021/acs.orglett.0c03038.

[201] Zhang J., Wang Q., Guo Y. *et al.* Visible-Light-Induced Benzylic C-H Functionalization for the Synthesis of 2-Arylquinazolines. *Eur. J. Org. Chem*. 2019. (34): 5934–5936. doi.org/10.1002/ejoc.201900996.

[202] Howard P., Twycross R., Shuster J. *et al.* Benzodiazepines. *J. Pain Symp. Manag*. 2014. **47**(5): 955–964. doi.org/10.1016/j.jpainsymman.2014.03.001.

[203] Ellis T.K., Ueki H., Yamada T. *et al.* Design, synthesis, and evaluation of a new generation of modular nucleophilic glycine equivalents for the efficient synthesis of sterically constrained α-amino acids. *J. Org. Chem*. 2006. **71**(22): 8572–8578. doi.org/10.1021/jo0616198.

[204] Soloshonok V.A., Ellis T.K., Ueki H., Ono T. Resolution/deracemization of chiral α-amino acids using resolving reagents with flexible stereogenic centers. *J. Am. Chem. Soc*. 2009. **131**(21): 7208–7209. doi.org/10.1021/ja9026055.

[205] Zou Y., Han J., Saghyan A.S. *et al.* Asymmetric synthesis of tailor-made amino acids us-

ing chiral Ni (II) complexes of Schiff bases. An update of the recent literature. *Molecules*. 2020. **25**(12): 2739. doi:10.3390/molecules25122739.

[206] Ueki H., Ellis T.K., Martin C.H., Soloshonok V.A. Efficient large-scale synthesis of picolinic acid-derived nickel (II) complexes of glycine. *Eur. J. Org. Chem*. 2003. (10): 1954–1957. DOI: 10.1002/ejoc.200200688.

[207] Ohkura H., Berbasov D.O., Soloshonok V.A. Chemo-and regioselectivity in the reactions between highly electrophilic fluorine containing dicarbonyl compounds and amines. Improved synthesis of the corresponding imines/enamines. *Tetrahedron*. 2003. **59**(10): 1647–1656. doi.org/10.1016/S0040-4020(03)00138-8.

[208] Soloshonok V.A., Kirilenko A.G., Kukhar V.P., Resnati G. Transamination of fluorinated β-keto carboxylic esters. A biomimetic approach to β-polyfluoroalkyl-β-amino acids. *Tetrahedron Lett*. 1993. **34**(22): 3621–3624. doi.org/10.1016/S0040-4039(00)73652-5.

[209] Soloshonok V.A., Ono T. The effect of substituents on the feasibility of azomethine-azomethine isomerization: New synthetic opportunities for biomimetic transamination. *Tetrahedron*. 1996. **52**(47): 14701–14712. doi.org/10.1016/0040-4020(96)00920-9.

[210] Wang Y., Jia D., Zeng J, *et al*. Benzocarbazole Synthesis via Visible-Light-Accelerated Rh (III)-Catalyzed C–H Annulation of Aromatic Amines with Bicyclic Alkenes. *Org. Lett*. 2021. **23**(20): 7740–7745. doi.org/10.1021/acs.orglett.1c02709.

[211] Kumar D., Sharma S., Kalra S. *et al.* Medicinal perspective of indole derivatives: recent developments and structure-activity relationship studies. *Curr. Drug Targets*. 2020. **21**(9): 864–891. doi.org/10.2174/1389450121666200310111 5327.

[212] Mo X., Rao D.P., Kaur K. *et al.* Indole derivatives: a versatile scaffold in modern drug discovery–an updated review on their multifaceted therapeutic applications (2020–2024). *Molecules*. 2024. **29**(19): 4770. doi.org/10.3390/molecules29194770.

[213] Kaushik N.K., Kaushik N., Attri P. *et al.* Biomedical importance of indoles. *Molecules.* 2013. **18**(6): 6620–6662. doi.org/10.3390/molecules18066620.

[214] Kumar S., Ritika. A brief review of the biological potential of indole derivatives. *Future J. Pharm. Sci.* 2020. 1–9. doi.org/10.1186/s43094-020-00141-y.

[215] Xie C, Mei H, Wu L, Soloshonok VA, Han J, Pan Y. LDA-promoted asymmetric synthesis of β-trifluoromethyl-β-amino indanone derivatives with virtually complete stereochemical outcome. *RSC Adv*. 2014. **4**(9): 4763–4768. DOI: 10.1039/C3RA45773G.

[216] Taber D.F., Tirunahari P.K. Indole synthesis: a review and proposed classification. *Tetrahedron.* 2011. **67**(38): 7195–7210. doi.org/10.1016/j.tet.2011.06.040.

[217] Gribble G.W. Recent developments in indole ring synthesis–Methodology and applications. *Contemp. Org. Synth.* 1994. **1**(3): 145–172. doi: 10.1039/CO9940100145.

[218] Qian P., Xie C., Wu L. *et al*. Asymmetric synthesis of (3*S*,1′*S*)-3-(1-amino-2,2,2-trifluoroethyl)-1-(alkyl)-indolin-2-one derivatives by addition of (*S*)-*N*-*t*-butylsulfinyl-3,3,3-trifluoroacetaldimine to 1-(alkyl)-indolin-2-ones. *Org. Biomol. Chem*. 2014. **12**(40): 7909–7913. DOI: 10.1039/C4OB01453G

[219] Wu L., Xie C., Zhou J. *et al*. General asymmetric synthesis of 2,2,2-trifluoro-1-(1*H*-indol-3-and-2-yl)ethanamines. *J. Fluor. Chem*. 2015. **170**: 57–65. doi:10.1016/j.jfluchem.2015.01.001

[220] Li T., Zhou S., Wang J. *et al.* Asymmetric synthesis of α-(1-oxoisoindolin-3-yl)glycine: synthetic and mechanistic challenges.

Chem. Commun. 2015 **51**(9): 1624–1626; doi: 10.1039/C4CC05659K.

[221] Xie C., Zhang L., Sha W. *et al.* Detrifluoroacetylative in situ generation of free 3-fluoroindolin-2-one-derived tertiary enolates: design, synthesis, and assessment of reactivity toward asymmetric Mannich reactions. *Org. Lett*. 2016. **18**(13): 3270–3273. doi.org/10.1021/acs.orglett.6b01516.

[222] Zhang L., Zhang W., Mei H. *et al*. Catalytic asymmetric aldol addition reactions of 3-fluoro-indolinone derived enolates. *Org. Biomolec. Chem*. 2017. **15**(2): 311–315. doi.org/10.1039/C6OB02454H.

[223] Hernández I., Domínguez G., Soloshonok V.A. *et al.* Promoted Deaminative Coupling of Gramines with *C*-and *N*-Nucleophiles. *J. Org. Chem*. 2024. **89**(23): 17291–17309. DOI: 10.1021/acs.joc.4c01895

[224] Domínguez G.,, Mujika A., Hernández I. et al. Deconstructing α-Amidoalkyl Sulfones as Dual d-Sulfonyl/a-Azomethine Synthons: Synthesis of 3-Sulfonylmethylindole Aminals, J. Org. Chem. 2025, 90, 11910−11922, doi.org/10.1021/acs.joc.5c01392. .

[225] Xiao Z., Li Y., Wu Y. *et al*. Asymmetric Synthesis of Unprotected Tryptophan Derivatives Using Gramines via Ni (II) Complexes. *J. Org. Chem*. 2025. **90**(9): 3155–3165. doi.org/10.1021/acs.joc.4c02406.

[226] Li J.T., Luo J.N., Wang J.L. *et al*. Stereoselective intermolecular radical cascade reactions of tryptophans or ϫ-alkenyl-α-amino acids with acrylamides via photoredox catalysis. *Nature Commun*. 2022. **13**(1): 1778. doi.org/10.1038/s41467-022-29464-5.

[227] Soloshonok V.A., Avilov D.V., Kukhar V.P. Asymmetric aldol reactions of trifluoromethyl ketones with a chiral Ni (II) complex of glycine: stereocontrolling effect of the trifluoromethyl group. *Tetrahedron*. 1996. **52**(38): 12433–12442. doi.org/10.1016/0040-4020(96)00741-7.

[228] Soloshonok V.A., Kukhar V.P., Galushko S.V. *et al*. General method for the synthesis of enantiomerically pure β-hydroxy-α-amino acids, containing fluorine atoms in the side chains. Case of stereochemical distinction between methyl and trifluoromethyl groups. X-Ray crystal and molecular structure of the nickel (II) complex of (2*S*,3*S*)-2 (trifluoromethyl)threonine. *J. Chem. Soc. Perkin Trans. 1*. 1993. (24): 3143–3155. doi.org/10.1039/P19930003143.

[229] Soloshonok V.A., Cai C., Hruby V.J., Van Meervelt L. Asymmetric synthesis of novel highly sterically constrained (2*S*,3*S*)-3-methyl-3-trifluoromethyl-and (2*S*,3*S*,4*R*)-3-trifluoromethyl-4-methylpyroglutamic acids. *Tetrahedron*. 1999. **55**(41): 12045–12058. doi.org/10.1016/S0040-4020(99)00710-3.

[230] Aceña J.L., Sorochinsky A.E., Soloshonok V. Asymmetric synthesis of α-amino acids via homologation of Ni (II) complexes of glycine Schiff bases. Part 3: Michael addition reactions and miscellaneous transformations. *Amino Acids*. 2014. **46**(9): 2047–2073. DOI: 10.1007/s00726-014-1764-5.

[231] Soloshonok V.A., Cai C., Hruby V.J. A practical asymmetric synthesis of enantiomerically pure 3-substituted pyroglutamic acids and related compounds. Angew. Chem. Int. Ed. 2000. **39**: 2172–2175. doi.org/10.1002/1521-3757(20000616)112:12<2256::AID-ANGE2256>3.0.CO;2-9

[232] Kim H.J., Fabry D.C., Mader S., Rueping M. Photoredox/rhodium catalysis in C–H activation for the synthesis of nitrogen containing heterocycles. *Org. Chem. Front*. 2019. **6**(14): 2319–2323. doi.org/10.1039/C9QO00206E.

[233] Lin S.N., Deng Y., Zhong H. *et al*. Visible Light-Induced Radical Cascade Difluoromethylation/Cyclization of Unactivated Alkenes: Access to CF_2H-Substituted Polycyclic Imidazoles. *ACS Omega*. 2024. **9**(26): 28129–28143. doi.org/10.1021/acsomega.4c01177.

[234] Soloshonok V.A., Hayashi T. Gold (I)-catalyzed asymmetric aldol reaction of methyl isocyanoacetate with fluorinated benzaldehydes. *Tetrahedron Lett*. 1994. **35**(17): 2713–2716. doi.org/10.1016/S0040-4039(00)77013-4.

[235] Soloshonok V.A., Hayashi T. Gold (I)-catalyzed asymmetric aldol reactions of fluorinated benzaldehydes with an α-isocyanoacetamide. *Tetrahedron: Asymm*. 1994. **5**(6): 1091–1094. doi.org/10.1016/0957-4166(94)80059-6.

[236] Soloshonok V.A., Kacharov A.D., Hayashi T. Gold (I)-catalyzed asymmetric aldol reactions of isocyanoacetic acid derivatives with fluoroaryl aldehydes. *Tetrahedron*. 1996. **52**(1): 245–254. doi.org/10.1016/0040-4020(95)00893-D.

[237] Liu Y.C., Chen P., Li X.J. *et al*. Visible-light-induced dual acylation of alkenes for the construction of 3-substituted chroman-4-ones. *J. Org. Chem*. 2022. **87**(6): 4263–4272. doi.org/10.1021/acs.joc.1c03100.

[238] Bravo P., Guidetti M., Viani F. *et al*. Chiral sulfoxide controlled asymmetric additions to C=N double bond. An efficient approach to stereochemically defined α-fluoroalkyl amino compounds. *Tetrahedron*. 1998. **54**(42): 12789–12806. doi.org/10.1016/S0040-4020(98)00779-0.

[239] Xie C., Dai Y., Mei H. *et al*. Asymmetric synthesis of quaternary α-fluoro-β-ketoamines via detrifluoroacetylative Mannich reactions. Chem. Commun. 2015. **51**(44): 9149–9152. DOI: 10.1039/c5cc02256h.

[240] Bravo P., Capelli S., Crucianelli M. *et al*. Asymmetric synthesis of α-arylglycinols via additions of lithium methyl *p*-tolyl sulfoxide to *N*-(PMP) arylaldimines followed by "non oxidative" Pummerer reaction. *Tetrahedron*. 1999. **55**(10): 3025–3040. doi.org/10.1016/S0040-4020(99)00064-2.

[241] Li W., Zhou L. Vinyldiazo compounds as 3-carbon radical acceptors: synthesis of 4-fluoroacridines via visible-light-promoted cascade radical cyclization. *Org. Lett*. 2021. **23**(11): 4279–4283. doi.org/10.1021/acs.orglett.1c01204.

[242] Xue L., Song X., Zhang X., Fan X. Synthesis of *O*-Heterocycle Spiro-Fused Cyclopentaquinolinones and Cyclopentaindenes through Visible Light-Induced Radical Cyclization Reactions. *J. Org. Chem*. 2023. **88**(17): 12641–12657. doi.org/10.1021/acs.joc.3c01317.

[243] Tyson J.J., Light J.C. Properties of two-component bimolecular and trimolecular chemical reaction systems. *J. Chem. Phys*. 1973. **59**(8): 4164–4173. doi.org/10.1063/1.1680609.

[244] Gershinowitz H., Eyring H. The theory of trimolecular reactions1. J. Am. Chem. Soc. 1935. **57**(6): 985–991. doi.org/10.1021/ja01309a007.

[245] Liang D., Rao L., Xiao C., Chen J.R. Intermolecular Hetero-Diels–Alder Reactions of Photogenerated aza-ortho-Quinone Methides with Aldehydes. *Org. Lett*. 2019. 21(21):8783–8. doi.org/10.1021/acs.orglett.9b03399.

[246] Geng X., Xu Z., Cai Y., Wang L. Visible-light-driven multicomponent cyclization by trapping a 1,3-vinylimine ion intermediate: A direct approach to pyrimido [1,2-*b*] indazole derivatives. *Org. Lett*. 2021. **23**(21): 8343–8347. doi.org/10.1021/acs.orglett.1c03076.

[247] Manna S., Prabhu K.R. Visible-light-mediated vicinal difunctionalization of activated alkynes with boronic acids: substrate-controlled rapid access to 3-alkylated coumarins and unsaturated spirocycles. *Org. Lett*. 2023. **25**(5): 810–815. doi.org/10.1021/acs.orglett.2c04333.

Стаття надійшла: 30.01.2026
Стаття прийнята до друку: 01.03.2026
Стаття опублікована: 25.03.2026